7-11-2015

TAFIa is a Novel Inhibitor of Tumour Angiogenesis in Breast Cancer

Jennifer Lynn Balun
University of Windsor

TAFIa is a Novel Inhibitor of Tumour Angiogenesis in Breast Cancer

By

Jennifer Balun

A Thesis
Submitted to the Faculty of Graduate Studies
through Chemistry and Biochemistry
in Partial Fulfillment of the Requirements for
the Degree of Master of Science
at the University of Windsor

Windsor, Ontario, Canada

2015

TAFIa is a Novel Inhibitor of Tumour Angiogenesis in Breast Cancer

by

Jennifer Balun

APPROVED BY:

_____

L. Porter

Department of Biological Sciences

_____

S. Pandey

Department of Chemistry & Biochemistry

_____

M. Boffa, Advisor

Department of Chemistry & Biochemistry

May 25, 2015

Declaration of Co-Authorship

I hereby declare that this thesis incorporates material that is result of joint research, as follows:

This thesis also incorporates the outcome of a joint research undertaken in collaboration with Zainab Bazzi under the supervision of Dr. Michael Boffa. The collaboration is covered in Chapter 2 of the thesis. In all cases, the key ideas, primary contributions, experimental designs, data analysis and interpretation, were performed by the author, and the contribution of coauthors was primarily through the production of rTM EGF3-6 clones, stable cell lines expressing the rTM EGF3-6 proteins, and some purification of the rTM EGF3-6 proteins.

I am aware of the University of Windsor Senate Policy on Authorship and I certify that I have properly acknowledged the contribution of other researchers to my thesis, and have obtained written permission from each of the co-author(s) to include the above material(s) in my thesis.

I certify that, with the above qualification, this thesis, and the research to which it refers, is the product of my own work.

I certify that, to the best of my knowledge, my thesis does not infringe upon anyone's copyright nor violate any proprietary rights and that any ideas, techniques, quotations, or any other material from the work of other people included in my thesis, published or otherwise, are fully acknowledged in accordance with the standard referencing practices. Furthermore, to the extent that I have included copyrighted material that surpasses the bounds of fair dealing within the meaning of the Canada Copyright Act, I certify that I have obtained a written permission from the copyright owner(s) to include such material(s) in my thesis and have included copies of such copyright clearances to my appendix.

I declare that this is a true copy of my thesis, including any final revisions, as approved by my thesis committee and the Graduate Studies office, and that this thesis has not been submitted for a higher degree to any other University or Institution.

Abstract

Thrombomodulin (TM) is known mostly for its role in the regulation of hemostasis, but it has also been shown to play an antimetastatic role in cancer. A previous study showed that the anitmetastatic effects of TM were dependent on thrombin binding. However, it is not known which substrate of thrombin-TM, protein C or TAFI, is responsible for these antimetastatic effects. We hypothesized that TAFI is responsible for the antimetastatic effects of TM, specifically tumour angiogenesis, due to its role in the inhibition of pericellular plasminogen activation. We determined the effect of TAFIa on tumour angiogenesis through inhibition of TAFIa and manipulation of cofactor ability of TM. We found inhibition of TAFIa resulted in increased proliferation, invasion, tube formation, and ECM proteolysis. We also found an inhibitory effect of TAFI activation by thrombin-TM on tube formation and ECM proteolysis. Our results suggest that TAFIa inhibits tumour angiogenesis in breast cancer cells.

Acknowledgements

First and foremost I would like to thank my supervisor Dr. Boffa for giving me the opportunity to work in his lab and on this project. Thank you for all of the guidance, advice, support, and encouragement. I'd also like to thank Dr. Koschinsky for her support and advice.

I would like to thank Dr. Pandey and Dr. Porter for agreeing to be a part of my committee and contributing their time and knowledge to this project. I would also like to thank Dr. Cavallo-Medved for sharing her expertise and taking time out of her busy schedule to provide insight on my project.

I'd like to thank the members of the Boffa lab group: Tanya, Dragana, Zainab, Christina, Justin, and Danielle. I'd also like to thank the members of the Koschinsky lab group: Corey, Rocco, Jackson, Sera, and Matt. Thank you everyone for the help and advice.

Finally, I would like to thank my mom for her love and patience throughout the completion of this thesis.

Table of Contents

List of Tables

List of Figures

List of Abbreviations

IIa	Thrombin
AAFR	N-(4-Methoxyphenylazoformyl)-Arg-OH · HCL
APC	Activated protein C
Bcl-2	B cell lymphoma-2
bFGF	Basic fibroblast growth factor
BK	Bradykinin
BSA	Bovine serum albumin
CM	Conditioned media
CPB	Carboxypeptidase B
CPN	Carboxypeptidase N
CPR	Carboxypeptidase R
CPU	Unstable carboxypeptidase
CS	Chondroitin sulfate
DIC	Differential interference contrast
DMEM	Dulbeco's modified eagle's medium
DQ	Dye-quenched
EBM-2	Endothelial Cell Basal Medium-2
ECM	Extracellular matrix
EDTA	Ethylenediamine-tetraacetic acid
EGF	Epidermal growth factor
EGM-2	Endothelial Cell Basal Medium-2
ELISA	Enzyme-linked immunosorbent assay
EMT	Epithelial-mesenchymal transition
EPCR	Endothelial protein C receptor
FBS	Fetal bovine serum
FDP	Fibrin degradation product
FGF	Fibroblast growth factor
Fibrin'	Partially degraded fibrin
GPI	Glycosyl phosphatidylinositol

HBS	HEPES buffered saline
HBSS	HEPES buffered saline solution
HEK293	Human Embryonic Kidney 293
HEPES	N-(2-Hydroxyethyl)piperazine-N'-(2-ethanesulfonic acid)
HIF-1	Hypoxia-inducible factor 1
HMGB1	High mobility group box chromosomal protein 1
HUVEC	Human umbilical vein endothelial cell
IL	Interleukin
ISV	Intersegmental vessel
MMP	Matrix metalloproteinase
MT-MMP	Membrane-type matrix metalloproteinase
NFκB	Nuclear factor κB
OPN	Osteopontin
PAI-1	Plasminogen activator inhibitor-1
PAI-2	Plasminogen activator inhibitor-2
PBS	Phosphate buffered solution
pCPB	Plasma procarboxypeptidase B
PCR	Polymerase chain reaction
PDGF	Platelet-derived growth factor
PEG	Polyethylene glycol
PGF	Placenta growth factor
Plg	Plasminogen
Pln	Plasmin
PPACK	D-phenylalanyl-prolyl-arginyl chloromethyl ketone
PS	Protein S
PTCI	Potato tuber carboxypeptidase inhibitor
PTEN	Phosphate and tensin homolog
RPE	Retinal pigment epithelium
rTM	Recombinant thrombomodulin
qRT-PCR	Quantitative real time polymerase chain reaction
S-2366	L-Pyroglutamyl-L-prolyl-L-argininep-Nitroaniline hydrochloride

SDS	Sodium dodecyl sulfate
SDS-PAGE	Sodium dodecyl sulfate-polyacrylamide gel electrophoresis
SEM	Standard error of the mean
SFM	Serum free media
SIV	Subintestinal vein
TAFI	Thrombin-activatable fibrinolysis inhibitor
TAFIa	Activated thrombin-activatable fibrinolysis inhibitor
TGF	Transforming growth factor
TF	Tissue Factor
TFPI	Tissue factor pathway inhibitor
TIMP	Tissue inhibitor of metalloproteinase
TM	Thrombomodulin
TNF	Tumour necrosis factor
tPA	Tissue-type plasminogen activator
uPA	Urokinase-type plasminogen activator
uPAR	Urokinase-type plasminogen activator receptor
uPAS	Urokinase plasminogen activation system
VEGF	Vascular endothelial growth factor
VEGFR	Vascular endothelial growth factor receptor
VPF	Vascular permeability factor
WST	Water soluble tetrazolium

Chapter 1 Introduction

1.1 Cancer

The body contains over 30 trillion cells whose growth and proliferation is highly controlled [1]. When these processes become uncontrolled a cell can become transformed [1]. There are more than one hundred different types of cancer and almost every tissue in the body is capable of forming tumours [1, 2]. Cancer is the leading cause of death in Canada [3]. In 2009, 40% of Canadians were expected to develop cancer in their lifetimes, and 25% of Canadians were expected to die from cancer [3]. There are multiple different theories of the mechanisms by which cancer arises, and it is likely that multiple combinations of these mechanisms lead to the disease.

The development of a malignant tumour involves a multistep process of consecutive alterations in many oncogenes, microRNAs, and tumour-suppressor genes in somatic cells [2, 4]. Germ-line mutations of these genes are also possible which could predispose a person to a heritable cancer [4]. Mutations can be caused from chemical compounds, viruses, and radiation [5]. Epigenetic events, such as promoter methylation, can lead to cancer [5]. Mutated cells have a greater survival advantage compared to non-mutated cells, which could lead to carcinogenesis [5]. Tumours are usually heterogeneous due to secondary and tertiary genetic alterations [4]. This heterogeneity of tumours can make treatment difficult because there are multiple different populations of cancer cells with differing vulnerability to treatment [4].

There are hallmark capabilities that most cancer cells exhibit. The six main hallmarks of cancer are: sustaining proliferative signaling, evading growth suppressors, enabling replicative immortality, resisting apoptosis, inducing angiogenesis, and activating invasion and metastasis [2, 6]. There are also two emerging hallmarks of cancer: reprogramming energy metabolism and evading immune destruction. Cancer cells can acquire sustained proliferative signaling by producing their own growth factors, overexpressing growth factor receptors, influencing tumour-associated stroma to secrete growth factors, and compromised negative feedback loops that inhibit proliferative signaling [2, 6]. Cancer cells can evade growth suppressors by disruptions in cell cycle progression pathways, or redirection of an antiproliferative pathway such as the TGF-β pathway towards activating the epithelial-mesenchymal transition (EMT) [2, 6]. Another hallmark is enabling replicative immortality which can be attributed to telomere maintenance and prevention of senescence [2, 6]. Cancer cells can resist apoptosis through the loss of tumour suppressor function, downregulating pro-apoptotic factors, increase in expression of anti-apoptotic regulators, or increasing expression of survival factors [2, 6]. During tumour formation the "angiogenic switch" occurs where normally quiescent vasculature becomes activated by increasing activation or expression of pro-angiogenic factors and decreasing expression or activation of anti-angiogenic factors [2, 6]. Metastasis of tumour cells is responsible for 90% of cancer deaths [2]. Activation of invasion and metastasis in cancer cells can occur through activation of extracellular proteases, altered binding specificities of integrins, cadherins, and cell-cell adhesion molecules [2, 6]. An emerging hallmark of cancer is the reprograming of energy metabolism by relying on glycolysis which leads to an "aerobic glycolysis" state that

fuels cell growth and uncontrolled proliferation [6]. The second emerging hallmark, evading immune destruction, has not been completely solved but it seems that tumours manage to avoid being destroyed by the immune system by disabling components of the immune system that have been sent to destroy them [6]. These hallmarks of cancer showcase the complexity of the disease and how treatment of the disease is complicated due to the amount of contributing factors.

Due to the prevalence and complexity of cancer there has been extensive research invested in finding new pathogenic pathways to better understand and treat this disease.

1.2 Angiogenesis

Angiogenesis is the process in which preexisting blood vessels sprout new capillaries. In adults, new vessels are formed predominantly through angiogenesis, as opposed to vasculogenesis which is the process of blood vessel formation from endothelial-cell precursors [7]. In adults, the vasculature is quiescent and is only normally activated through wound healing and female reproductive processes such as ovulation [8].

New capillaries from quiescent vasculature can be formed in response to a stimulus which activates the vasculature [8]. Once activated, endothelial cells locally degrade the vascular basement membrane and extracellular matrix allowing the cells to invade the surrounding stroma [8, 9]. The endothelial cells begin to proliferate into the perivascular space toward the stimulus forming a migrating column [8, 9]. Extravascular

fibrin is deposited and acts as a temporary matrix scaffold for the migrating endothelial cells [10]. The endothelial cells in the migrating column enter a differentiation zone where the cells stop proliferating and begin to change shape and tightly adhere to each other to form the lumen of the new capillary [8, 9]. The sprouting tubes fuse and coalesce into loops allowing circulating blood to flow through the new capillary [8]. Finally, there is further proliferation in the blood vessel wall to increase diameter, and perivascular cells are attracted to the new vessel to form a new basal lamina [9]. Once the new blood vessel has formed, the vessel becomes quiescent.

The process of angiogenesis in normal processes like the female reproductive cycle and wound healing is usually not harmful, but overactive angiogenesis can lead to many diseases. Angiogenesis is overactive in macular degeneration, endometriosis, psoriasis, rheumatoid arthritis, and cancer [11, 12].

1.3 Tumour Angiogenesis

Sustained angiogenesis is one of the hallmarks of cancer [2, 6]. The key role that angiogenesis plays in cancer has been recognized since the early 1970s. In 1971, Folkman published an article stating that vascularization of a tumour was necessary for expansion of the tumour [13]. His group found that tumours could not grow beyond 1-2 mm^3 in size without angiogenesis because the tumour could not receive enough oxygen and nutrients [14]. Without angiogenesis, the tumour maintains a balance of proliferation and apoptosis preventing growth and causing it to be dormant [11]. Folkman's initial

findings were controversial since it was widely believed that tumour growth was not dependent on angiogenesis [15]. Moreover, there was a general belief that tumours grew around existing vasculature and recruitment of blood vessels was not possible [15]. Eventually, the scientific evidence grew to support Folkman's initial findings and a vast amount of research has gone into discovering how tumour angiogenesis occurs. Now it is firmly established that highly angiogenic tumours have a higher metastatic potential than less vascular tumours [16].

When blood vessels are quiescent, there is a balance between pro-angiogenic factors and anti-angiogenic factors. Where there is an increase in pro-angiogenic factors and a decrease in anti-angiogenic factors, the "angiogenic switch" occurs and angiogenesis is activated [8]. Tumour angiogenesis goes through two phases separated by the "angiogenic switch": an avascular phase and a vascular phase [9]. In the avascular phase the dormant tumour is in a steady state of proliferation and apoptosis [9]. Only a small subset of the avascular tumours reach the vascular phase in which exponential tumour growth occurs due to tumour angiogenesis [9]. Tumours can release diffusible angiogenic factors, such as VEGF and bFGF, that can signal quiescent vasculature to begin angiogenesis [8]. Negative regulators of angiogenesis, such as thrombospondin-1 and endostatin, must also be decreased for tumour angiogenesis to occur [11]. Different factors such as hypoxia in the tumour can cause an increase in VEGF secretion from tumour cells and surrounding stromal cells [9]. The tumour suppressor gene p53 upregulates thrombospondin-1; p53 is lost in half of all cancers which could lead to a decrease of thrombospondin-1 [6, 9].

The blood vessels formed through tumour angiogenesis differ from blood vessels formed through normal angiogenesis. Vessels formed by tumour angiogenesis do not become quiescent, and the constant growth of new blood vessels within a tumour causes them to have a different physiology [9]. Structurally, tumour blood vessels are dilated, irregularly shaped, have dead ends, and can have cancer cells integrated into the vessel wall [9]. The blood vessels aren't organized into normal structures like capillaries, arterioles, and venules: they are instead chaotically organized with excessive vessel branching [17]. The blood flow in tumour vessels is erratic, it is slow moving and sometimes oscillating; this leads to acidic and hypoxic regions in tumours [9, 18]. Tumour vessels are leaky due to overproduction of VEGF and thus experience microhemorrhaging [9]. There is high interstitial pressure within the tumour due to the leakiness of the tumour vasculature [17]. Tumour vessels have altered endothelial cell-pericyte interactions, which results in defective surrounding basement membrane [17]. The endothelial cells within the tumour vessel have abnormal gene expression and require growth factors for survival [17]. Overall, tumour vessels are functionally and structurally different than normal blood vessels.

Blood vessels within the tumour can act as an escape route for a tumour to metastasize. Metastasis follows a step-wise sequence sometimes referred to as the invasion-metastasis cascade [6, 19]. First, tumour cells locally invade and intravasate into the blood vessel within or surrounding the tumour [19]. The cancer cells then travel and survive through the blood stream, arrest in a capillary bed, and extravasate from the blood stream into the parenchyma of distant tissues [19, 20]. The cancer cells proliferate in their new environment and form a micrometastatic lesion, through the process of colonization

[19]. Once the micrometastatic lesion has formed, vascularization of the new tumour can occur and the process of metastasis can begin again [19]. Cancer cells can metastasize through either blood vessels or through lymphatic vessels [19].

The process of tumour angiogenesis is necessary for the growth of a tumour past a dormant avascular stage [9, 11, 13, 14]. Tumour angiogenesis provides nutrients and oxygen to a tumour and also can act as an escape route allowing metastasis to occur [14, 19].

1.4 Vascular Endothelial Growth Factor

Vascular endothelial growth factor (VEGF) is a key mediator of angiogenesis. VEGF is responsible for vascular permeability and growth [21]. Originally, VEGF was identified by different groups as two different proteins named based on its two main activities [21]. Senger and colleagues first identified a protein they named "tumour vascular permeability factor" (VPF) in 1983 and suggested that this protein could be responsible for the high permeability of tumour blood vessels [22]. Ferrara and Henzel identified a protein they named "vascular endothelial growth factor" (VEGF) in 1989 due to the protein being an endothelial cell specific mitogen [23]. Eventually, cDNA cloning of both VPF and VEGF determined that they were the same protein [21]. VEGF is also referred to as VEGF-A, as it belongs to a family of proteins including VEGF-B, VEGF-C, VEGF-D, and placenta derived growth factor (PDGF) [21]. The other VEGF proteins, VEGF-B, VEGF-C, and VEGF-D do not play a role in endothelial angiogenesis [21].

VEGF-C and VEGF-D play a role in lymphatic angiogenesis [21]. VEGF-A (hereafter referred to simply as "VEGF") exists as four main isoforms produced by alternative splicing: $VEGF_{121,}$ $VEGF_{165}$, $VEGF_{189}$, and $VEGF_{206}$, with $VEGF_{165}$ being the most prominent isoform [21]. VEGF binds to two receptors, VEGFR-1 and VEGFR-2, both of which are receptor tyrosine kinases [21]. VEGF binding to VEGFR-2 leads to the mitogenic activity while VEGFR-1 acts as a decoy receptor by sequestering VEGF leading to less VEGF availability for VEGFR-2 [21].

VEGF expression is upregulated most effectively by hypoxia due to the transcription factor hypoxia-inducible factor 1 (HIF-1) [21]. The inflammatory cytokines IL-1 and IL-6 upregulate the expression of VEGF [21]. Many growth factors upregulate VEGF expression such as PDGF, TGF-α, TGF-β, FGF, and EGF; these growth factors are frequently expressed by tumours [21, 24]. Activation of Ras and mutations in the Wnt-signaling pathway result in increased VEGF expression [21]. VEGF expression can also be upregulated by mutations in the tumour suppressors PTEN and p53 [21, 25]. Biologically active $VEGF_{189}$, $VEGF_{206}$, and, to a lesser extent, $VEGF_{165}$ can be released from the extracellular matrix (ECM) by the proteolytic enzyme plasmin or the glycosaminoglycan heparin [26].

1.4.1 Role of VEGF in Cancer

VEGF acts as a key mediator of angiogenesis by promoting endothelial cell growth, vascular permeability, chemotaxis, extracellular matrix (ECM) degradation, and endothelial cell survival [21, 25]. In endothelial cells, VEGF induces the expression of

the anti-apoptotic proteins Bcl-2 and survivin [21]. VEGF induces expression of urokinase-type plasminogen activator (uPA), tissue-type plasminogen activator (tPA), and plasminogen activator inhibitor-1 (PAI-1) [27]. uPA is involved in extracellular proteolysis and cell migration [27]. VEGF also upregulates the expression of urokinase-type plasminogen activator receptor (uPAR) in endothelial cells; uPAR greatly increases the rate of plasminogen activation [28]. In retinal pigment epithelium (RPE) cells there is a positive feedback loop that exists between VEGF and matrixmetaloproteinase-9 (MMP9), where MMP9 is involved in ECM degradation [29].

VEGF is the key mediator of angiogenesis and it is upregulated by hypoxia, growth factors frequently expressed in tumours, loss of tumour suppressors, and over-activation of oncogenes [21, 24, 25]. VEGF has been found to be overexpressed in many human tumours including kidney, colon, pancreas, bladder, breast, stomach, and glioblastomas [30]. VEGFR-1 and VEGFR-2 are expressed in many human tumours [31]. Elevated levels of VEGF in cancer are associated with a poorer prognosis [24]. Due to these factors inhibiting the VEGF became an attractive cancer therapeutic target. Many drugs have been made to target VEGF and the VEGFRs. While these drugs have been successful in treating mouse tumours, they only have modest effects on human cancers [32]. Bevacizumab, a human antibody against VEGF-A, was the first FDA approved drug for cancer treatment that inhibited VEGF [21]. Bevacizumab seems to be only slightly beneficial to advanced colon cancer patients by prolonging life for 4 to 5 months [32]. The FDA has revoked the approval of bevacizumab for the treatment of metastatic breast cancer [33]. In phase III clinical trials VEGF or VEGFR inhibitors were shown to have modest effects on human cancers [32, 34]. A potential explanation for the minimal

benefit of these therapies is the tumour cells that are resistant to anti-VEGF therapy could upregulate many other growth factors that can stimulate tumour angiogenesis [32]. The failure of the anti-VEGF therapeutics suggests that new molecular targets need to be found to treat tumour angiogenesis [32].

1.5 Urokinase Plasminogen Activation System

The urokinase plasminogen activation system (uPAS) is involved in many different processes including tissue and vascular remodeling, cell migration, cell invasion, cell adhesion, tumour development, angiogenesis, and metastasis [35]. uPAS consists of urokinase-type plasminogen activator (uPA), urokinase-type plasminogen receptor (uPAR), and two inhibitors: plasminogen activator inhibitor-1 (PAI-1), and plasminogen activator inhibitor-2 (PAI-2) [36]. The uPAS system is involved in the conversion of the zymogen plasminogen to the active enzyme plasmin (Fig. 1.1) [36].

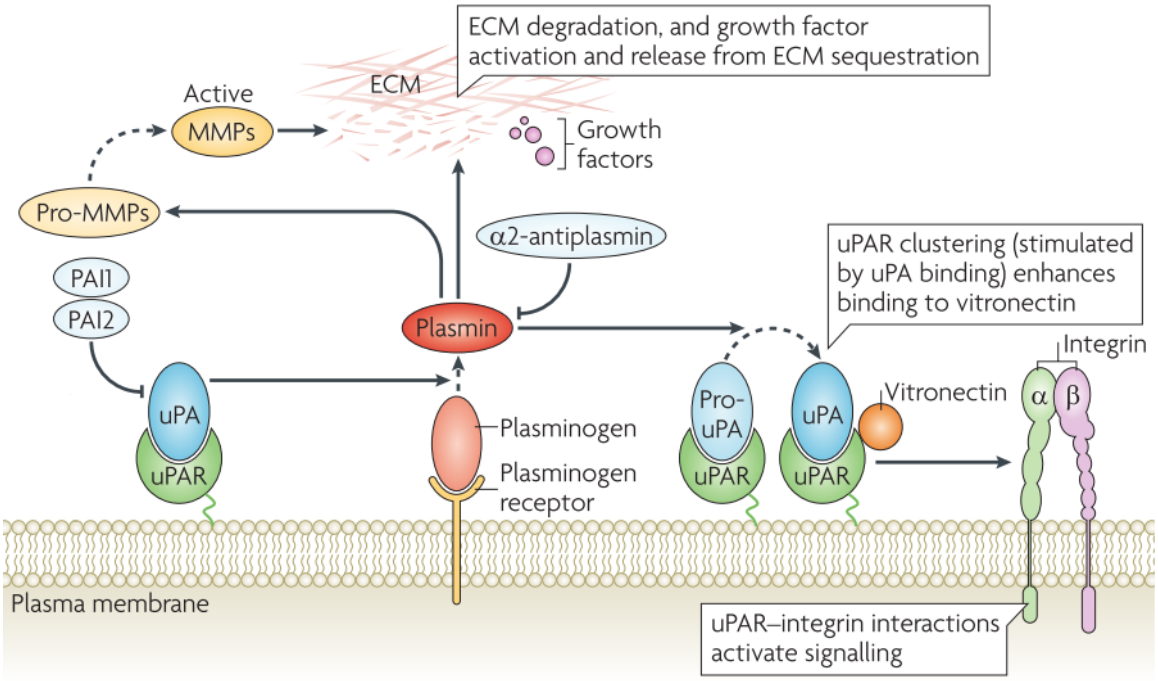

Figure 1.1 Activation of plasminogen by the urokinase plasminogen activation system

Urokinase-type plasminogen activator receptor (uPAR) can bind both the zymogen urokinase-type plasminogen activator (pro-uPA) and the active form uPA with the same affinity. Plasmin can activate pro-uPA to uPA, and uPA can activate plasminogen to plasmin. Both of these processes are more efficient when the zymogen forms are bound to their cell surface receptors, uPAR or plasminogen receptor. Plasmin degrades the extracellular matrix (ECM) and activates and releases matrix metalloproteinases (MMPs). Both plasmin and the active MMPs can activate and release growth factors from the ECM. uPA bound to uPAR can bind to the ECM protein vitronectin. uPA-uPAR bound to vitronectin can interact with integrins to activate intracellular signaling events. uPA is antagonized by plasminogen activator inhibitor 1 (PAI-1) and plasminogen activator inhibitor 2 (PAI-2). Plasmin activity can be inhibited by α_2-antiplasmin. (Image adapted from ref. 41).

Plasminogen is the zymogen form of plasmin, its activation plays a role in fibrinolysis, inflammation, and cancer [37]. Plasminogen is produced by the liver and circulates at a relatively high concentration through interstitial fluids and plasma [38]. The concentration of plasminogen can be upregulated in response to injury or inflammation [38]. Plasminogen circulates under physiological conditions as Glu-plasminogen [37]. Glu-plasminogen consists of a single chain with a carboxyl-terminal serine protease domain, five kringle domains, and an amino-terminal glutamic acid [37]. Plasminogen can bind to proteins with carboxyl-terminal lysine through the lysine-binding site in kringle domains 1, 2, 4, and 5 [37]. Glu-plasminogen is in a tight conformation; proteolysis by plasmin of the amino-terminal portion results in the cleavage of the amino-terminal portion and generates Lys-plasminogen [36]. Plasminogen is in the tight conformation under physiological conditions to limit the amount of plasminogen activation in the blood [36]. Lys-plasminogen is in an open conformation and is susceptible to cleavage from proteolytic enzymes such as uPA and tissue-type plasminogen activator (tPA) to form plasmin [36].

There are more than twelve known plasminogen receptors possibly present on the cell surface, most with a carboxyl-terminal lysine residue to which the kringle domains of plasminogen can bind [39]. Activation of plasminogen by uPA or tPA is enhanced through binding of plasminogen to a cell surface plasminogen receptor [39]. Plasmin is protected from inhibitors by being bound to a plasminogen receptor [37]. Binding of plasminogen to a cell surface plasminogen receptor localizes plasminogen activation to the cell surface (Fig. 1.1) [37].

Plasmin is a serine protease with activity toward a broad range of substrates. In the blood, fibrin is the main substrate of plasmin [40]. Plasmin mediates fibrinolysis by degrading and clearing fibrin blood clots [41]. Plasmin also degrades a range of basement membrane and ECM components including proteoglycans, fibronectin, vitronectin, type IV collagen, and laminin (Fig. 1.1) [36]. Plasmin can release many growth factors from the ECM that promote migration, growth and angiogenesis such as VEGF, EGF, bFGF, and TGF-β (Fig. 1.1) [36]. Many of these growth factors then act to upregulate the expression of uPAR, uPA, and PAI-1 [36]. Plasmin also activates many matrix metalloproteinases (MMPs) that can further degrade the ECM and release growth factors (Fig. 1.1) [38]. Plasmin activates MMP1, 2, 3, 9, 13, and 14 [38]. Plasmin has been shown to have activity toward osteopontin (OPN); proteolytic cleavage of OPN can result in increased cell adhesion of tumour cells [42]. Angiostatin, an inhibitor of angiogenesis, is a fragment of plasminogen and plasmin that can be produced from plasmin autoproteolysis or degradation by MMPs [35]. Overall, plasmin acts to regulate fibrinolysis and tissue remodeling.

There are two different plasminogen activators: uPA and tPA [43]. tPA is involved in plasminogen activation in the blood which leads to the lysis of fibrin clots [38]. uPA is involved in plasminogen activation which leads to tissue remodeling [43]. uPA is secreted as a single-chain zymogen pro-uPA [35, 36]. Single chain pro-uPA can be converted to the two chain active form of uPA by proteases such as plasmin and trypsin [35, 36]. There is reciprocal zymogen activation between plasmin and uPA: plasmin is the main activator of pro-uPA, and plasminogen is the main substrate of uPA (Fig. 1.1) [36]. Pro-uPA and uPA bind with the same affinity to uPAR, and the

conversion of pro-uPA to uPA is more efficient when pro-uPA is bound to uPAR (Fig. 1.1) [35, 36]. This localization of the activation of pro-uPA to uPAR leads to pericellular generation of uPA [36].

uPAR is involved in regulating extracellular proteolysis, cell signaling, and cell adhesion [41]. uPAR localizes to cell-cell contacts, cell-ECM contacts, and the leading edge of migrating cells [36]. uPAR has low expression in normal cells and it is upregulated by injury and inflammation and during ECM remodeling [41]. uPAR does not contain a transmembrane domain: instead it is associated with the cell surface by a glycosyl phosphatidylinositol (GPI) anchor [36]. uPAR binds both pro-uPA and uPA and it enhances the production of uPA at the cell surface (Fig. 1.1) [36]. Another ligand of uPAR is the ECM protein vitronectin [36, 43]. Vitronectin binds to a different location on uPAR than pro-uPA/uPA; therefore, both vitronectin and pro-uPA/uPA can simultaneously bind to uPAR [41]. Binding of uPAR to vitronectin is enhanced by uPA binding to uPAR [41]. Vitronectin binding to uPAR results in cell adhesion [41]. The GPI anchor attached to uPAR allows it to localize to lipid rafts which have a higher concentration of vitronectin and integrins [41]. Integrins are cell surface receptors that transduce signals from the extracellular environment; some integrins are co-receptors of vitronectin [40]. uPAR or uPAR associated with vitronectin may interact with integrins which results in cell signaling leading to cell survival, cell proliferation, cytoskeleton remodeling, and cell mobility (Fig. 1.1) [41, 43]. uPAR regulates extracellular proteolysis through uPA, cell adhesion through vitronectin, and cell signaling through vitronectin and potentially through integrins [41].

There are inhibitors of the uPAS which act to regulate the amount of uPA and plasmin generation: PAI-I, PAI-2, α_2-antiplasmin, and α_2-macroglobin [36, 37, 43]. PAI-1 and PAI-2 are plasminogen activator inhibitors while α_2-antiplasmin and α_2-macroglobin inhibit plasmin [36, 37, 43]. PAI-1 and PAI-2 are serine protease inhibitors (serpins). PAI-1 is considered the main inhibitor of uPA and tPA (Fig. 1.1) [43]. PAI-2 can inhibit tPA and uPA, albeit to a lesser extent than PAI-1 (Fig. 1.1) [35]. PAI-1 inactivates tPA and uPA in a 1:1 ratio and it can also moderately inhibit plasmin [36, 43]. PAI-1 is stabilized in its active conformation by an interaction with vitronectin and PAI-1 bound to vitronectin can still bind to uPA [43]. PAI-1 bound to uPA loses its affinity for vitronectin [35]. uPA bound to uPAR is not protected from inhibition by PAI-1 and PAI-2 [43]. α_2-antiplasmin is the main inhibitor of plasmin (Fig. 1.1) [35]. Cell surface bound plasmin is protected against inhibition from α_2-antiplasmin and α_2-macroglobin circulating in the plasma, this acts to restrict active plasmin to the cell surface [43].

1.1.1 Urokinase Plasminogen Activation System in Cancer

uPA, uPAR, and PAI-1 expression has been found to be upregulated in cancer and associated with a poorer prognosis [36]. These uPAS components are upregulated in many cancers including lung, bladder, breast, colon, ovary, cervix, kidney, stomach, brain, thyroid, bladder, and endometrium [36]. In breast cancer specifically, high levels of uPA and PAI-1 are robust prognostic markers associated with poor relapse-free survival and overall survival [44]. The uPAS system is involved in tumour cell migration, invasion, tumour angiogenesis, proliferation and adhesion [36].

The uPAS has been implicated in tumour angiogenesis. While uPA and uPAR levels are undetectable in normal quiescent endothelial cells, their production is induced at the leading edge of migrating endothelial cells by pro-angiogenic factors such as VEGF [10, 27, 45]. PAI-1 is highly expressed in tumour associated endothelial cells [10]. The major angiogenic stimulator hypoxia can induce uPAR and PAI-1 [10]. MMPs released from the ECM and activated by plasmin play a role in angiogenesis by degrading the ECM and basement membrane of existing vasculature to allow movement and proliferation of endothelial cells into the surrounding stroma [36]. uPA expression can be induced by NFκB; in many cancers NFκB is constitutively active [36]. The uPA promoter has also been found to be hypomethylated in many cancer cells leading to increased uPA production [36]. The tumour suppressor p53 can bind to a sequence in the untranslated region of uPAR mRNA, resulting in an increase in its mRNA degradation by other proteins [36]. In more than 50% of cancers there are loss-of-function mutations of p53 which could account for the upregulation of uPAR in many cancers [36].

The upregulation of PAI-1 in cancers seems paradoxical since PAI-1 inhibits uPA. A study from Bajou *et al.* showed prevention of tumour vascularization and invasion of transplanted keratinocytes in PAI-1 deficient mice [46]. When PAI-1 expression was restored in the PAI-I deficient mice there was invasion and tumour vascularization of the transplanted keratinocytes [46]. This study showed that PAI-1 expression is essential for tumour angiogenesis and invasion [46]. Excessive ECM and basement membrane proteolysis hinder angiogenesis because there is the absence of a scaffold for migrating endothelial cells to adhere [10]. PAI-1 prevents excessive proteolysis which therefore supports angiogenesis [10]. PAI-1 can bind to vitronectin,

and when PAI-1 binds to uPA it loses affinity for vitronectin [35, 43]. In this manner, PAI-1 could regulate cell adhesion: when PAI-1 interacts with vitronectin it inhibits cell adhesion while when PAI-1 complexes with uPA adhesion is promoted [47]. In the absence of uPA, cells would be nonadherent and motility of the cells would increase [47]. When PAI-1 is bound to vitronectin it can block the binding of vitronectin to integrin $\alpha_v\beta_3$ which leads to a decrease in migration on the substratum [48]. Binding of PAI-1 to uPA restores binding of vitronectin to integrin $\alpha_v\beta_3$, therefore increasing cell migration on the substratum [48]. PAI-I can regulate both adherence and migration on the cell surface [47, 48]. PAI-1 could favour tumour progression by preventing excessive proteolysis, regulating cell adhesion, and regulating migration on the substratum [10, 47, 48].

Inhibiting different components of the uPAS has become an attractive target for cancer therapeutics. Drugs targeting the uPAS have showed promise *in vitro* and *in vivo* and many have entered clinical trials [36]. For example, WX-UK1, an inhibitor of uPA, has shown promise in phase I and II clinical trials [36]. However, there have also been many drugs that showed promise *in vitro* and *in vivo* but have failed in clinical trials such as surmin, a competitive inhibitor of uPA binding to uPAR [36]. Plasminogen receptors, like uPAR, also localize plasmin generation to the cell surface which is essential for the metastatic role of plasmin [37, 39]. It may be more beneficial to target cell surface plasminogen receptors than uPAR because they are directly involved in the localization of plasminogen activation on the cell surface [39]. Therefore a potential therapeutic target could be the inhibition of pericellular plasminogen activation.

1.6 Matrix Metalloproteinases

Matrix metalloproteinases (MMPs) constitute a family of 23 zinc-dependent endopeptidases known mainly for their involvement in extracellular proteolysis [10]. MMPs play a role in organ development, regulating inflammatory processes, and tissue remodeling [49]. They also play a role in diseases such as rheumatoid arthritis and cancer [49, 50]. MMPs can be placed into two broad structural categories: secreted MMPs and membrane-type MMPs (MT-MMPs) [10]. Most MMPs share three common domains: a pro-domain with a conserved cysteine residue, a catalytic domain containing a zinc ion, and a carboxyl-terminal hemopexin-like domain linked to the catalytic domain with a hinge region [49, 50]. MMPs are synthesized as zymogens, and are kept inactive through a covalent coordination of the zinc ion in the catalytic domain to the conserved cysteine in the pro-domain [50]. MMPs are activated through a mechanism called cysteine switch, during which the cysteine zinc coordination is disturbed either by chemical modification of the cysteine residue or proteolytic removal of the pro-domain [51]. Plasmin is a major protease involved in the removal of the pro-domain and subsequent activation of MMPs [52]. While there are many inhibitors of MMPs such as α_2-macroglobin and α_1-proteinase inhibitor, the main inhibitors of MMPs are tissue inhibitors of metalloproteinases (TIMPs) [49]. TIMPs form reversible 1:1 complexes with active MMPs [49]. MMPs degrade components of the ECM including collagens, proteoglycans, and glycoproteins [53]. MMPs are also involved releasing growth factors embedded in the ECM [53]. Other MMP substrates include cytokines, chemokines, growth factor receptors, tyrosine kinase receptors, and cell adhesion molecules [50, 53].

1.1.2 Involvement of Matrix Metalloproteinases in Cancer

MMPs are upregulated in many cancers and high levels of MMPs are correlated with poorer prognosis [50]. MMPs are expressed in many cells found in the tumour microenvironment including fibroblasts, endothelial cells, and inflammatory cells [49]. MMPs degrade the ECM which leads to cell invasion and metastasis [49]. MMPs are involved in increasing the bioavailability of many growth factors in the tumour microenvironment leading to cell proliferation [49]. MMPs are also involved in the regulation of apoptosis through cleavage of receptors or ligands that are pro-apoptotic [49]. MMPs can activate many inflammatory mediators which can lead to tumour-associated inflammation [49]. MMPs have been found to be highly involved in tumour angiogenesis [49]. Many MMPs have been found to have tumour-suppressing functions as well, such as the production of angiostatin formed through proteolytic cleavage of plasminogen by MMP2, 3, 7, 9, and 12 [35, 53].

MMPs have been implicated in tumour angiogenesis, specifically MMP2, 9, and 14 [53]. Endothelial cells have been found to express MMP2, 3, 7, 14, and 19 as well as TIMP1, and 2 [49]. Mice deficient in MMP2 have reduced tumour angiogenesis [54]. Mice deficient in MMP9 and MMP14 have impaired angiogenesis during development [55, 56]. MMP2 and MMP9 are known as gelatinases since one of their substrates is gelatin, but they can also degrade other substrates such as collagen type IV, laminin, and fibrin [53]. MMP14 is a MT-MMP that can degrade substrates such as collagen types I, II, III, fibrin, and fibronectin [53]. These MMPs could be playing a role in tumour angiogenesis by degrading the vascular basement membrane and ECM [53]. MMP9 can release VEGF from the ECM [49]. MMP9 has been shown to be in a positive feedback

loop with VEGF in RPE cells [29]. MMP3, 7, 9, and 16 can cleave matrix-bound VEGF producing truncated versions that cause vascular dilation of existing vessels, whereas non-truncated VEGF induces vessel sprouting [57]. The angiostatin that MMPs can create from plasminogen can act to inhibit angiogenesis [35, 53]. The effects that MMPs have on angiogenesis are diverse since they can generate pro- and anti-angiogenic effects.

Since MMPs have been associated with multiple cancers there have been many MMP inhibitor drugs made. They have, however, had disappointing results in clinical trials [49]. Many of these drugs lacked specificity toward particular MMPs as many MMPs are structurally similar [53]. Another potential reason for the failure of these drugs could be that they were tested on late-stage tumours that had already metastasized and/or had established vasculature [53]. Since MMPs are implicated in tumour angiogenesis, MMP inhibitor drugs may be more beneficial in treating early-stage tumours to prevent tumour angiogenesis and metastasis [53].

1.7 Coagulation and Fibrinolysis

While the activation of plasmin on the cell surface is involved in cancer amongst other effects, its activation in the blood plays a key role in the fibrinolytic system [41, 43, 58]. Maintaining vascular blood fluidity an essential physiological process [59]. There is a delicate balance between blood clot deposition and removal known as hemostasis that occurs under normal physiological conditions [59]. Normal hemostasis regulates the maintenance of blood fluidity while protecting against excessive bleeding resulting from vascular injury [59]. The coagulation system is responsible for the formation of a fibrin

clot at the site of an injury, whereas the fibrinolytic system is responsible for the degradation of the fibrin clot [59]. Imbalances in hemostasis can lead to the formation of a thrombus that can occlude blood flow leading to a heart attack or stroke or to diseases involving a bleeding tendency, such as hemophillia [58, 60]. There are control mechanisms present in both the coagulation and fibrinoytic systems – as well as between the systems – that act to ensure the hemostatic balance is maintained [60].

Endothelial cells provide a barrier between blood and tissues, and they act to maintain blood fluidity, and protect against vascular injury by producing thromboresistant and vasoprotective molecules [61]. Under normal conditions, the surface of endothelial cells is thromboresistant which ensures that platelets and other blood cells do not adhere [61]. Upon vascular injury platelets adhere to the endothelial cell surface due to the loss of endothelial cell protective molecules and expression of prothrombotic factors and adhesive molecules [61]. Vascular injury can expose ECM components, mainly collagen, to the blood which platelets can come into contact with and adhere to [62]. After platelets adhere to the ECM components platelet activation and aggregation occur [62]. The cycle of platelet adhesion, activation, and aggregation continues and results in the formation of a platelet plug [61, 62].

The platelet plug is the first hemostatic structure; after it forms the coagulation cascade is initiated [59, 63]. The function of the coagulation system is to add to the platelet plug and form a stable fibrin clot at the site of injury to prevent excessive bleeding [58, 63]. Thrombin is the main enzyme produced in the coagulation cascade, and is responsible for the formation of the fibrin clot [63]. The coagulation cascade is further divided into the extrinsic and intrinsic pathways [63]. The extrinsic pathway of

the coagulation cascade produces the thrombin needed for initial fibrin clot formation, while the intrinsic pathway of the coagulation cascade leads to a large burst of thrombin formation within the clot which protects the clot from fibrinolysis (Fig. 1.2) [63, 64].

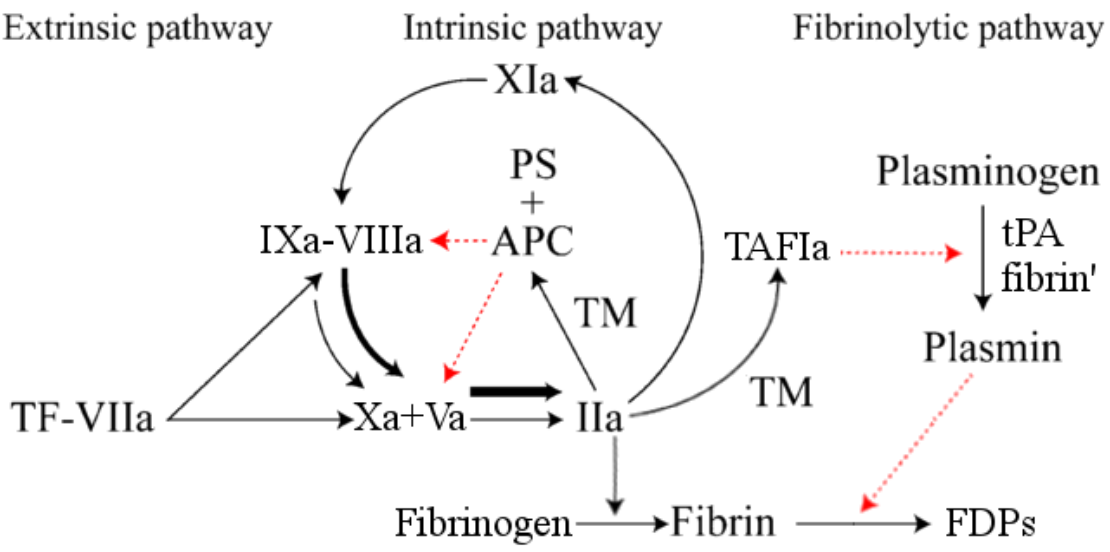

Figure 1.2 Coagulation and fibrinolytic pathways

The coagulation cascade is initiated upon vascular injury in which tissue factor (TF) is exposed to the bloodstream. Initially the extrinsic pathway is activated, by which TF binds to activated factor VII (VIIa). The TF-VIIa complex activates limited quantities of factors X and IX. Activated factor X (Xa) along with its cofactor factor Va activate prothrombin to thrombin (factor IIa) on the surface of activated platelets. IIa converts the soluble zymogen fibrinogen to the insoluble fibrin. The formation of fibrin forms a fibrin clot. IIa can activate factor XI, which activates factor IX. TF-VIIa can also catalyze the production of IXa. IXa along with its cofactor factor VIIIa activate factor X and lead to further production of IIa. The intrinsic pathway makes large amounts of IIa which can consolidate the clot forming a thrombus. The fibrinolytic cascade is initiated after the formation of a thrombus. Initially limited digestion of the fibrin clot occurs by plasminogen converted by tissue-type plasminogen activator to plasmin forming fibrin' which contains carboxyl-terminal lysine residues that make fibrin' an effective cofactor for plasminogen activation thereby mediating positive feedback in the fibrinolytic cascade. Digestion of fibrin into soluble fibrin degradation products (FDPs) dissolves the clot. IIa can bind to the transmembrane cofactor thrombomodulin (TM) to activate protein C and thrombin-activatable fibrinolysis inhibitor (TAFI). Activated protein C (APC) along with its cofactor Protein S can inhibit coagulation by degrading factors Va and VIIIa. TAFIa can remove the carboxyl-terminal lysine residues from fibrin' therefore inhibiting the positive feedback loop in fibrinolysis. (Image adapted from ref. 63).

The initial step in the coagulation cascade involves the expression of membrane bound tissue factor (TF) [65]. TF is not normally exposed to the blot clotting factors under physiological conditions, but when blood enters the interstitium after vascular injury it is exposed to TF [65]. TF recruits circulating factor VIIa and forms a catalytically active complex [63, 66]. The TF-VIIa complex activates limited quantities of factors IX and X to factors IXa and Xa (Fig. 1.2) [66, 67]. Factor Xa is involved in the common pathway while factor IXa is involved in the intrinsic pathway [63]. The extrinsic pathway proceeds with factor Xa along with its cofactor Va and the activated platelet surface forming a complex known as prothombinase which activates prothrombin to thrombin (Fig. 1.2) [66]. Thrombin then cleaves soluble fibrinogen into insoluble fibrin forming a fibrin clot (Fig. 1.2) [66]. The amount of thrombin generated through the extrinsic pathway is relatively small, being only around 5% of the total thrombin generated during coagulation [63]. The TF-VIIa complex is rapidly inactivated by tissue factor pathway inhibitor (TFPI) which results in trace amounts of Xa formation and consequently low amounts of thrombin formation formed through the extrinsic pathway [65]. The small amount of thrombin generated through this pathway is sufficient to form a fibrin clot but cannot stabilize the clot [63, 67]. The majority of thrombin is generated through the intrinsic pathway in order to protect the newly formed fibrin clot [63]. Thrombin generated through the extrinsic pathway can activate factor XI, which can then activate factor IX (Fig. 1.2) [63]. TF-VIIa complex also catalyzes the production of factor IXa (Fig. 1.2) [66, 67]. Factor IXa along with its cofactor VIIIa and an activated platelet surface form a complex known as intrinsic tenase [66]. Tenase activates factor X which can further activate prothrombin to thrombin [66]. This pathway leads to a large

amplification of thrombin generation (Fig. 1.2) [67]. The thrombin generated can activate factors V, VIII, and XIII, platelets, and can convert fibrinogen to fibrin [66]. Activated factor XIII (XIIIa) is a transglutaminase that cross-links fibrin to stabilize the clot [66]. The insoluble fibrin mesh binds to the platelets forming a platelet-fibrin thrombus at the site of the vascular injury [59].

For wound healing and tissue remodeling to occur after vascular injury the formed thrombus must be broken down through fibrinolysis (Fig. 1.2) [67]. tPA can activate plasminogen to plasmin, however this conversion is slow in the absence of a fibrin cofactor, accounting for the localization of fibrinolysis to the thrombus itself (Fig. 1.2) [58]. Plasmin can proteolytically cleave fibrin into soluble fibrin degradation products (FDPs) (Fig. 1.2) [58]. Partial cleavage of fibrin by plasmin generates carboxyl-terminal lysine residues that can bind tPA and plasminogen greatly enhancing the efficiency of tPA activation of plasminogen (Fig. 1.2) [68]. These carboxyl-terminal lysines therefore mediate positive feedback in the fibrinolytic cascade. An additional positive feedback mechanism mediated by carboxyl-terminal lysines in fibrin is acceleration of plasmin-mediated conversion of Glu-plasminogen to Lys-plasminogen [62, 67]. Lys-plasminogen is in an open conformation and is a better substrate for tPA [36]. The serine protease inhibitors α_2-antiplasmin and PAI-1 can downregulate fibrinolysis by irreversibly binding to plasmin and tPA, respectively [58, 64]. Plasmin bound to carboxyl-terminal lysine residues on partially-degraded fibrin is protected from inactivation by α_2-antiplasmin [69]. Therefore, the generation of carboxyl-terminal lysine residues on fibrin is an important regulatory mechanism that promotes fibrinolysis [63].

Within both the coagulation and fibrinolytic systems there are regulatory mechanisms such as the anticoagulant pathway involving protein C and the antifibrinolytic pathway involving thrombin-activatable fibrinolysis inhibitor (TAFI) (Fig. 1.2) [64]. Both of these mechanisms are mediated by the endothelial transmembrane enzyme thrombomodulin (TM) in complex with thrombin [64]. TM binds thombin and prevents it from its procoagulant functions and directs it toward the activation of either protein C or TAFI [64]. When TM concentrations are low the activation of TAFI is favoured, whereas high TM concentrations favour protein C activation [70]. Thrombin bound to TM is both anticoagulant through the activation of protein C and antifibrinolytic through the activation of TAFI [64]. The protein C anticoagulant pathway is an important mechanism for controlling thrombosis [71]. The thrombin-TM complex can activate protein C more than 1000-fold more efficiently than thrombin alone [72]. Once activated protein C (APC) is formed, it along with its cofactor protein S (PS) can proteolytically degrade cofactors Va and VIIIa (Fig. 1.2) [66, 73]. This inhibits the formation of prothrombinase and intrinsic tenase leading to an overall decrease of thrombin production and an overall downregulation of coagulation [66, 73]. The TAFI antifibrinolytic pathway is an important mechanism in regulating the positive feedback loop of the fibrinolytic pathway (Fig. 1.2) [68]. This antifibrinolytic pathway creates a direct molecular link between the coagulation and fibrinolytic pathways since activation of coagulation produces thrombin that can then inhibit fibrinolysis through activation of TAFI [74]. The thrombin-TM complex is the most likely physiological activator of TAFI, with a 1250-fold increase in activation efficiency over thrombin alone [75]. The burst of thrombin generation during the intrinsic coagulation cascade can trigger the activation of

TAFI [68]. TAFIa can cleave carboxyl-terminal lysine and arginine residues from partially degraded fibrin, therefore attenuating the effect of these residues on positive feedback via plasminogen activation, Glu- to Lys-plasminogen conversion, and protection of plasmin from α_2-antiplasmin [62, 76, 77]. Therefore, TAFIa leads to a decrease in plasmin formation and delays the lysis of the fibrin clot [64].

1.8 Thrombomodulin

Thrombomodulin (TM) is transmembrane glycoprotein that plays a role in regulating vascular hemostasis and has recently been linked to cancer. It is mainly found on endothelial cells but is also present in monocytes, platelets, megakaryocytes, chondrocytes, smooth muscle cells, osteoblasts, keratinocytes, astrocytes, and in various tumour cells [78, 79]. In the vasculature, TM concentration is higher within capillaries compared to arteries and veins [78]. TM acts as a cofactor for thrombin in the activation of protein C and TAFI [64].

TM contains 557 amino acids and has a theoretical molecular mass of 75 kDa [80]. TM is usually present in a highly glycosylated form with an apparent molecular mass of 100 kDa [80]. TM contains five domains: an amino-terminal lectin-like domain, six-epidermal growth factor (EGF)-like repeats, a serine-threonine rich domain, a transmembrane domain, and a carboxyl-terminal cytoplasmic tail (Fig. 1.3) [80]. The amino-terminal lectin-like domain makes up the majority of the extracellular component of TM and contains two potential sites for *N*-linked glycosylation [78]. The lectin-like domain plays a role in inflammation, cell proliferation, and cell adhesion [78]. The EGF-

like domains are responsible for activation of protein C and TAFI (Fig. 1.3) [78]. EGF-like repeats 5 and 6 are specifically responsible for thrombin binding (Fig. 1.3) [78]. EGF-like repeats 3-6 are essential for TAFI activation, while EGF-like repeats 4-6 are essential for protein C activation [78]. There are specific residues within the EGF-like domains that are essential for substrate binding, residing in EGF-like repeat 3 for TAFI activation and EGF-like repeat 4 for protein C activation [81, 82]. Mutation to alanine of Val340, Asp341, and Glu343 in EGF-like repeat 3 of TM result in more than a 90% reduction in TAFI activation with marginal loss in protein C activation [82]. Mutation to alanine of Phe376 in EGF-like repeat 4 of TM results in a 90% reduction in protein C activation and retains approximately 80% TAFI activation [81, 82]. Mutation to alanine of Asp349, Glu357, Tyr358, and Gln387 in EGF-like domain 4 of TM results in loss of both TAFI and protein C activation [81, 82]. Mutation of Gln387 to proline results in the greatest loss of both TAFI and protein C activation by abolishing thrombin binding to TM [81, 82]. The serine-threonine rich domain contains four potential sites for *O*-linked glycosylation [78]. The serine-threonine rich domain also supports the attachment of chondroitin sulfate (CS) (Fig. 1.3) [78]. CS is a glycosoaminoglycan with approximately 20 repeating disaccharide units and a trisaccharide terminus [78]. CS is important for the protein C cofactor ability of TM and it acts as a second lower affinity binding site for thrombin [78].

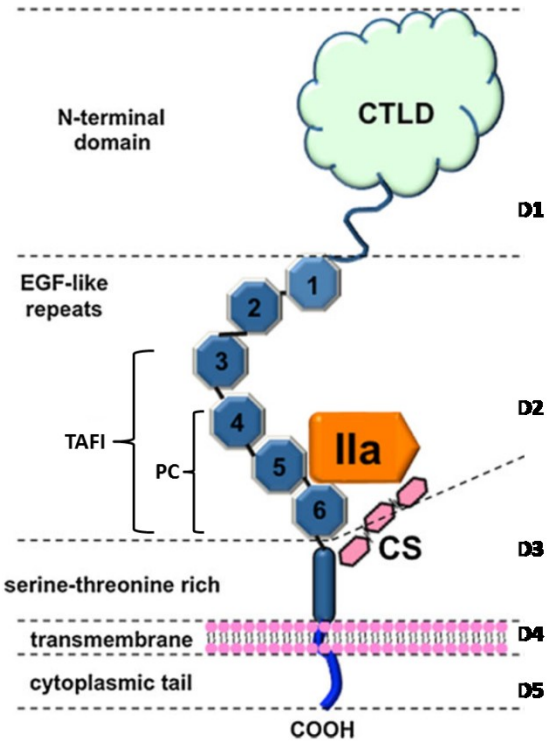

Figure 1.3 Schematic diagram structure of thrombomodulin

Thrombomodulin (TM) contains five domains: amino-terminal lectin-like domain (D1), epidermal growth factor (EGF)-like domain (D2), serine-threonine rich domain (D3), transmembrane domain (D4) and a cytoplasmic tail (D5). The lectin-like domain is involved in cell proliferation, inflammation and adhesion. The EGF-like domain is responsible for substrate activation. EGF-like repeats 5-6 are responsible for thrombin binding (IIa). Activation of thrombin activatable-fibrinolysis inhibitor (TAFI) by the TM-IIa complex is achieved through EGF-like repeats 3-6. Activation of protein C by the TM-IIa complex is achieved through EGF-like repeats 4-6. The serine-threonine rich domain supports the attachment of chondroitin sulfate (CS). (Image adapted from ref. 78)

Many factors have been found to modulate TM cellular expression. TM can be upregulated by factors such as VEGF, thrombin, heat shock, histamines, and statins [78, 83]. Factors that can downregulate TM expression include hypoxia, inflammatory cytokines, TGF-β, and shear stress [78, 83]. There are also regulatory mechanisms of TM which can regulate its cofactor activity towards its substrates. Oxidation of Met388 which is in the linker region between EGF-like repeats 5 and 6 results in an 80% loss in protein C activation by thrombin-TM but does not affect TAFI activation [82, 84]. Concentration of TM is another regulatory mechanism for substrate activation of TM: when TM concentration is high protein C activation is favoured, when TM concentration is low TAFI activation is favoured [70]. Within the capillaries the concentration of TM is high which would lead to protein C activation and reduced coagulation [71, 78].

The main function of TM is being a cofactor to thrombin in the activation of TAFI and protein C, but TM has been shown to play a role in inflammation, cell adhesion, and cancer [78]. The lectin-like domain plays a role in maintaining cell-cell adhesion [85]. The lectin-like domain has also been shown to attenuate inflammation through binding to HMGB1 and Lewis Y antigen [78, 85]. HMGB1 is a pro-inflammatory protein and binding of HMGB1 to the lectin-like domain of TM sequesters HMGB1 from its inflammatory pathway therefore inhibiting inflammation [78, 85]. The Lewis Y antigen is a carbohydrate present in lipopolysaccharide component of the cell wall of gram-negative bacteria that is highly involved in strong inflammatory processes during infection [85]. Binding of the lectin-like domain of TM to the Lewis Y antigen can block the inflammatory reaction [85]. TM can also indirectly inhibit inflammation by sequestering thrombin [78]. Thrombin has many pro-inflammatory functions, of which

many are mediated through activation of protease activated receptors (PARs) [78]. Thrombin bound to TM is prevented from activating PARs therefore the pro-inflammatory effects of thrombin are inhibited [78].

1.1.3 Role of Thrombomodulin in Cancer

Expression of TM has been found to be inversely correlated to tumour malignancy and prognosis [86, 87]. Patients with TM-positive tumours have a significantly higher survival rate than patients with TM-negative tumours [88]. In breast cancer patients low TM is strongly correlated with high relapse rate and poor prognosis [89]. Soluble TM has been shown to reduce invasion and metastasis *in vivo* [90]. TM expression has also been shown to decrease cell proliferation [79, 87]. Zhang *et al.* found that TM decreased tumour cell growth and that it was dependent on TM containing a functional lectin-like domain [79]. Conversely, Horowitz *et al.* found that TM does not affect established tumour growth, rather TM has a role in metastatic potential and survival of newly metastasized tumour cells in the lungs [86, 91]. Horowitz *et al.* also found that TM is an important regulator of metastasis and this was dependent on thrombin binding to TM [91]. They made a strain of mice containing a Q387P mutation "knocked in" to the gene encoding TM, a mutation that leads to a severe reduction in TM cofactor activity toward TAFI and protein C by abolishing thrombin binding [82, 91, 92]. The presence of the Q387P mutation in the mice had no effect on tumour growth but significantly increased metastatic potential and spontaneous metastasis, and increased the probability of a metastatic focus forming from circulating tumour cells [91]. Furthermore,

Horowitz *et al.* performed the same experiments using mice expressing a form of TM lacking the lectin-like domain and did not find significant impact on metastasis [91]. These findings suggest that thrombin binding to TM, not the lectin-like domain of TM, is required for the antimetastatic effects of TM [91].

TM has recently been shown to play a role in angiogenesis. Shi *et al.* reported that recombinant TM containing the six EGF-like repeats and the serine-threonine rich domain (rTMD23) promoted angiogenesis [93]. Kuo *et al.* performed a follow-up to the work of Shi *et al.* and made mutations within the rTMD23 of E357A, R385S, and D400A; these mutations do not allow for the activation of protein C [94]. They found that the mutations of the rTMD23 increased angiogenesis but did not alter the angiogenic potential compared to the non-mutated rTMD23 [94]. Their result suggested that rTMD23 induced angiogenesis in a manner independent of activation of protein C [94]. Kuo *et al.* published another study suggesting that TM could be inhibiting angiogenesis through the lectin-like domain [95]. They found that the lectin-like domain of TM could be inhibiting angiogenesis through interaction with the Lewis Y antigen [95]. The Lewis Y antigen has been shown to increase angiogenesis, therefore the lectin-like domain could inhibit angiogenesis by sequestering the Lewis Y antigen [95]. These studies suggest that TM could be playing both pro- and anti-angiogenic roles and therefore further studies are required to determine the role of TM in angiogenesis.

1.9 Protein C

Protein C is plasma zymogen that is activated by thrombin-TM to form activated protein C (APC) a serine protease involved in inhibiting coagulation [73]. Thrombin can convert protein C into APC, however this conversion is very slow [73]. Binding of thrombin to TM can increase the rate of activation of protein C by thrombin 1000-fold [72]. The endothelial protein C receptor (EPCR), which binds protein C, can increase the rate of activation of protein C by thrombin-TM another 20-fold [71]. EPCR aligns protein C to the thrombin-TM [71]. Once formed, APC can decrease thrombin production by inhibiting both the intrinsic and common coagulation pathways [66, 73]. APC along with its cofactor protein S can degrade factors VIIIa and Va [66]. APC-mediated degradation of FVIIIa also requires inactive factor V as a cofactor [66]. The result of decreasing thrombin production by APC is decreased coagulation as well as enhanced fibrinolysis (*vide infra*) [66]. APC has functions independent of the coagulation pathway including cytoprotective and anti-inflammatory functions [66]. EPCR binds to both protein C and APC with equal affinity [71]. APC bound to EPCR can activate protease-activated receptor 1 (PAR-1) [73]. Activation of PAR-1 by APC can result in cytoprotective effects including anti-apoptotic activities, protection of endothelial cell barrier, anti-inflammatory activities and altered gene expression [96].

1.9.1 Role of Protein C in Cancer

APC may play a role in cancer however there are conflicting reports on whether it is playing an antimetastatic or prometastatic role. Studies have found that APC promotes cancer cell invasion, migration, angiogenesis, DNA synthesis, and proliferation as well as inhibits apoptosis and these effects were due to EPCR-bound APC activation of PAR-1 [97–100]. Conversely, one study found that APC limited cancer cell extravasation through PAR-1 signaling [101]. Another study found that transgenic mice over expressing EPCR reduced metastases in the liver and lung [102]. In contrast, another study found overexpression of EPCR in lung adenocarcinoma cells was prometastatic and silencing EPCR decreased metastasis [103]. Further studies are needed to determine whether APC is playing a prometastatic or antimetastatic role in cancer.

1.10 Thrombin-Activatable Fibrinolysis Inhibitor

Thrombin-Activatable Fibrinolysis Inhibitor (TAFI) is a plasma zymogen that plays a role in attenuating fibrinolysis. TAFI was originally discovered by different groups as carboxypeptidase U, R, and B. Initially, Hendriks *et al.* identified a basic carboxypeptidase in human serum similar to but distinct from the stable basic carboxypeptidase N (CPN) [104]. This carboxypeptidase showed unstable basic carboxypeptidase activity at 37°C, it was therefore named 'unstable' carboxypeptidase (CPU) [104]. Campbell and Okada found an unstable enzyme that exhibited carboxypeptidase activity preferentially towards arginine over lysine residues that was

generated during coagulation and named it carboxypeptidase R (CPR) [105]. Eaton and colleagues found a pro-enzyme contaminant that bound to a plasminogen affinity column when purifying α_2-antiplasmin and named it plasma procarboxypeptidase B (pCPB) because its activated form had similar activity to pancreatic carboxypeptidase B (CPB) [106]. Wang *et al.* determined that pCPB and CPU were the same enzyme [107]. At the same time, Bajzar and coworkers discovered TAFI when trying to solve the conundrum that the anti-coagulant APC appeared to have profibrinolytic activity [108]. It was determined that the profibrinolytic effect of APC was actually an indirect effect through inhibition of thrombin generation by APC which lead to an attenuation of TAFI activation [108, 109]. Bajzar and coworkers also determined that TAFI was the same protein as pCPB [108]. TAFI, CPU, CPR, and CPU were all determined to be the same protein [60, 107, 108].

Plasma TAFI is primarily produced in the liver, but there are extrahepatic sources of TAFI including monocytes, endothelial cells, adipocytes, macrophages, and megakaryocytes [110, 111]. Unpublished data from our laboratory indicate that TAFI is also expressed in breast cancer cells.

The mature TAFI protein has a theoretical molecular mass of 45 kDa and consists of 401 amino acids after the removal of a 22 amino acid signal peptide [60, 68]. However, TAFI is glycosylated and thus the apparent molecular mass of TAFI on SDS-PAGE is 60 kDa [60]. The structure of TAFI consists of an activation peptide containing 92 residues and a catalytic domain containing 309 residues [112]. The activation peptide contains four *N*-linked glycosylation sites at Asn22, Asn51, Asn63, and Asn86 that are always glycosylated [112]. Within the catalytic domain there is a catalytic zinc ion

coordinated by His159, Glu162, and His288 [112]. Cleavage at Arg92 removes the activation peptide resulting in the activation of TAFI (TAFIa) [112]. After removal of the activation peptide, TAFIa has a molecular mass of approximately 35 kDa [113, 114]. There is a dynamic flap with considerable mobility that resides within the catalytic domain of TAFI from residues 296-350 [112]. When the activation peptide is present, the dynamic flap (consisting of coil-helix-coil secondary structure) is stabilized by hydrophobic interactions between Val35 and Leu39 in the activation peptide and Tyr 341 in the dynamic flap [112]. Once the activation peptide is removed the stabilizing interactions are lost and the dynamic flap becomes mobile [112]. An irreversible conformational change occurs over time as a consequence movement of the dynamic flap which disrupts the catalytic site thus inactivating TAFI (TAFIai) [112]. During the irreversible conformational change TAFIa activity is destroyed due to the displacement of the critical residues Tyr341 and Asp348 [112]. Tyr341 is involved in stabilizing interactions and Asp348 is responsible for substrate specificity of TAFI [112]. The irreversible conformational change also exposes a cryptic thrombin cleavage site at Arg302 in TAFIai [112].

TAFI can be activated by cleavage at Arg92 by thrombin, plasmin and, most effectively, by thrombin in complex with TM [75, 106, 109]. Both thrombin and plasmin are relatively weak activators of TAFI and need high concentrations in order to activate TAFI. The thrombin-TM complex increases activation of TAFI 1250-fold over thrombin alone [75]. The large thrombin generation that occurs during the intrinsic coagulation pathway is sufficient to activate TAFI, even in the absence of TM [60].

Glycosaminoglycans, which can be found in the ECM exposed by vascular injury, can increase the rate of plasmin-mediated TAFI activation by 20-fold [115].

TAFIa has no known physiological inhibitors, and therefore its intrinsic thermal instability regulates its inactivation [104, 113]. At 37°C, TAFIa has a half-life of approximately ten minutes [113]. Cleavage by thrombin at Arg302 occurs after inactivation of TAFI, therefore thrombin cleavage is a consequence of TAFIa inactivation and not a cause [60, 112]. Plasmin can cleave TAFI at Arg302, Lys327, and Arg330 [116]. Some of these plasmin cleavage sites are available when TAFI is in the zymogen form, therefore plasmin could cleave the zymogen resulting in a decrease in TAFI activation [60, 116]. APC indirectly inhibits TAFI activation by decreasing thrombin generation [108]. Due to the catalytic zinc ion, TAFI is susceptible to inhibition by chelating agents such as EDTA [68]. There are synthetic TAFIa inhibitors and naturally occurring inhibitors that have been found to inhibit TAFIa [68]. As an example, potato tuber carboxypeptidase inhibitor (PTCI) is a reversible inhibitor of TAFIa [76].

TAFIa plays a role in attenuating fibrinolysis after activation by the thrombin generated through the intrinsic coagulation pathway [68]. Very low concentrations of TAFIa are required to attenuate fibrinolysis; 1 nM (less than 2% of the total plasma concentration of TAFI) was shown to be sufficient to half-maximally inhibit fibrinolysis [75]. TAFIa removes carboxyl-terminal lysine and arginine residues from fibrin partially degraded by plasmin cleavage [64], thereby interfering with several positive feedback mechanisms in the fibrinolytic cascade (*vide supra*). Overall TAFIa attenuates fibrinolysis which ensures consolidation of the fibrin clot [67].

1.10.1 Role of TAFI in Inflammation

TAFIa also plays a role in inflammation by cleaving carboxyl-terminal lysine and arginine residues from inflammatory mediators such as bradykinin (BK), C5a, C3a, and thrombin-cleaved osteopontin (OPN) [77, 117]. BK is an important part of the inflammatory response, as it leads to vascular permeability, vasodilation, as well as the four classic signs of inflammation redness, heat, pain, and swelling [63, 77]. The anaphylatoxins, C3a and C5a, are potent leukocyte chemoattractants [63, 77]. OPN plays a role in cell-matrix interactions, adhesion, and inflammatory responses [77]. OPN is a chemoattractant and it also stimulates cell motility and survival [77]. Thrombin cleavage of OPN results in a carboxyl-terminal arginine residue (OPN-R) [118]. OPN-R appears to increase migration, adhesion, and spreading of various cell types [119]. Thrombin-cleavage of OPN up-regulates the pro-inflammatory properties of OPN while cleavage of OPN-R by TAFIa decreases these pro-inflammatory effects [77]. Experiments using TAFI knockout mice revealed that neutrophil recruitment was enhanced and unexpectedly the mice were protected from liver damage which could potentially be attributed to increased C3a and C5a levels [120]. These results suggest that TAFIa is playing a role in downregulating inflammation.

1.10.2 Role of TAFI in Wound Healing

TAFIa has been shown to play a role in two distinct types of wound healing: cutaneous wounds and colonic anastomoses [121]. The plasminogen activation system plays an important role in wound healing through regulation of ECM remodeling [35]. In

plasminogen knockout mice wound healing is impaired [122] . A study done by te Velde *et al*. showed that TAFI knockout mice had impaired secondary wound healing of cutaneous wounds, and impaired healing of colonic anastomoses [121]. Primary wound healing occurs in sutured wounds, secondary wound healing occurs in unsutured wounds [121]. Secondary wound healing, as opposed to primary wound healing, involves epithelial cell migration toward opposite edges of the wound to cover the wound [121]. The general wound healing process involves tissue exudate and clotted blood forming a scab and the wound is then filled in by granulation tissue beneath the scab [121, 123]. Subsequently, fibroblasts arrive at the wound and begin to make ECM proteins and angiogenesis occurs [121, 123]. Wound healing is completed through re-epithelialization and formation of a collagen scar [121, 123]. During re-epithelialization, as well as formation of granulation tissue, fibrin acts as a provisional matrix [121, 123]. The collagen scar is formed through contraction of the wound after the degradation of the provisional matrix [121]. Wound healing is impaired when the balance between production and degradation of ECM is disrupted [121]. In cutaneous wound healing migration of keratinocytes is important, whereas wound healing of colonic anastomoses depends on angiogenesis and matrix remodeling [121]. Colonic anastomoses are a higher risk wound, where impaired healing can lead to death [121]. During healing of colonic anastomoses proteolytic degradation of the ECM and ECM remodeling must be controlled [121]. The TAFI knockout mice had impaired re-epithelialization of keratinocytes during secondary cutaneous wound healing. However, complete wound healing of the TAFI knockout mice did occur, albeit significantly delayed [121]. Fibrinogen deficient mice showed similar secondary cutaneous wound healing to TAFI

deficient mice, as both had impaired keratinocyte migration [121, 124]. This similarity could indicate absence of TAFI could lead to increased removal of fibrin from the provisional matrix leading to impaired wound healing [121, 123]. During healing of colonic anastomoses, TAFI knockout mice had poorer postsurgical recovery [121]. TAFI knockout mice had decreased anastomotic strength of the healed colon, as well as a higher rate of postsurgical mortality, peritonitis, and bleeding complications [121]. In this type of wound healing, absence of TAFI could lead to increased plasminogen activation leading to increased angiogenesis and matrix remodeling [36, 121]. Healing of colonic anastomoses requires matrix remodeling which involves pericellilar plasminogen activation [35, 121]. Many plasminogen activation components and MMPs reside in the leading edge of migrating cells in wound healing [41, 123]. Crucially, TAFIa has been shown to inhibit plasminogen binding to cell surface receptors by removing carboxyl-terminal lysine residues [76, 125]. These experiments show that TAFI plays a role in wound healing through fibrinolysis and potentially through inhibition of cell surface plasminogen receptors [76, 121, 123].

1.10.3 Role of TAFI in Cancer

TAFI could also be playing a role in cancer. TAFIa has been shown to reduce plasminogen binding to the surface of cells [76]. In hepatocytes, silencing of TAFI led to increased plasmin activity on the cell surface and increased cell proliferation [126]. TAFIa has been shown to remove carboxyl-terminal lysine residues from cell surface plasminogen receptors leading to inhibition of cell migration in TAFI deficient mice

[125]. Reijerkerk *et al.* published a study stating that TAFIa does not affect tumour growth and metastasis in TAFI deficient mice [127]. However, this study used B16 melanoma cells and Lewis lung carcinoma cells which do not support TAFI activation [127]. Higuchi *et al.* found that activation of TAFI by TM in HT1080 fibrosarcoma cells inhibited plasminogen activation and resulted in decreased cell invasion [128]. Atkinson *et al.* found that inhibition of TAFIa leads to increased levels of ECM breakdown due to decreased inhibition of plasminogen activation by TAFIa [129]. Guimarães *et al.* showed that TAFIa can inhibit both endothelial tube formation in a 3D plasma clot matrix and endothelial cell migration [130]. They suggested that the 3D plasma clot matrix served as an *in vitro* model of wound healing angiogenesis since the plasma clot used for endothelial tube formation mimics a thrombus [130]. This study showed that TAFIa controlled wound healing angiogenesis through inhibition of plasminogen activation [130]. Overall these results suggest that TAFI could be playing a role in cancer through inhibition of pericellular plasminogen activation leading to metastasis, and TAFI could be playing a role in tumour angiogenesis since it was shown to play a role in wound healing angiogenesis.

1.11 Research Rationale

The antimetastatic role of TM is well established, however the mechanism of these effects has not yet been determined. The study by Horowitz *et al.* showed that the antimetastatic effects of TM were dependent on its ability to bind thrombin [91]. However this study did not determine which substrate of thrombin-TM, TAFI or protein

C, was responsible for the antimetastatic effects of TM. With regards to the role of protein C in cancer, there are conflicting reports of whether it is playing an antimetastatic or a prometastatic role [97–103]. TAFIa has been shown to inhibit pericellular plasminogen activation through cleavage of carboxyl-terminal lysine residues *in vitro* and *in vivo* [76, 125, 126]. Pericellular plasminogen activation has been shown to be upregulated in cancer and plays a role in metastasis and tumour angiogenesis through degradation of ECM, release of growth factors from ECM, and regulation of MMP activity [36]. Higuchi *et al.* found decreased invasion of HT1080 fibrosarcoma cells due decreased plasminogen activation by TAFIa activated by TM [128]. The study published by Reijerkerk *et al.* stated TAFIa did not affect metastasis and tumour growth in TAFI deficient mice [127]. However, the cell lines used in that study do not support TAFI activation, therefore this study does not clearly rule out a role for TAFI in cancer. TAFIa has been implicated in reducing degradation of ECM, this result could be anti-metastatic in a cancer cell microenvironment [129]. It has also been shown that TAFIa can inhibit wound healing angiogenesis on a plasma clot [130]. Since TAFIa has been shown to inhibit pericellular plasminogen activation and angiogenesis on a plasma clot, TAFIa could be playing a role in inhibition of tumour angiogenesis. Due to the ability of TAFIa to inhibit pericellular plasminogen activation it is hypothesized that TAFI, and not protein C, is responsible for the antimetastatic effects of TM (Fig. 1.4).

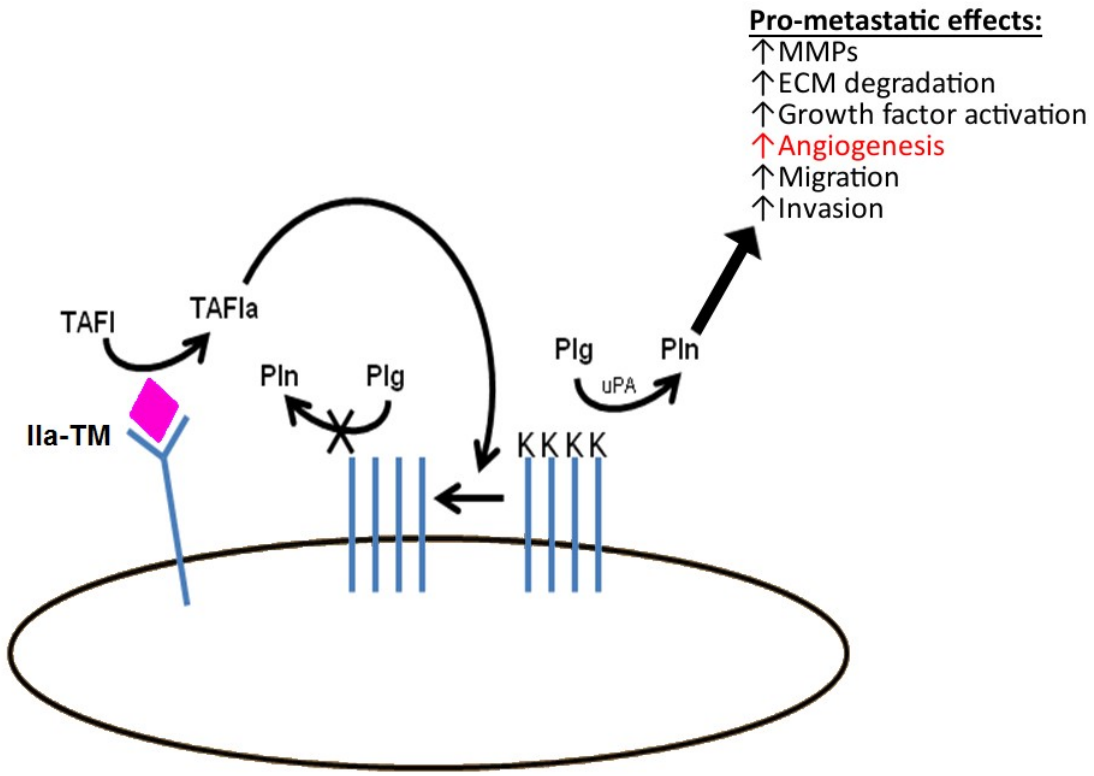

Figure1.4 Hypothesized model of TAFIa inhibition of pericellular plasminogen activation

TAFI is activated by thrombin (IIa) in complex with the transmembrane cofactor thrombomodulin (TM). Activated TAFI (TAFIa) can cleave the carboxyl-terminal lysine (K) residues from cell surface plasminogen receptors. Removal of the carboxyl-terminal lysine residues from cell surface plasminogen receptors results in inhibition of plasminogen (Plg) binding to the cell surface receptor, and consequently a decrease in plasminogen activation. The decrease in pericellular plasminogen activation leads to a decrease in plasmin (Pln) formation. Plasmin plays a role in many metastatic activities including: extracellular matrix (ECM) degradation, release and activation of matrix metalloproteinases (MMPs) from the ECM, and release and activation of growth factors from the ECM. Cell invasion and migration occur as a result of plasmin activation due to the breakdown of ECM surrounding the cell. Plasmin can lead to increased angiogenesis due to increase in growth factors, ECM breakdown, and MMPs. TAFIa inhibits plasmin formation therefore it is hypothesized that TAFIa can inhibit the pro-metastatic effects of plasmin.

1.12 Research Objectives

TAFIa plays a role in inhibiting pericellular plasminogen activation and therefore is hypothesized to inhibit the prometastatic effects of plasmin specifically, for this thesis, those on tumour angiogenesis. In breast cancer patients, low TM is strongly correlated with poor prognosis and high relapse rate [89]. Unpublished data from our laboratory shows that breast cancer cells express TAFI. Endothelial cells have also been shown to express TAFI [110]. Unpublished data from our laboratory also shows that TAFIa inhibits plasminogen activation in breast cancer cells. Therefore endothelial cells and breast cancer cells will be used in the following objectives to determine the role TAFIa plays in tumour angiogenesis. It is hypothesized that TAFIa will inhibit tumour angiogenesis.

The specific objectives to show the role TAFIa plays in tumour angiogenesis are:

1. To inhibit TAFIa activity, with potato tuber carboxypeptidase inhibitor (PTCI), to determine the role of TAFIa in endothelial cell invasion, proliferation, tube formation, ECM proteolysis, MMP mRNA expression and secretion either in cultured endothelial cells alone or in a co-culture system containing both endothelial cells and breast cancer cells

2. To promote TAFI activation using mutant forms of soluble TM with differing substrate activation capability to determine the role of TAFIa in endothelial tube formation and ECM proteolysis either in cultured endothelial cells alone or in a co-culture system containing both endothelial cells and breast cancer cells.

Chapter 2 Materials and Methods

2.1 Cell Lines and Culture

SUM149 and MDA-MB-231 cell lines were a gift from Dr. Lisa Porter (Department of Biological Sciences, University of Windsor, Windsor, ON, Canada), and the HUVEC cell line was purchased from the American Type Culture Collection (ATCC) (Manassas,VA, USA). SUM149 cells were grown in Dulbecco's Modified Eagles Medium (DMEM) (Gibco, Mississauga, ON, Canada) supplemented with 10% fetal bovine serum (FBS) (Gibco), 1% antibiotic/antimycotic (Gibco), 10 μg/mL insulin (Sigma-Aldrich, Oakville, ON, Canada) and 0.5 μg/mL hydrocortisone (Sigma-Aldrich). MDA-MB-231 cells were supplemented with DMEM (Gibco) completed with 10% FBS (Gibco), 1% antibiotic/antimycotic (Gibco). HUVECs were supplemented with Endothelial Cell Basal Medium-2 (EBM-2) (Lonza, Walkerville, MD, USA) completed with 2% FBS (Lonza) and Endothelial Cell Growth Media-2 (EGM-2) SingleQuots Kit (Lonza). HUVECs were used at passage five for all experiments. These cells were maintained at 37°C and 5% CO_2.

2.2 Cloning of rTM EGF3-6 and rTM EGF3-6 mutants

To clone rTM EGF3-6, first the desired mutations, V340A/D341A and F376A, were made in TM within the puc19TM15 vector (ATCC) using the QuikChange II Site-Directed Mutagenesis Kit (Angilent Technologies, Santa Clara, CA, USA), as per the manufacturer's protocol. The primer sequences that were used for the V340A/D341A and

F376A mutations are located in Table 2.1. The wild-type TM and mutated TM in puc19TM15 were cut out using EcoRI and ligated to pcDNA4/*myc*-His A (Invitrogen), which was linearized using EcoRI.

Next, wild-type, V340A/D341A, and F376A TM within pcDNA4/*myc*-His A were used as template DNA in PCR, using Q5 high fidelity polymerase (New England BioLabs, Whitby, ON, Canada), as per the manufacturer's protocol. The primers in Table 2.2 were used to amplify the lectin-like domain and EGF-like repeats 1-6 (hereafter called rTMD12) in wild-type, V340A/D341A, and F376A TM in pcDNA4/*myc*-His A. Both the PCR amplicon and pcDNA4/*myc*-His A were digested with EcoRI and AgeI to insert rTMD12 into pcDNA4/*myc*-His A.

The next step in the process of making rTM EGF3-6 involved removal of the lectin-like domain and EGF1-2 without removal of the signal sequence. Using site-directed mutagenesis EcoRV restriction sites were engineered. The EcoRV sites were engineered downstream of the signal peptide and upstream of EGF3. Introduction of these sites were done simultaneously using the QuikChange II Site-Directed Mutagenesis Kit (Angilent Technologies) with wild-type rTMD12 in pcDNA4/*myc*-His A as the template DNA. The primers used for the introduction of the EcoRV sites using site-directed mutagenesis are located in Table 2.3. Once the sites were introduced, the mutagenesis product was ligated back on itself through digestion with EcoRV which formed rTM EGF3-6.

After rTM EGF3-6 was made, wild-type, V340A/D341A, and F376A rTMD12 in pcDNA4/*myc*-His A were digested with KpnI, this was used as the insert. rTM EGF3-6

was also digested with KpnI, this was used as the vector. The various mutations were inserted into rTM EGF3-6 producing wild-type, V340A/D341A, and F376A rTM EGF3-6[1].

Table 2.1 Primer sequences used for site-directed mutagenesis to make mutations in TM in puc19TM15

Primer name	Sequence (5'→3')
V340A/D341A sense	TAA CTA CGA CCT GGC GGC CGG CGA GTG TGT GG
V340A/D341A anti-sense	CCA CAC ACT CGC CGG CCG CCA GGT CGT AGT TA
F376A sense	CTG CGC CGA GGG CGC CGC GCC CAT TCC C
F376A anti-sense	GGG AAT GGG CGC GGC GCC CTC GGC GCA G

Table 2.2 Primer sequences used to amplify rTMD12

Primer name	Sequence (5'→3')
5' Primer (TM 5' EcoRI)	GAA TTC GGC AGC GCG CAG CGG CAA GAA
3' Primer (EGF3-6 3' AgeI)	ACC GGT ACA GTC GGT GCC AAT GTG GCG

Table 2.3 Primer sequences for site-directed mutagenesis removal of lectin-like domain and EGF1-2 in rTMD12

Primer name	Sequence (5'→3')
Signal Peptide EcoRV sense	CCC CGC ACC CGC AGA TAT CCA GCC GGG TGG CAG C
Signal Peptide EcoRV anti-sense	GCT GCC ACC CGG CTG GAT ATC TGC GGG TGC GGG G
EGF3 EcoRV sense	CTG GCG GCC GAC GAA CAC CGG GAT ATC GAC GTG GAT GAC TGC ATA CTG
EGF3 EcoRV anti-sense	CAG TAT GCA GTC ATC CAC GTC GAT ATC CCG GTG TTG GTC GGC CGC CAG

[1] Cloning of rTM EGF3-6 was completed by Zainab Bazzi under the supervision of Dr. Michael Boffa

2.3 Protein Purification and Quantification

The rTM EGF3-6 mutants were transfected using polyethylenimine (Sigma-Aldrich) into HEK293 cells (ATCC), and stably expressing lines were selected for using 3 mg/mL zeocin (Life Technologies Inc.). The recombinant proteins were purified using His-tag purification. Briefly, binding buffer (50mM NaH_2PO_4, 0.5M NaCl, 1mM β-ME, 5mM imidazole, 10% glycerol, pH 7.9) was passed over a nickel column, then the protein harvest containing the same components as the binding buffer was passed over the column, a wash was completed (binding buffer with 10mM imidazole), and then protein was eluted (binding buffer with 400mM imidazole). The eluted protein was dialyzed in storage buffer (20 mM HEPES, 150 mM NaCl, 10% glycerol, pH 7.9). The dialyzed samples were concentrated with polyethylene glycol (PEG)-20 000 (Sigma), and dialyzed in storage buffer. The purified proteins were checked for purity using a silver stain. Protein concentrations were determined using a Pierce™ BCA Protein Assay Kit (Life Technologies Inc.) according to the manufacturer's instructions. rTM EGF3-6 mutants were stored at -70°C in aliquots until use[2].

2.4 TAFIa Activity Assay

An AAFR assay was used to determine the initial rate of TAFI activation with the rTM EGF3-6 mutants. In a 96-well plate 10 nM of each rTM EGF3-6 mutant was added in triplicate with and without 25 nM of thrombin (IIa) (Haematologic Technologies Inc.,

[2] Production of stable cell lines and some purification of the rTM EGF3-6 proteins were completed by Zainab Bazzi under the supervision of Dr. Michael Boffa.

Essex Junction, VT, USA). Rabbit soluble TM was used as a control (Haematologic Technologies Inc.). All the wells received 5 mM of $CaCl_2$, and 200 nM of TAFI (His-tag purified), and HBST (20 mM HEPES pH 7.4, 150 mM NaCl, 0.01% (v/v) Tween 20) was added to each well to make each reaction up to a final volume of 50 µL. Following the addition of IIa, TAFI was allowed to activate for ten minutes at room temperature. Then 0.24 mM N-(4-Methoxyphenylazoformyl)-Arg-OH · HCL (AAFR) (BaChem, Torrance, CA, USA), and 200 nM D-phenylalanyl-prolyl-arginyl chloromethyl ketone (PPACK) (Calbiochem, Darmstadt, Germany) diluted in HBST was added to each well for a final volume of 100 µL. AAFR is a colorimetric substrate that absorbs strongly at 350 nm. TAFIa, and other enzymes with carboxypeptidase B activity, can cleave the anisylazoformyl moiety from AAFR [131]. The resulting products no longer absorb at 350 nm [131]. PPACK inhibits IIa, and therefore stops the reaction. Absorbance was read at 350 nm for one hour using a SpectraMax Plus384 Absorbance Microplate Reader (Molecular Devices, Sunnyvale, CA, USA).

2.5 Activated Protein C Activity Assay

An S-2366 assay was used to determine the initial rate of protein C activation in the rTM EGF3-6 mutants. In a 96-well plate 10 nM of each rTM EGF3-6 mutant was added in triplicate with and without 25 nM of IIa (Haematologic Technologies Inc.). Rabbit soluble TM was used as a control (Haematologic Technologies Inc.). All the wells received 5 mM of $CaCl_2$, and 100 nM of protein C (Haematologic Technologies Inc), and HBS with 0.1% BSA was added to each well to make each reaction up to a final volume

of 50 µL. Following the addition of IIa, protein C was allowed to activate for 30 minutes at 37°C. Then 200 µM of L-Pyroglutamyl-L-prolyl-L-argininep-Nitroaniline hydrochloride (S-2366) (Chromogenix, Orangeburg NY, USA), and 200 nM PPACK (Calbiochem) diluted in HBS (20 mM HEPES pH 7.4, 150 mM NaCl) with 0.1% BSA was added to each well for a final volume of 100 µL. S-2366 is a colorimetric substrate, which initially does not absorb at 405 nm [132]. Upon cleavage by activated protein C the products of cleaved S-2366 absorb at 405 nm [132]. Absorbance was read at 405 nm for one hour using a SpectraMax Plus384 Absorbance Microplate Reader (Molecular Devices).

2.6 Proliferation Assay

Cell proliferation was determined in HUVECs using the WST-1 assay (Roche Diagnostics, Laval, QC, Canada). WST-1 is a stable tetrazolium salt that can be cleaved to formazan due to the glycolytic production of NAD(P)H in viable cells [133]. This assay measures metabolic activity of viable cells which can be used an index of proliferation. HUVECs were seeded at 10 000 cells/well in a total volume of 100 µL in a 96-well plate in EBM-2 media (Lonza). Cells were treated in quadruplicate with either 50 ng/mL Vascular Endothelial Growth Factor (VEGF) (VEGF-A_{165}, R&D systems, Minneapolis, MN, USA), or 25 µg/mL potato tuber carboxypeptidase inhibitor (PTCI) (Sigma-Aldrich). VEGF was used as a positive control, and PTCI is an inhibitor of TAFIa. Twenty-four hours after treatment, 10 µL of WST-1 was added to each well and incubated for 2 hours at 37°C. The cleavage of WST-1 to formazan by metabolically

active cells can be measured at 450 nm. Using a SpectraMax Plus384 Absorbance Microplate Reader (Molecular Devices) absorbance values were measured at 450 nm.

2.7 Endothelial Cell Invasion Assay

Transwell invasion assays were used to assess the effect of inhibiting TAFIa on endothelial cell invasion. BD Falcon™ Cell culture inserts 8 μm pore size PET track-etched membranes (BD Biosciences, Mississauga, ON, Canada) were coated with 150 μL of 2 mg/mL Cultrex® Basement Membrane Extract without Phenol Red (Trevigen, Gaithersburg, MD, USA) in an 24-well plate for one hour. Cultrex was diluted to 2 mg/mL from a stock solution with serum and supplement free EBM-2 media (Lonza). Following the incubation the inserts were washed thrice with HEPES Buffered Saline Solution (HBSS) (Lonza). In the bottom of each well in the 24-well plate 600 μL of supplement free EBM-2 with 0.2% FBS with and 50 ng/mL VEGF or 25 μg/mL PTCI was added. Coated inserts were placed in the wells and 50 000 HUVECs/well in 100 μL of serum and supplement free EBM-2 media were added into the coated inserts. Cells were allowed to invade into the Cultrex for 20 hours, after which non-invaded cells were removed with a cotton swab, and the invaded cells were fixed in methanol. The invaded cells were stained with 0.25% Crystal Violet (Sigma-Aldrich). The cells in five different fields of view were counted under a 20× objective using an Olympus CKX415F2 Inverted Microscope (Olympus America, Center Valley, PA).

2.8 Tube Formation Assay

2.8.1 HUVEC Tube Formation Assay

HUVECs were grown in T25 flasks to ~80% confluency, washed four times with HBSS (Lonza), and were labelled with 5 µM Cell Tracker™ Orange CMTMR (Life Technologies Inc.) in EBM-2 with 0.75% FBS for one hour at 37°C. The labelled cells were then washed four times with HBSS (Lonza) and incubated in complete EBM-2 for one hour at 37°C. Next, 50 µL of Cultrex (Trevigen) was used to coat a 35 mm glass bottom culture dish (MatTek, Ashland, MA, USA), then the coated dish was incubated for 10 minutes at 37°C to allow the Cultrex to solidify. After incubation with complete media, 20 000 HUVECs in 50 µL of EBM-2 with 0.75% FBS were seeded on top of the solidified Cultrex and were allowed to attach for 40 minutes at 37°C. Subsequently, complete EBM-2 media with 2% Cultrex and treatment (50 ng/mL VEGF, 25 µg/mL PTCI, 10 nM wild-type rTM EGF3-6, 10 nM rTM EGF3-6 V340A/D341A, and/or 10 nM rTM EGF3-6 F376A) was added. The assay was incubated at 37°C for 18 hours to allow formation of tube-like structures [134, 135]. The assay was imaged using an Olympus IX81 confocal microscope (Olympus America, Center Valley PA, USA). Tube formation in eight to ten different fields of view was imaged under a 10× objective. Relative tube length was calculated using ImageJ software by determining total tube length and dividing by total number of tubes and comparing the values to the control.

2.8.2 Co-culture Tube Formation Assay

SUM149 or MDA-MB-231 cells were grown in T25 flasks to ~80% confluency, washed four times with phosphate buffered saline (PBS), and were labelled with 5 μM CellTrace Far Red DDAO-SE (Life Technologies Inc.) in serum free DMEM (Gibco) for one hour at 37°C. The labelled cells were then washed four times with PBS, and incubated in complete DMEM for one hour at 37°C. Next, Cultrex was used to coat a 35mm glass bottom culture dish as previously described in section 2.8.1. After incubation with complete media, breast cancer cells [20 000 SUM149 cells or 7000 MDA-MB-231 cells in 50 μL serum free DMEM] were seeded on top of the solidified Cultrex, and were allowed to attach for 40 minutes at 37°C. Then complete DMEM media with 2% Cultrex was added. The assay was incubated at 37°C for 24 hours, after which the media was aspirated off. Thereafter, 20 000 HUVECs prelabelled with Cell Tracker™ Orange CMTMR (Life Technologies Inc.) were seeded on top of the embedded breast cancer cells using the same procedure as described in 2.8.1. Again treatment included 50 ng/mL VEGF, 25 μg/mL PTCI, 10 nM wild-type rTM EGF3-6, 10 nM rTM EGF3-6 V340A/D341A, and/or 10 nM rTM EGF3-6 F376A. The assay was incubated at 37°C for 18 hours, and was imaged and quantified as previously described in section 2.8.1.

2.9 Proteolysis Assay

2.9.1 HUVEC Proteolysis Assay

Proteoysis of DQ-collagen IV by HUVECs was assessed as previously described [136, 137]. The HUVEC proteolysis assay was set up the same way as the HUVEC tube formation assay in section 2.8.1, except 50 µL of a solution containing 25 µg/ml DQ-collagen IV (Life Technologies Inc.) mixed with Cultrex (Trevigen) was used to coat a 35 mm glass bottom culture dish (MatTek). Again treatment included 50 ng/mL VEGF, 25 µg/mL PTCI, 10 nM wild-type rTM EGF3-6, 10 nM rTM EGF3-6 V340A/D341A, and/or 10 nM rTM EGF3-6 F376A. The assay was incubated at 37°C for 18 hours, and was imaged using an Olympus IX81 confocal microscope (Olympus America). Three to four z-stacks with fourteen 2.5 µm slices were imaged using a 20× objective with a zoom of three. Amount of proteolysis was determined using ImageJ software by calculating total fluorescence of the DQ-collagen type IV divided by HUVEC area.

2.9.2 Co-culture Proteolysis Assay

Proteolysis of DQ-collagen IV by co-cultured HUVECs and breast cancer cells was assessed as previously described [138]. Cultrex mixed with 25 µg/ml DQ-collagen IV was used to coat a 35 mm glass bottom culture dish as previously described in section 2.9.1. Next, breast cancer cells prelabelled with CellTrace Far Red DDAO-SE (Life Technologies Inc.) were seeded on top of the DQ-Collagen type IV-Cultrex mixture seeding the same cell number and using the same procedure as described for the co-

culture tube formation assay in section 2.8.2. Again treatment included 50 ng/mL VEGF, 25 µg/mL PTCI, 10 nM wild-type rTM EGF3-6, 10 nM rTM EGF3-6 V340A/D341A, and/or 10 nM rTM EGF3-6 F376A. The assay was incubated at 37°C for 18 hours, and was imaged as previously described in section 2.9.1. Areas to images were selected by finding areas were HUVEC tubes were in contact with a breast cancer spheroid. Amount of proteolysis was determined using ImageJ software by calculating total fluorescence of the DQ-collagen type IV divided by combined HUVEC and breast cancer cell areas.

2.10 Preparation of HUVEC and SUM149 Conditioned Media Samples

SUM149 cells were seeded into a 6-well plate at 250 000 cells/mL and were either untreated, or treated with 50 ng/mL VEGF or 25 µg/mL PTCI. After 24 hours of incubation with treatment, SUM149 cells were washed thrice with PBS and 1 mL of serum free DMEM was added. HUVECs were seeded into a 6 well plate and were grown to 60% confluency and were either untreated, or treated with 50 ng/mL VEGF or 25 µg/mL PTCI. After 24 hours of incubation with treatment, HUVECs were washed thrice with HBSS (Lonza) and 1 mL of EBM-2 with 0.2% FBS media was added. Both the treated SUM149 cells and HUVECs were serum starved for 24 hours. Then media was collected and centrifuged for 5 minutes at room temperature at 700 *g* to pellet cells [139]. The supernatant was collected and centrifuged for 10 minutes at 4°C at 2000 *g* to remove cell debris [139]. Lysates from both cell types were collected by adding 100 µL of lysis buffer [50 mM Tris-HCl (pH 7.4), 1% Nonidet P-40, 0.25% sodium

deoxycholate, 150 mM NaCl, 1 mM EDTA], shaking on ice for 10 minutes, and centrifuging for 10 minutes at 12000 *g*. Cell lysate concentration was determined using a Pierce™ BCA Protein Assay Kit (Life Technologies Inc.) according to the manufacturer's instructions.

2.11 Treatment of HUVECs with SUM149 Conditioned Media

HUVECs were grown to 60% confluency in a 6-well plate were washed thrice with HBSS (Lonza) and the supernatant from untreated, VEGF, or PTCI treated SUM149 cells as described in 2.10, was mixed 1:1 with complete EBM-2 media and added to the HUVECs. Also, a non-treated HUVEC well was seeded as a control. After 24 hours of incubation with SUM149 conditioned media (CM) the HUVECs were washed thrice with HBSS and placed in EBM-2 media with 0.2% FBS. Twenty-four hours after incubation in EBM-2 media with 0.2% FBS, the supernatant and lysate were collected, and lysate concentration was determined as previously described in section 2.10.

2.12 Gelatin Zymography

MMP2 and MMP9 enzymatic activities in SUM149, HUVEC, and HUVEC treated with SUM149-CM media samples were determined by SDS-PAGE gelatin zymography as described by Mohamed *et al.* [139]. Samples were mixed with 2X SDS sample buffer and were loaded equally (20 µg/lane SUM149 samples, 6 µg/lane HUVEC samples) without heating or reducing, and electrophoresed in 10% SDS-PAGE

containing 1% gelatin (w/v) at 125 V for 2.5 hours at 4°C. Human recombinant MMP2 (5 ng) and MMP9 (2.5 ng) (R&D Systems) were also loaded as positive controls. After electrophoresis, gels were incubated twice in renaturing buffer (2.5% Triton X-100) for 15 minutes with gentle shaking at room temperature. Thereafter, gels were washed twice with water for 15 minutes with gentle shaking at room temperature. Gels were then placed in developing buffer (50 mM Tris-HCl pH 7.8, 5 mM $CaCl_2$, 0.05% Brij 35) and incubated with gentle shaking overnight at 37°C. Subsequently, gels were stained for one hour in Coomassie brilliant blue R-250 (50% methanol, 10% acetic acid, 40% water, 0.5% Coomassie brilliant blue R-250), and destained (50% methanol, 10% acetic acid, 40% water) until clear bands of proteolytic activity appeared. Relative proteolytic activity of the samples was determined by densitometry using FluoroChem® Q imaging system software (Alpha Innotech Corporation, Santa Clara, CA, USA).

2.13 RNA Extraction

Total RNA was extracted from SUM149, HUVEC, and HUVECs treated with SUM149-CM cells using RNeasy Mini Kit (Qiagen, Toronto, ON, Canada) as per manufacturer's protocol. RNA concentrations were measured using a NanoDrop 2000 UV-Vis Spectrophotometer (Thermo Scientific, Wilmington, DE, USA).

2.14 Quantitative Real Time PCR

qRT-PCR was carried out using iTaq Universal SYBR Green One-Step Kit (BioRad, Mississauga, ON, Canada) as per the manufacturer's protocol on a BioRad CFX96 Real-Time System to determine relative amounts of MMP2 and MMP9 mRNA in VEGF or PTCI treated HUVECs, SUM149 cells, and HUVECs treated with SUM149-CM. 300 ng of RNA was used in each qRT-PCR experiment. The primer sequences that were used can be found in Table 2.4, primers were constructed as per Wang *et al* [140]. Thermocycling conditions used for all reactions were: 50°C for 10 minutes, 95°C for 1 minute, 40 cycles of 95°C for 12 seconds and 60°C for 30 seconds. Also, no reverse transcriptase controls and a no template control were run as negative controls to ensure there was no contamination of the RNA samples with genomic DNA, or contamination of the reagents, respectively. Relative mRNA expression as compared to the control was calculated using the $2^{-\Delta\Delta CT}$ method [141].

Table 2.4 Primer sequences used for qRT-PCR

Primer Name	Sequence (5'→3')
MMP2 Forward	CAG GGA ATG AGT ACT GGG TCT ATT
MMP2 Reverse	ACTCCAGTTAAAGGCAGCATCTAC
MMP9 Forward	AATCTC TTCTAGAGACTGGGAAGGAG
MMP9 Reverse	AGCTGATTGACTAAA GTA GCT GGA
GAPDH Forward	AGA GAG AGG CCC TCA GTT GCT
GAPDH Reverse	TTG TGA GGG AGA TGC TCA GTG T

2.15 Statistical Analysis

Results are expressed as a mean ± SEM from at least three independent experiments. Statistical analysis was performed with IBM SPSS Statistics V22.0 software using one-way ANOVA test with post-hoc Tukey HSD. $p<0.05$ was considered significant.

Chapter 3 Results

3.1 Inhibition of TAFIa increases endothelial cell proliferation

One of the main steps in angiogenesis involves proliferation of endothelial cells in response to an angiogenic stimulus [8, 9]. To assess the role that TAFIa plays in endothelial cell proliferation, potato tuber carboxypeptidase inhibitor (PTCI) was used to inhibit TAFIa. PTCI is a small 39-residue protein purified from potatoes that binds tightly to and inhibits both the carboxypeptidase A and B family of proteases [142, 143]. Even though PTCI can inhibit other proteases, in this system only TAFIa is present. PTCI specifically inhibits TAFIa, and has no effect on the TAFI zymogen [144]. PTCI reversibly binds to TAFIa [68]. Human umbilical vein endothelial cells (HUVECs) were treated with either PTCI or VEGF. After incubation with the treatment, proliferation was quantified using the WST-1 assay. WST-1 is a tetrazolium salt that can be cleaved to formazan through a bioreduction mechanism that is dependent on the glycolytic production of NAD(P)H in viable cells [133]. The production of formazan can be quantified, and is a measure of metabolically active cells which can be used as an index of proliferation. VEGF was used as a positive control since it is the key mediator of angiogenesis [21]. Inhibition of TAFIa by PTCI significantly increased endothelial cell proliferation, 1.3-fold increase compared to control (Fig. 3.1). Inhibition of TAFIa using PTCI resulted in same increase in cell proliferation compared to control as VEGF (Fig. 3.1). This result suggests that TAFIa inhibits endothelial cell proliferation, although further experiments will need to be completed to confirm proliferation is being affected such as flow cytometry.

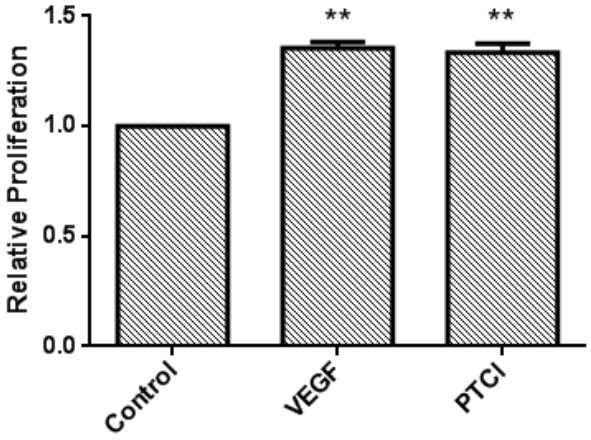

Figure 3.1 Inhibition of TAFIa increases proliferation of endothelial cells
Effect of inhibiting TAFIa with PTCI on HUVEC proliferation determined by WST-1 proliferation assay, measured by absorbance at 450 nm. HUVECs were treated for 24 hours with 50 ng/mL VEGF or 25 µg/mL PTCI. Significantly increased production of formazan, therefore increased metabolically active cells, was observed by both VEGF and PTCI treatment of HUVECs represented relative to the control. The amount of metabolically active cells can be a measure of cell proliferation. Values are expressed as mean ± SEM from 5-6 independent experiments performed in quadruplicate. ** $p < 0.01$ versus control.

3.2 Inhibition of TAFIa increases endothelial cell invasion

For angiogenesis to occur, endothelial cells must locally degrade the vascular basement membrane and invade into the surrounding stroma [8, 9]. Transwell inserts coated in Cultrex can mimic the basement membrane endothelial cells need to invade through during angiogenesis. HUVECs were seeded in the top chamber of a Cultrex coated transwell insert, and either VEGF or the TAFIa inhibitor PTCI were added to the lower chamber. PTCI significantly increased invasion of HUVECs (Fig. 3.2B). PTCI increased invasion of HUVECs 4.6-fold relative to the control, while the positive control VEGF increased invasion of HUVECs 6-fold relative to the control (Fig. 3.2B). This result suggests that TAFIa could decrease endothelial cell invasion.

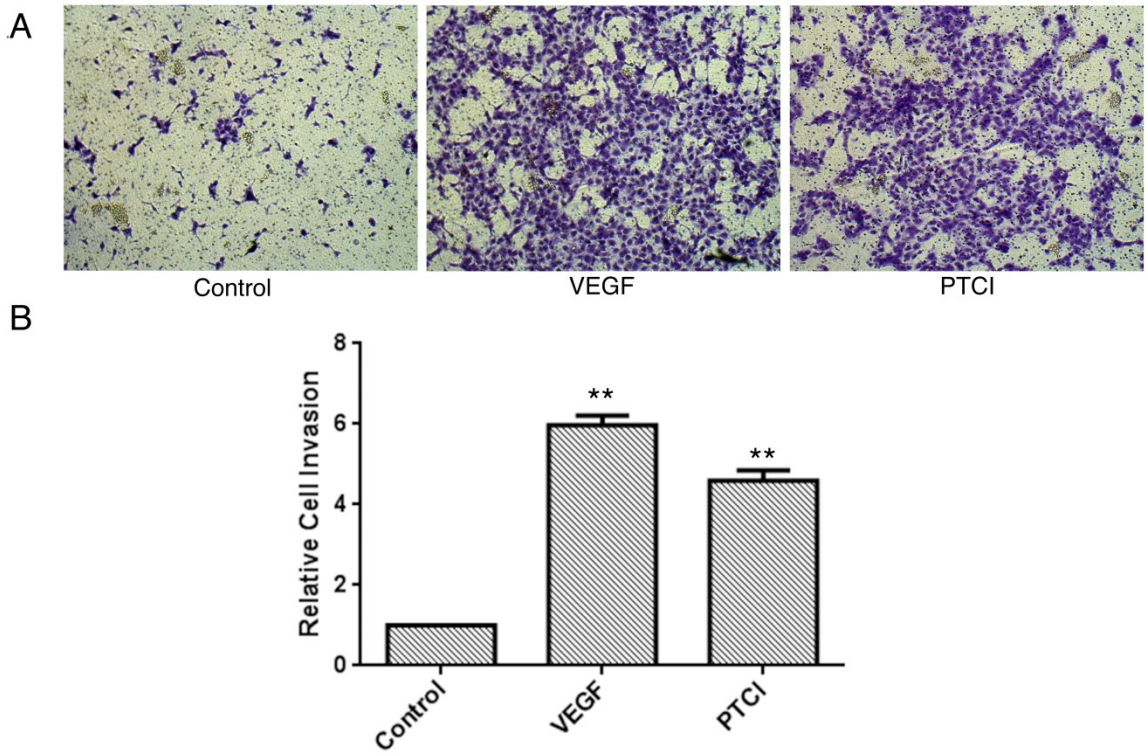

Figure 3.2 Inhibition of TAFIa increases endothelial cell invasion

Effect of inhibition of TAFIa with PTCI on endothelial cell invasion. **(A)** HUVECs were added to a transwell chamber coated with Cultrex, either 50 ng/mL VEGF or 25 µg/mL PTCI were added to the bottom chamber. Cells were allowed to invade for 20 hours after which cells were fixed, stained and imaged. Images above were obtained at 4× magnification. **(B)** Quantification of HUVEC invasion. Cells were counted from 5 different fields of view at 20× magnification, and cell numbers expressed relative to control. Both VEGF and PTCI significantly increased invasion of HUVECs. Values are expressed as mean ± SEM from four independent experiments. ** $p < 0.01$ verses control.

3.3 Inhibition of TAFIa increases tube formation in endothelial cells and in co-culture systems containing endothelial and breast cancer cells

Another aspect of angiogenesis is the formation of tube-like structures [8]. Previous studies have shown that inhibition of TAFIa increases endothelial tube formation in a 3D plasma clot matrix [130]. This result demonstrated a role for TAFI in wound healing angiogenesis [130], however, the role of TAFI endothelial tube formation in regards to tumour angiogenesis has yet to be studied. The role of TAFIa on angiogenesis was assessed using a plasma clot which consisted of a fibrin matrix as the ECM [130]. Studies have not been conducted determining a role for TAFIa on tube formation on reconstituted basement membrane as the ECM. An endothelial tube formation assay was used to determine the effect on tube formation when TAFIa was inhibited. HUVECs were seeded on top of reconstituted basement membrane (Cultrex), and were treated with either VEGF, as a positive control, or the TAFIa inhibitor PTCI. HUVECs formed capillary tube-like structures on Cultrex (Fig. 3.3A). The formation of tube-like structures on Cultrex represents a process of attachment, migration, and differentiation of endothelial cells into tube-like structures in a manner that mimics the *in vivo* process of tube formation [135, 145]. PTCI significantly increased relative tube length (1.3-fold) compared to the control (Fig. 3.3B). PTCI increased relative tube length similarly to VEGF (Fig. 3.3B).

The effect of inhibition of TAFIa on endothelial tube formation was also completed with co-culture systems consisting of HUVECs and either SUM149 cells (Fig. 3.4A) or MDA-MB-231 cells (Fig. 3.5A), both of which are breast cancer cell lines. The

breast cancer cells form spheroid structures on top of the Cultrex, while the endothelial cells form tube-like structures. These co-culture systems function to mimic a tumour microenvironment. The tumour cell microenvironment consists of cancer cells as well as stromal cells, such as endothelial cells [49]. There is a dynamic interplay between cancer cells and endothelial cells [49]. Both the endothelial cells [110] and the breast cancer cells could be a source of TAFI (unpublished data from our laboratory).Therefore co-culture systems containing endothelial cells and breast cancer cells were used to look the effect of inhibition of TAFIa on endothelial tube formation by both endothelial and breast cancer cells in the same environment. Interaction between HUVECs and breast cancer cells can be seen in merge images combining differential interference contrast (DIC), HUVEC fluorescence, and breast cancer cell fluorescence images (Fig. 3.4A & Fig. 3.5A). The co-culture systems were treated with either VEGF or PTCI. The co-culture systems produced nearly identical results between the two breast cancer cell lines used. PTCI significantly increased relative tube length compared to the control with a 1.4-fold increase in both the SUM149 and HUVEC co-culture (Fig. 3.4B), and in the MDA-MB-231 and HUVEC co-culture (Fig. 3.5B). PTCI treatment increased relative tube length similar to treatment with VEGF in both co-culture systems (Fig. 3.4B & Fig. 3.5B).

Overall these results suggest that TAFIa could decrease endothelial tube formation in both endothelial cells in isolation and in and co-culture systems containing endothelial cells and breast cancer cells.

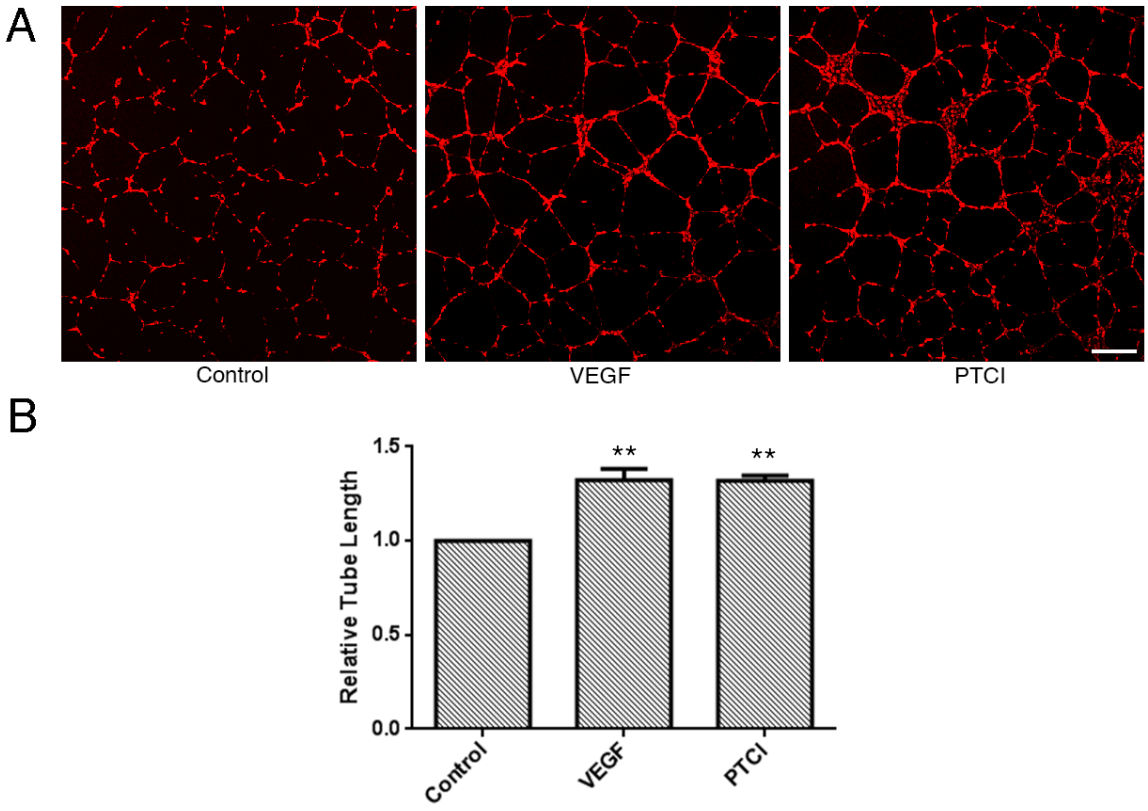

Figure 3.3 Inhibition of TAFIa increases endothelial tube formation

Effect of inhibition of TAFIa with PTCI on tube formation of endothelial cells. **(A)** HUVECs labelled with Cell Tracker Orange (red) were seeded on top of Cultrex in a 35 mm glass bottom culture dish and treated with either 50 ng/mL VEGF or 25 µg/mL PTCI. Cells were imaged 18 hours after seeding HUVECs using confocal microscopy. Images above were obtained at 40× magnification. Scale bar, 400 µm. **(B)** Quantification of endothelial tube formation. To quantify tube formation 8-10 images were obtained at 100× magnification. Tube length was determined by measuring total tube length divided by total tube number, and is expressed relative to that in the control untreated cells. Treatment with either VEGF or PTCI significantly increased relative tube length of HUVECs. Values are expressed as mean ± SEM from six independent experiments. ** $p < 0.01$ verses control.

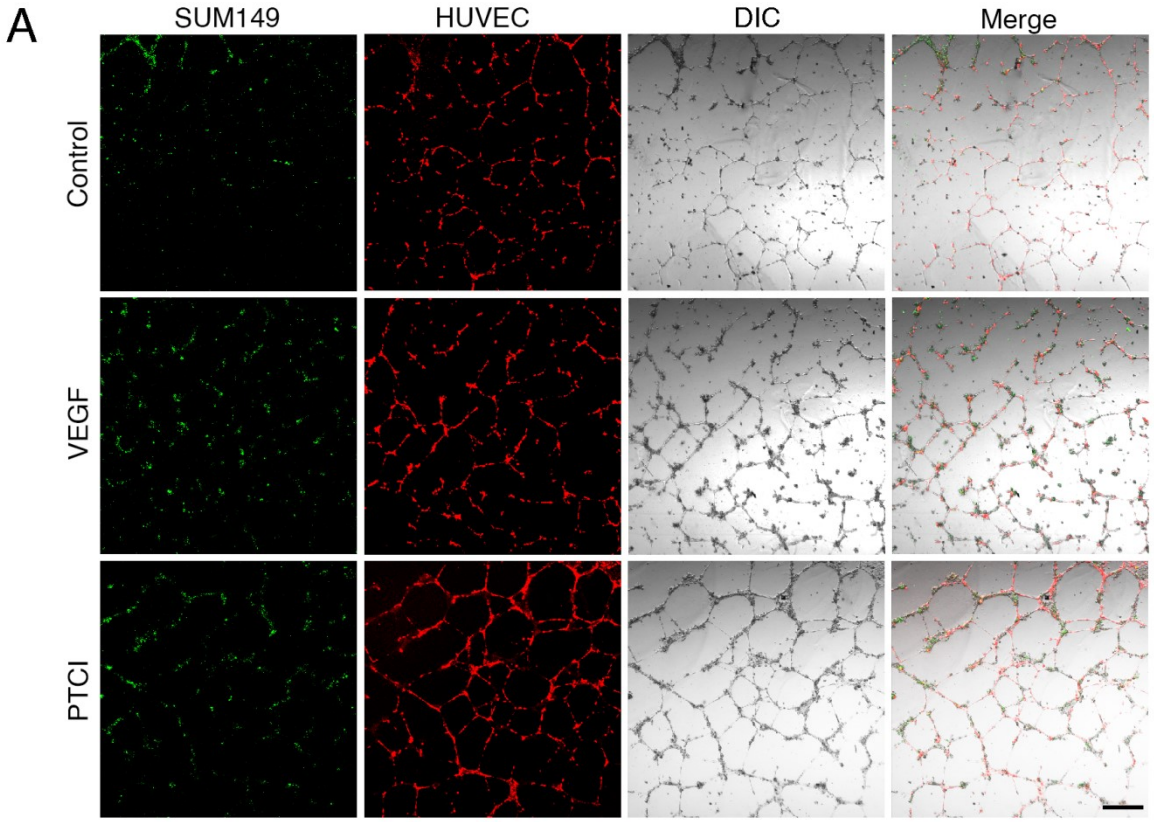
A
SUM149
HUVEC
DIC
Merge
Control
VEGF
PTCI

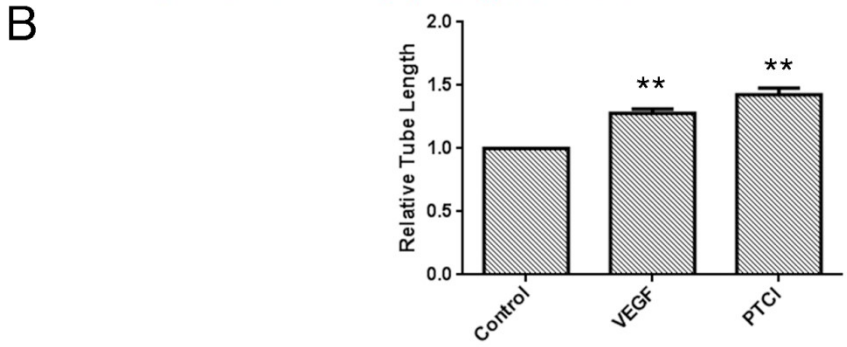
B
Relative Tube Length
2.0
1.5
1.0
0.5
0.0
**
**
Control
VEGF
PTCI

Figure 3.4 Inhibition of TAFIa increases endothelial tube formation in a co-culture system containing HUVECs and SUM149 cells

Effect of inhibition of TAFIa with PTCI on tube formation of endothelial cells co-cultured with SUM149 breast cancer cells. **(A)** SUM149 cells labelled with Cell Trace Far Red (green) were seeded on top of Cultrex in a 35 mm glass bottom culture dish. After 24 hours HUVECs labelled with Cell Tracker Orange (red) were seeded on top of the SUM149 cells and Cultrex. The co-cultures were treated with either 50 ng/mL VEGF or 25 μg/mL PTCI. Cells were imaged 18 hours after HUVECs were seeded using confocal microscopy. Images above were obtained at 40× magnification. Scale bar, 500 μm. **(B)** Quantification of endothelial tube formation. To quantify tube formation 8-10 images were obtained at 100× magnification. Tube length was determined by measuring total tube length divided by total tube number, and is expressed relative to that in the control untreated cells. Treatment with either VEGF or PTCI significantly increased relative tube length of HUVECs. Values are expressed as mean ± SEM from six independent experiments. ** $p < 0.01$ verses control.

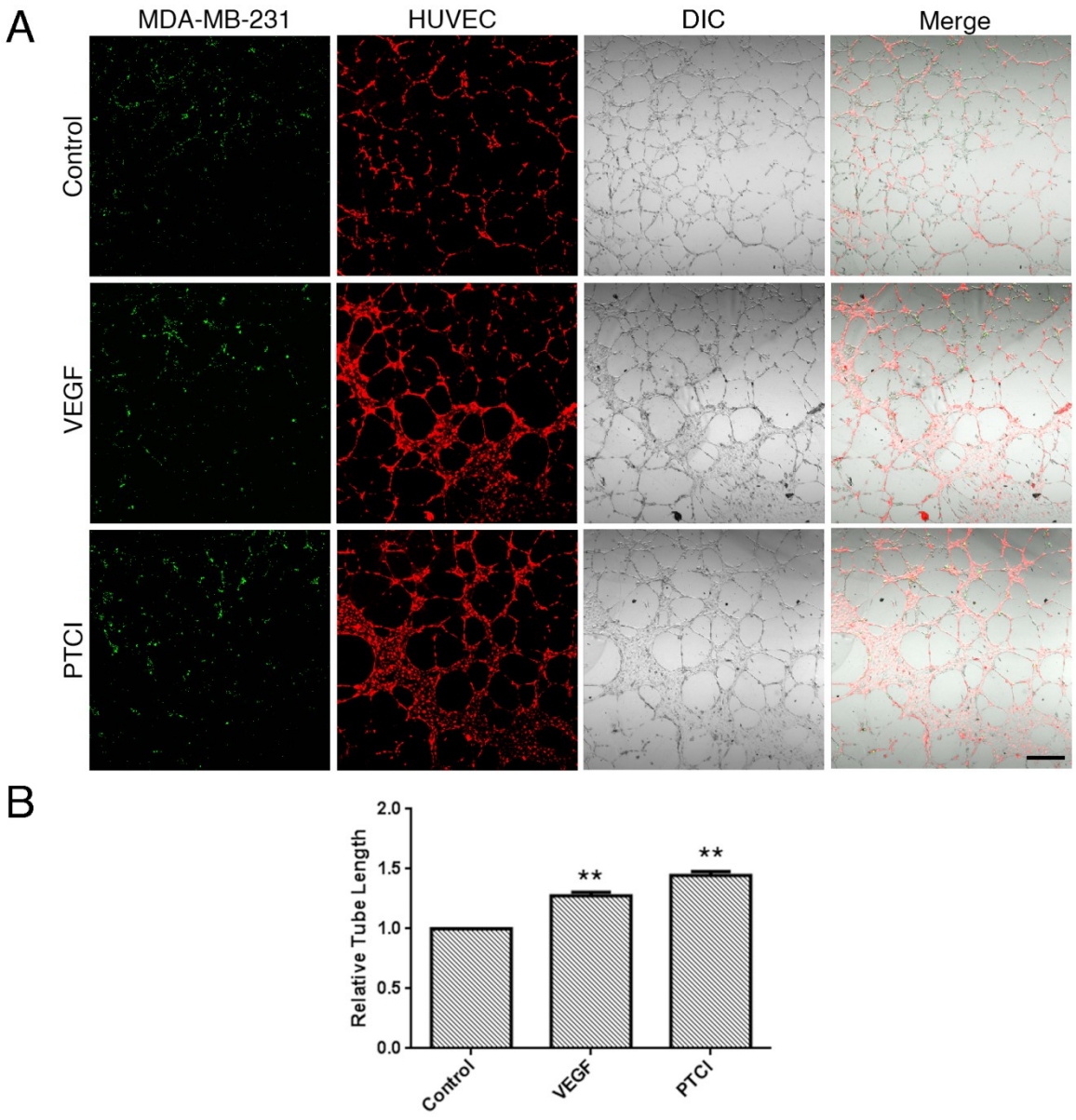
A
MDA-MB-231
HUVEC
DIC
Merge
Control
VEGF
PTCI
B
Relative Tube Length
2.0
1.5
1.0
0.5
0.0
**
**
Control
VEGF
PTCI

Figure 3.5 Inhibition of TAFIa increases endothelial tube formation in a co-culture system containing HUVECs and MDA-MB-231 cells

Effect of inhibition of TAFIa with PTCI on tube formation of endothelial cells co-cultured with MDA-MB-231 breast cancer cells. **(A)** MDA-MB-231 cells labelled with Cell Trace Far Red (green) were seeded on top of Cultrex in a 35 mm glass bottom culture dish. After 24 hours HUVECs labelled with Cell Tracker Orange (red) were seeded on top of the MDA-MB-231 cells and Cultrex. The co-cultures were treated with either 50 ng/mL VEGF or 25 μg/mL PTCI. Cells were imaged 18 hours after HUVECs were seeded using confocal microscopy. Images above were obtained at 40× magnification. Scale bar, 500 μm. **(B)** Quantification of endothelial tube formation. To quantify tube formation 8-10 images were obtained at 100× magnification. Tube length was determined by measuring total tube length divided by total tube number, and is expressed relative to that in the control untreated cells. Treatment with either VEGF or PTCI significantly increased relative tube length of HUVECs. Values are expressed as mean ± SEM from six independent experiments. ** $p < 0.01$ verses control.

3.4 Inhibition of TAFIa increases proteolysis of DQ-collagen IV by endothelial cells and by co-cultured endothelial and breast cancer cells

Degradation of the ECM is an important aspect of angiogenesis. One of the initial steps of angiogenesis involves degradation of vascular ECM and basement membrane [8, 9]. Pericellular plasminogen activation has been implicated in angiogenesis and metastasis though regulation of MMP activity, release of growth factors from the ECM, and degradation of the ECM [36]. VEGF has been shown to upregulate components of the plasminogen activation system in the leading edge of migrating endothelial cells [10, 27, 45]. Moreover, tube formation has been shown to spatially correlate to ECM proteolysis *in vitro* [146]. TAFIa has been shown to inhibit pericellular plasminogen activation *in vitro* and *in vivo* [76, 125, 126]. Therefore, we wanted to determine the effect of TAFIa on proteolysis of DQ-collagen IV, the most abundant type of collagen found in the basement membrane [147], by endothelial cells. HUVECs were seeded on top of Cultrex mixed with DQ-collagen IV, and were treated with either VEGF or PTCI (Fig. 3.6A). Once DQ-collagen IV, an initially quenched fluorescent substrate, is cleaved by proteases DQ-collagen IV degradation products are produced (green) (Fig. 3.6A). Degradation products of DQ-collagen IV were localized predominantly intracellularly (Fig. 3.6A), although treatment with VEGF did increase pericellular (outside the cell or on the cell membrane [146]) localization of DQ-collagen IV degradation products (Fig. 3.6A). Treatment of HUVECs with PTCI significantly increased proteolysis of DQ-collagen IV, 2-fold relative to the control (Fig. 3.6B).

Within the tumour cell microenvironment, consisting of cancer cells and stromal cells, there is a dynamic interplay between cancer cells and stromal cells, such as endothelial cells [49]. Degradation of the ECM of endothelial cells can lead to metastasis of tumour cells [19]. Therefore co-culture systems containing endothelial cells and breast cancer cells were used to look the effect of inhibition of TAFIa on proteolysis of DQ-collagen IV by both endothelial and breast cancer cells in the same environment. HUVECs co-cultured with SUM149 cells (Fig. 3.7A) or MDA-MB-231 cells (Fig. 3.8A) were treated with PTCI or VEGF. In both co-culture systems there was a mix of intracellular and pericellular proteolysis (Fig. 3.7A & Fig. 3.8A). The co-culture system containing HUVECs and MDA-MB-231 cells exhibited predominately pericellular proteolysis (Fig. 3.8A). In both co-culture systems treatment with VEGF or PTCI increased both pericellular and intracellular proteolysis as compared to the control (Fig. 3.7A & Fig. 3.8A). PTCI significantly increased proteolysis of DQ-collagen IV in the co-culture system containing both HUVECs and SUM149 cells, 1.6-fold compared to the control (Fig. 3.7B). In the co-culture system containing HUVECs and MDA-MB-231 cells, PTCI also significantly increased proteolysis of DQ-collagen IV by the co-cultured cells, 1.5-fold as compared to the control (Fig. 3.8B). In both co-culture systems, treatment with PTCI increased proteolysis of DQ-collagen IV similarly to the positive control VEGF (Fig. 3.7B & Fig. 3.8B).

Taken together these results suggest that TAFIa could be playing a role in inhibiting ECM proteolysis in both endothelial cells, as well as in a tumour cell microenvironment containing both endothelial and breast cancer cells.

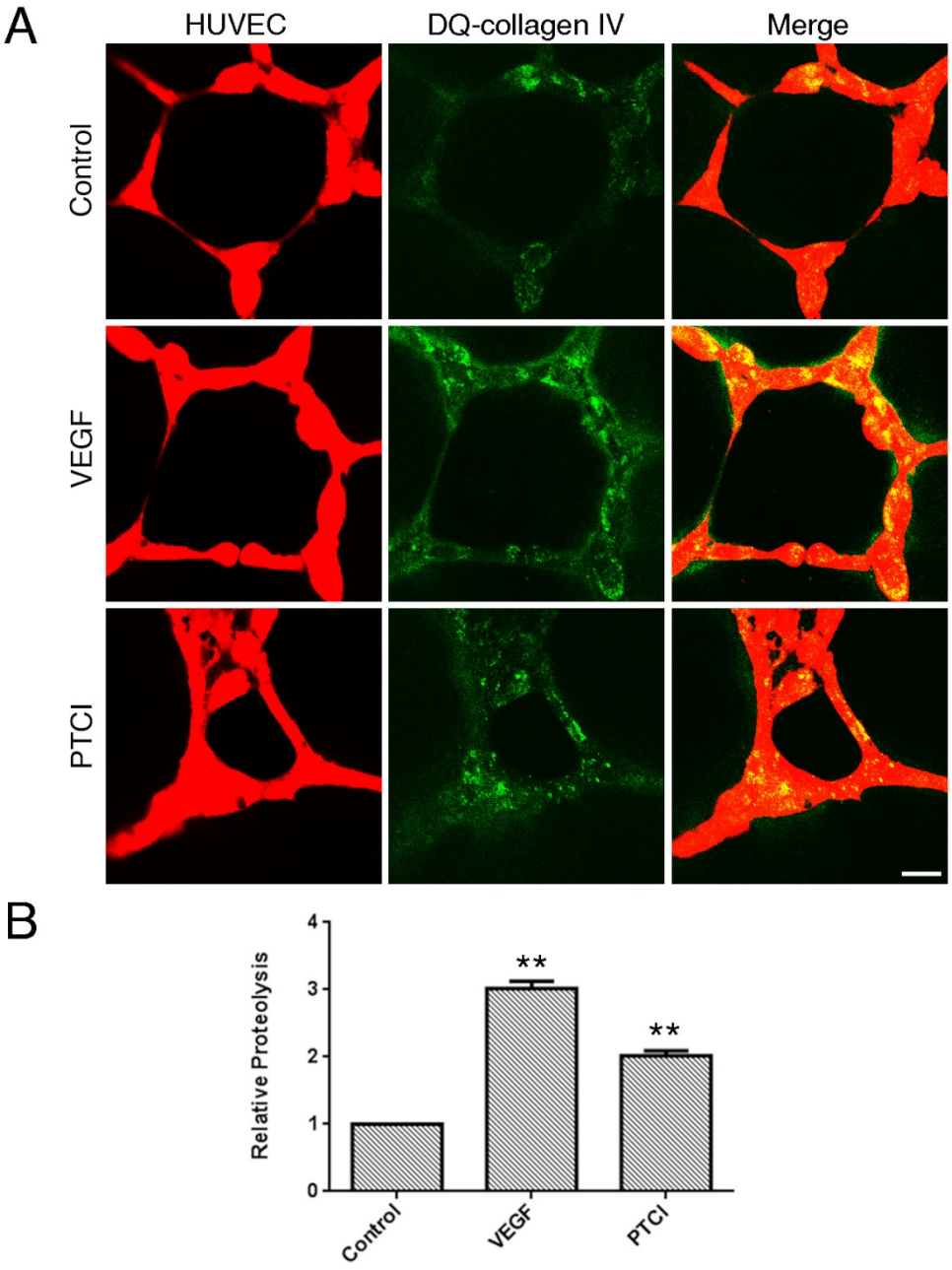
A
HUVEC
DQ-collagen IV
Merge
Control
VEGF
PTCI
B
Relative Proteolysis
4
3
2
1
0
**
**
Control
VEGF
PTCI

Figure 3.6 Inhibition of TAFIa increases proteolysis of DQ-collagen IV by endothelial cells

Effect of inhibition of TAFIa with PTCI on proteolysis of DQ-collagen IV by endothelial cells. **(A)** HUVECs labelled with Cell Tracker Orange (red) were seeded on top of Cultrex mixed with DQ-collagen IV in a 35 mm glass bottom culture dish and treated with either 50 ng/mL VEGF or 25 μg/mL PTCI. Cells were imaged 18 hours after seeding HUVECs using confocal microscopy. DQ-collagen IV cleavage products (green) were present predominantly intracellularly. Merge images show intracellular (yellow) and pericellular proteolysis (green). Images were obtained at 600× magnification. Representative images from the equatorial plane of a Z-stack are shown. Scale bar, 30 μm. **(B)** Quantification of proteolysis of DQ-collagen IV. To quantify proteolysis three equatorial planes from 3-4 different images from one experiment were quantified. Total integrated intensity of DQ-collagen IV florescence divided by total HUVEC area was calculated and expressed relative to the control. Treatment with either VEGF or PTCI significantly increased proteolysis of DQ-collagen IV by HUVECs. Values are expressed as mean ± SEM from 3-5 independent experiments. ** $p < 0.01$ verses control.

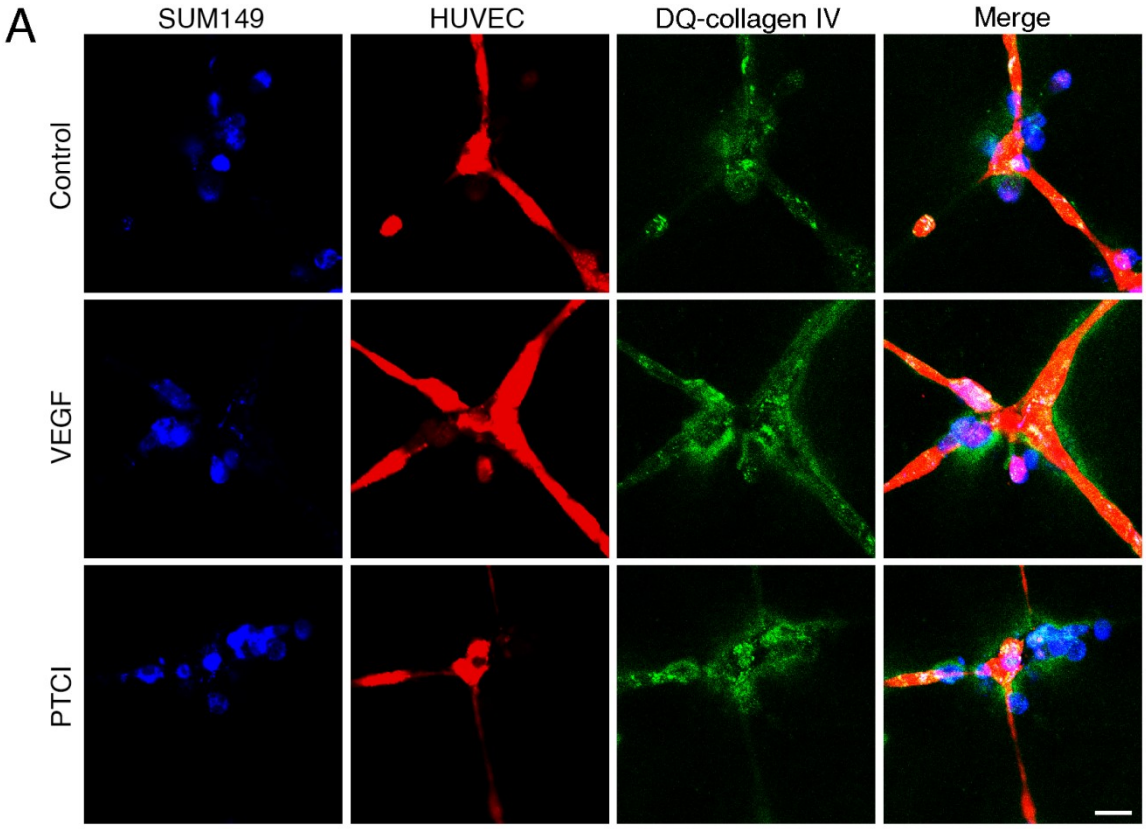
A
SUM149
HUVEC
DQ-collagen IV
Merge
Control
VEGF
PTCI

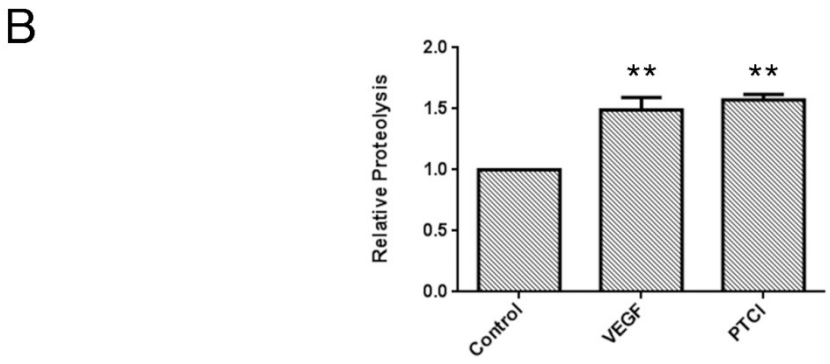
B
Relative Proteolysis
2.0
1.5
1.0
0.5
0.0
**
**
Control
VEGF
PTCI

Figure 3.7 Inhibition of TAFIa increases DQ-collagen IV proteolysis by co-cultured HUVECs and SUM149 cells

Effect of inhibition of TAFIa with PTCI on DQ-collagen proteolysis by co-cultured HUVEC and SUM149 cells. **(A)** SUM149 cells labelled with Cell Trace Far Red (blue) were seeded on top of Cultrex mixed with DQ-collagen IV in a 35 mm glass bottom culture dish. After 24 hours HUVECs labelled with Cell Tracker Orange (red) were seeded on top of the SUM149 cells and Cultrex mixed with DQ-collagen IV. The co-cultures were treated with either 50 ng/mL VEGF or 25 μg/mL PTCI. Cells were imaged 18 hours after HUVECs were seeded using confocal microscopy. DQ-collagen IV cleavage products (green) were present both intracellularly and pericellularly. Merged images show pericellular proteolysis (green) surrounding the co-cultured cells. Images were obtained at 600× magnification. Representative images from the equatorial plane of a Z-stack are shown. Scale bar, 30 μm. **(B)** Quantification of proteolysis of DQ-collagen IV. To quantify proteolysis three equatorial planes from 3-4 different images from one experiment were quantified. Total integrated intensity of DQ-collagen IV florescence divided by total combined cell area of HUVECs and SUM149 cells was calculated and expressed relative to the control. Treatment with either VEGF or PTCI significantly increased proteolysis of DQ-collagen IV. Values are expressed as mean ± SEM from 5-6 independent experiments. ** $p < 0.01$ verses control.

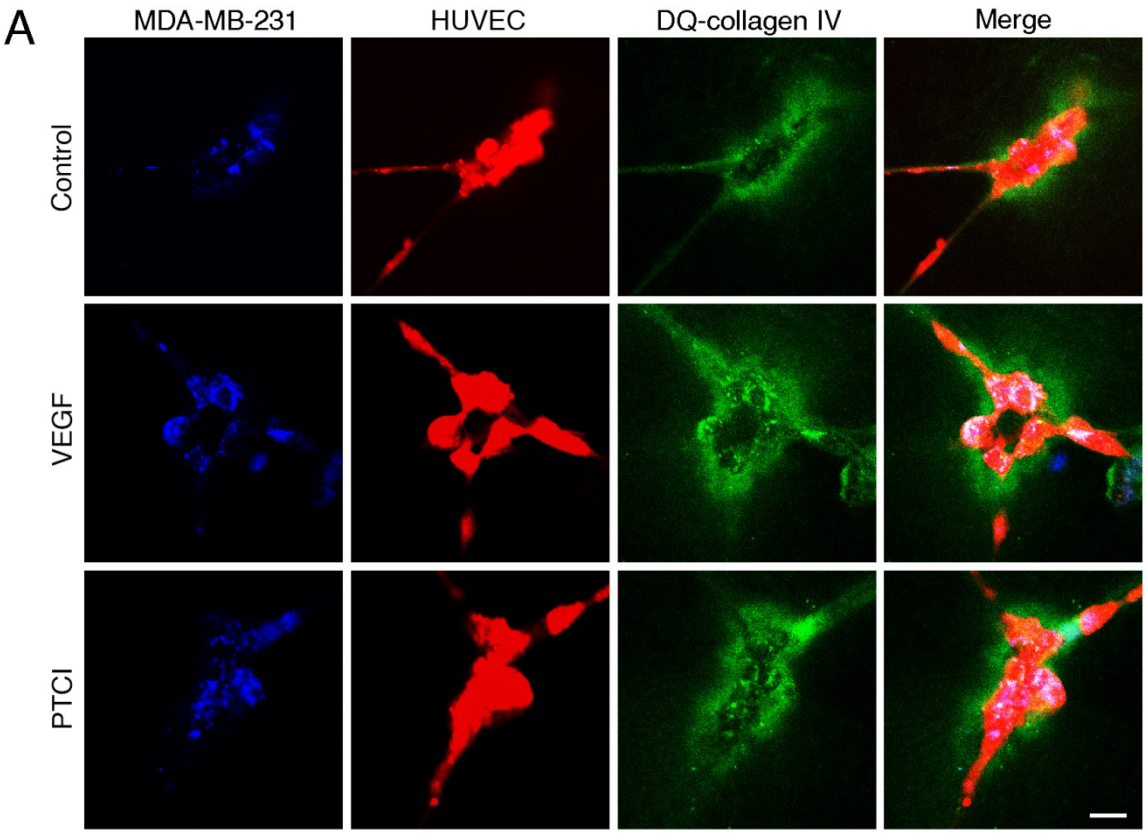
A
MDA-MB-231
HUVEC
DQ-collagen IV
Merge
Control
VEGF
PTCI

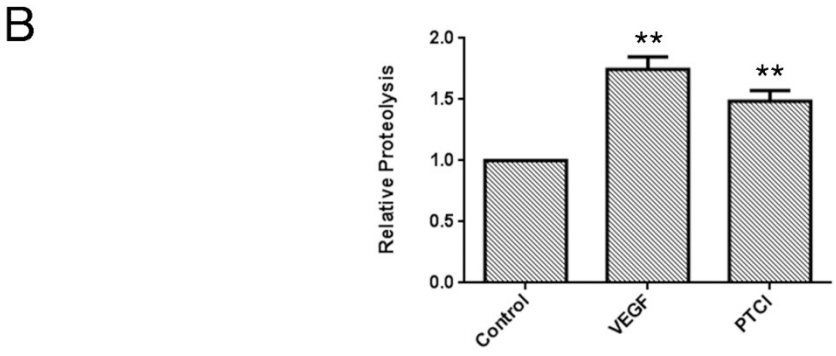
B
Relative Proteolysis
2.0
1.5
1.0
0.5
0.0
**
**
Control
VEGF
PTCI

Figure 3.8 Inhibition of TAFIa increases DQ-collagen IV proteolysis by co-cultured HUVECs and MDA-MB-231 cells

Effect of inhibition of TAFIa with PTCI on DQ-collagen proteolysis by co-cultured HUVEC and MDA-MB-231 cells. **(A)** MDA-MB-231 cells labelled with Cell Trace Far Red (blue) were seeded on top of Cultrex mixed with DQ-collagen IV in a 35 mm glass bottom culture dish. After 24 hours HUVECs labelled with Cell Tracker Orange (red) were seeded on top of the MDA-MB-231 cells and Cultrex mixed with DQ-collagen IV. The co-cultures were treated with either 50 ng/mL VEGF or 25 μg/mL PTCI. Cells were imaged 18 hours after HUVECs were seeded using confocal microscopy. DQ-collagen IV cleavage products (green) were present predominately pericellularly. Merge images show pericellular proteolysis (green) surrounding the co-cultured cells. Images were obtained at 600× magnification. Representative images from the equatorial plane of a Z-stack are shown. Scale bar, 30 μm. **(B)** Quantification of proteolysis DQ-collagen IV. To quantify proteolysis three equatorial planes from 3-4 different images from one experiment were quantified. Total integrated intensity of DQ-collagen IV florescence divided by total combined cell area of HUVECs and MDA-MB-231 cells was calculated and expressed relative to the control. Treatment with either VEGF or PTCI significantly increased proteolysis of DQ-collagen IV. Values are expressed as mean ± SEM from six independent experiments. ** $p < 0.01$ verses control.

3.5 Effect of inhibition of TAFIa on MMP2 and MMP9 mRNA expression and secretion

Since inhibition of TAFIa was shown to increase proteolysis of DQ-collagen IV by endothelial cells and by endothelial cells co-cultured with breast cancer cells, we next wanted to look at whether inhibition of TAFIa increased mRNA expression and secretion of MMPs involved in ECM proteolysis. Pericellular plasminogen activation is involved in ECM remodelling, as well as the release and activation of MMPs from the ECM [36]. MMP2 and MMP9 have been shown to be implicated in tumour angiogenesis [54]. MMP2 and MMP9 are gelatinases, but also degrade other ECM proteins such as collagen type IV [53]. VEGF has been shown to be in a positive feedback loop with MMP9 in RPE cells [29], therefore it was used as a positive control in these experiments. Gelatin zymography was used to determine the effect of inhibition of TAFIa on secretion of MMP2 and MMP9. Using gelatin zymography gelatinolytic activity of latent and active MMP2 and MMP9 can be visualized [148]. Samples are run using gel electrophoresis under denaturing and non-reducing conditions [148]. Active and latent MMP2 and MMP9 can be separated based on their molecular mass [148]. Gels are then renatured which causes activation of latent forms of these MMPs in the gel [148]. Both latent MMP2 and MMP9 can then proteolytically degrade gelatin in the gel [148]. After coomassie blue staining and destaining, clear zones where the staining has disappeared represent areas of proteolytic activity [148]. Quantitative RT-PCR was used to determine the effect of TAFIa inhibition on mRNA expression of MMP2 and MMP9.

PTCI or VEGF were used to treat SUM149 breast cancer cells. Bands from the SUM149 media samples migrated identically to recombinant pro-MMP2 and pro-MMP9

controls, which suggests that they are likely pro-MMP9 and pro-MMP2 (Fig. 3.9A). It was determined that PTCI significantly increased secretion of both pro-MMP2 (1.7-fold) and pro-MMP9 (2.6-fold) compared to the control (Fig. 3.9A). Preliminary qRT-PCR results suggest that PTCI does not affect the mRNA expression of either MMP2 or MMP9 (Fig. 3.9B).

PTCI or VEGF were used to treat HUVEC cells. Bands from the HUVEC media samples migrated identically to recombinant pro-MMP2 which was loaded as a control (Fig. 3.10A). This suggests that the gelatinolytic activity was likely due to pro-MMP2. It was determined that PTCI does not significantly affect the secretion of pro-MMP2 (Fig. 3.10A). We could not detect secretion of MMP9 (Fig. 3.10A). Preliminary qRT-PCR results suggest that PTCI increases the mRNA expression of both MMP2 (1.8-fold) and MMP9 (2.3-fold) compared to control (Fig. 3.10B).

Conditioned media (CM) from PTCI or VEGF treated SUM149 cells was used to treat HUVECs. Bands from the HUVEC media samples migrated identically to recombinant pro-MMP2 which was loaded as a control (Fig. 3.11A). This suggests that the gelatinolytic activity was likely due to pro-MMP2. Treatment of HUVECs with CM from untreated SUM149 cells resulted in a 1.2-fold increase in pro-MMP2 secretion compared to the untreated HUVEC control, although this was not significant (Fig. 3.11A). Treatment of HUVECs with CM from PTCI treated SUM149 cells significantly increased the secretion of pro-MMP2, 1.6-fold relative to the untreated HUVEC control (Fig. 3.11A). Preliminary qRT-PCR results show that treatment of HUVECs with CM from untreated SUM149 cells decreased MMP2 mRNA expression 2-fold and did not affect MMP9 mRNA expression compared to the untreated HUVEC control (Fig. 3.11B).

PTCI increased mRNA expression of MMP2 (4.8-fold) and MMP9 (1.5-fold) compared to the untreated HUVEC control (Fig. 3.11B).

Taken together these results suggest that inhibition of TAFIa in SUM149 breast cancer cells can increase the secretion of pro-MMP2 and pro-MMP9, and inhibition of TAFIa in SUM149 cells can increase the secretion of pro-MMP2 and increase the expression of MMP2 and MMP9 mRNA in HUVECs. The results therefore indicate that TAFIa has an opposite effect to the pro-angiogenic VEGF. These results also suggest that TAFIa is playing a different role in MMP2 and MMP9 secretion and expression in different cell types.

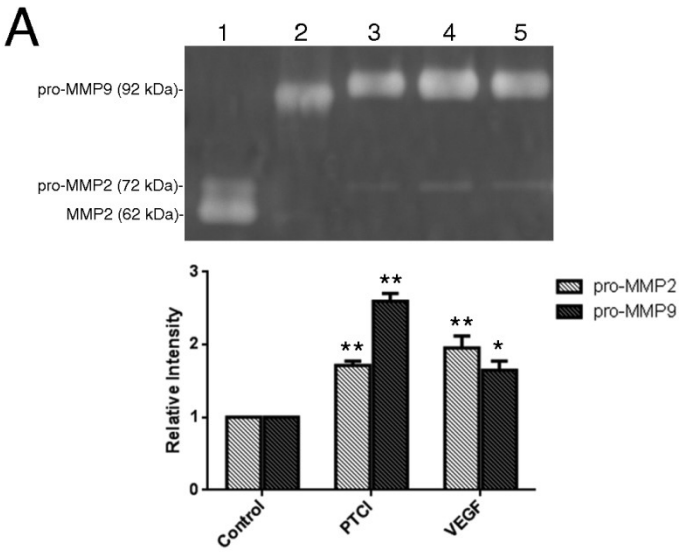
A
1
2
3
4
5
pro-MMP9 (92 kDa)-
pro-MMP2 (72 kDa)-
MMP2 (62 kDa)-
Relative Intensity
3
2
1
0
**
**
**
*
pro-MMP2
pro-MMP9
Control
PTCI
VEGF

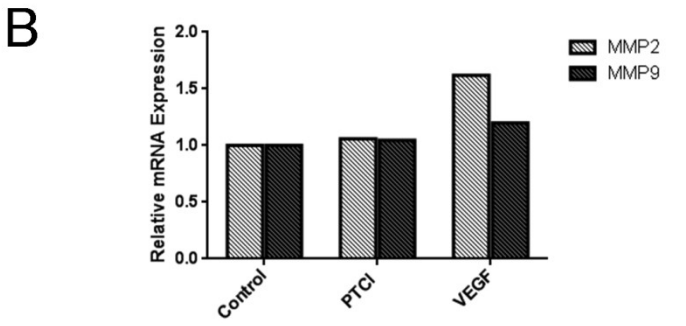
B
Relative mRNA Expression
2.0
1.5
1.0
0.5
0.0
MMP2
MMP9
Control
PTCI
VEGF

Figure 3.9 Inhibition of TAFIa in SUM149 cells increases secretion of pro-MMP2 and pro-MMP9, but does not affect mRNA expression of MMP2.
(A) Representative zymogram depicting gelatinolytic activity of pro-MMP9 (92 kDa), pro-MMP2 (72 kDa) secreted by SUM149 breast cancer cells treated with either 25 μg/mL PTCI or 50 ng/mL VEGF for 24 hours. Lanes 1 and 2 are control lanes for recombinant MMP2 (pro-MMP2 72 kDa, active MMP2 62 kDa) and pro-MMP9 (92 kDa), respectively. Lane 3 represents the control untreated SUM149 cells. Lanes 4 and 5 represent PTCI and VEGF treated SUM149 cells, respectively. Bands of gelatinolytic activity from SUM149 media samples migrate similarly to the recombinant MMP controls suggesting that the samples contain pro-MMP9 and pro-MMP2. Densitometry was performed and reported as relative intensity as compared to the control. Both PTCI and VEGF treatment significantly increased secretion of pro-MMP2 and pro-MMP9 in SUM149 cells. Data represent results of 3-6 independent experiments and are presented as mean ± SEM. * $p<0.05$, ** $p<0.01$ verses control. **(B)** MMP2 and MMP9 mRNA levels in PTCI and VEGF treated SUM149 cells using qRT-PCR. GAPDH was used as an internal control. Data represented as relative mRNA expression as compared to the control from one independent experiment. PTCI treatment of SUM149 cells did not affect mRNA expression of MMP2 or MMP9, while VEGF treatment increased mRNA expression of both MMP2 and MMP9.

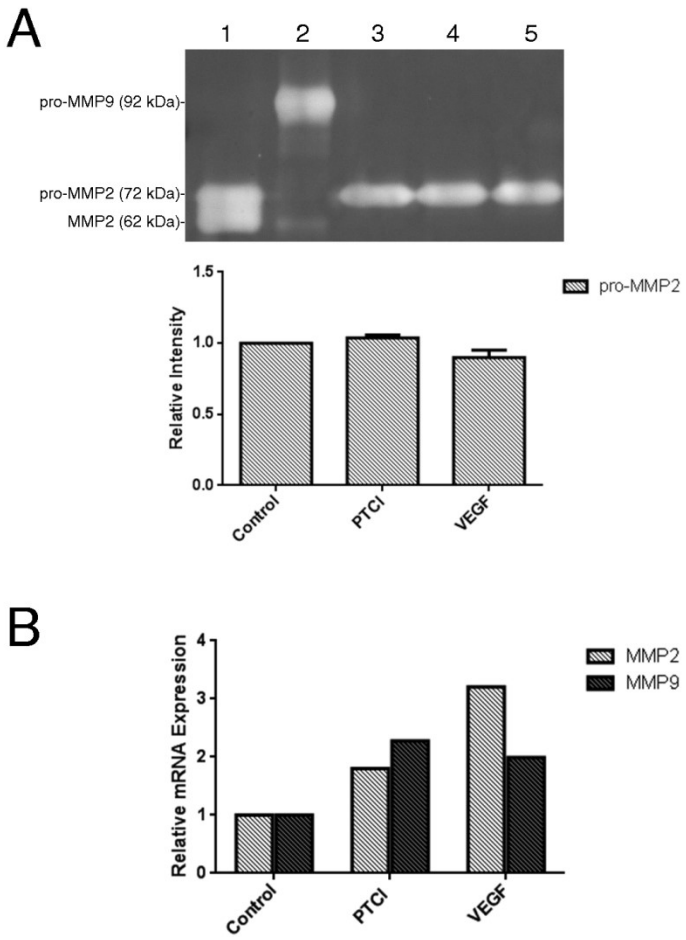

Figure 3.10 Inhibition of TAFIa in HUVECs does not affect secretion of pro-MMP2, but increases mRNA expression of MMP2 and MMP9.

(A) Representative zymogram depicting gelatinolytic activity of pro-MMP2 (72 kDa) secreted by HUVECs treated with either either 25 µg/mL PTCI or 50 ng/mL VEGF for 24 hours. Lanes 1 and 2 are control lanes for recombinant MMP2 (pro-MMP2 72 kDa, active MMP2 62 kDa) and pro-MMP9 (92 kDa), respectively. Lane 3 represents the control untreated HUVECs. Lanes 4 and 5 represent PTCI and VEGF treated HUVECs, respectively. Bands of gelatinolytic activity from HUVEC media samples migrate similarly to the recombinant pro-MMP2 control suggesting that the samples contain pro-MMP2. Densitometry was performed and reported as relative intensity as compared to the control. Neither PTCI nor VEGF treatment significantly affected secretion of pro-MMP2 in HUVECs. Data represent results of eight independent experiments and are presented as mean ± SEM. **(B)** MMP2 and MMP9 mRNA levels in PTCI and VEGF treated HUVECs using qRT-PCR. GAPDH was used as an internal control. Data represented as relative mRNA expression as compared to the control from one independent experiment. Both PTCI and VEGF treatment increased mRNA expression of MMP2 and MMP9.

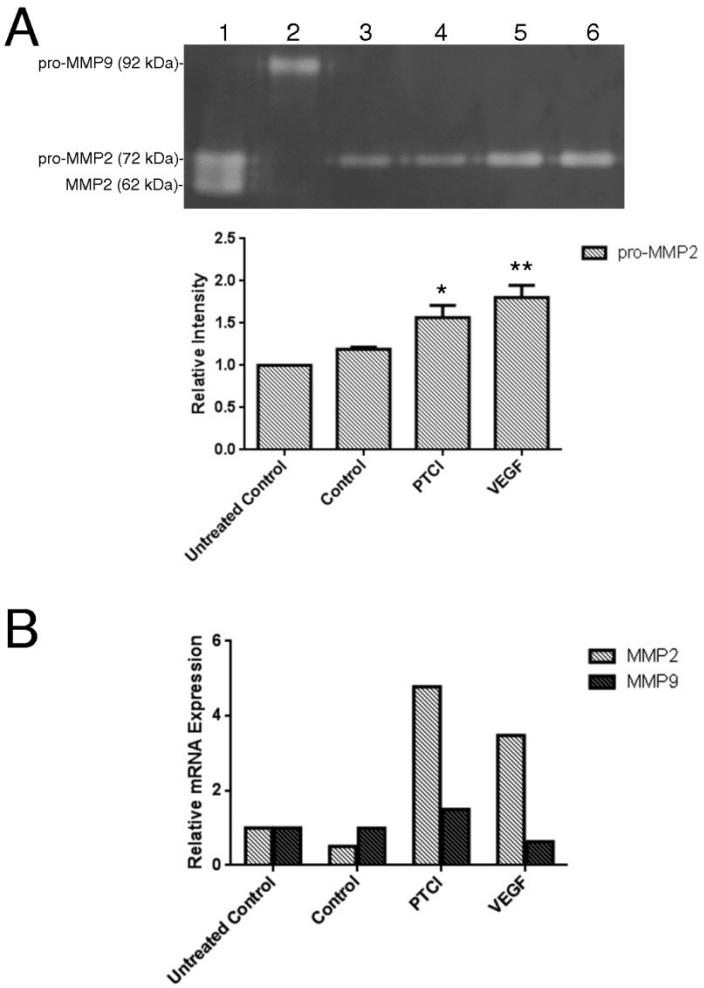
A
1
2
3
4
5
6
pro-MMP9 (92 kDa)-
pro-MMP2 (72 kDa)-
MMP2 (62 kDa)-
pro-MMP2
Relative Intensity
2.5
2.0
1.5
1.0
0.5
0.0
*
**
Untreated Control
Control
PTCI
VEGF
B
Relative mRNA Expression
6
4
2
0
MMP2
MMP9
Untreated Control
Control
PTCI
VEGF

Figure 3.11 Treatment of HUVECs with conditioned media from SUM149 cells treated with TAFIa inhibitor increases secretion of pro-MMP2 and mRNA expression of MMP2 and MMP9.

(A) Representative zymogram depicting gelatinolytic activity of pro-MMP2 (72 kDa) secreted by HUVECs treated with conditioned media (CM) from either 25 μg/mL PTCI or 50 ng/mL VEGF treated SUM149 cells. Lanes 1 and 2 are control lanes for recombinant MMP2 (pro-MMP2 72 kDa, active MMP2 62 kDa) and pro-MMP9 (92 kDa), respectively. Lane 3 represents the untreated control of untreated HUVECs. Lane 4 represents the control of HUVECs treated with untreated SUM149 CM. Lanes 5 and 6 represent HUVECs treated with CM from PTCI and VEGF treated SUM149 cells, respectively. Bands of gelatinolytic activity from HUVEC media samples migrate similarly to the recombinant pro-MMP2 control suggesting that the samples contain pro-MMP2. Densitometry was performed and reported as relative intensity as compared to the untreated control. CM treatment of HUVECs from PTCI and VEGF treated SUM149 cells significantly increased secretion of pro-MMP2. Data represent results of 4-5 independent experiments and are presented as mean ± SEM. * $p<0.05$, ** $p<0.01$ verses control. **(B)** MMP2 and MMP9 mRNA levels in HUVECs treated with CM from PTCI and VEGF treated SUM149 cells using qRT-PCR. GAPDH was used as an internal control. Data represented as relative mRNA expression as compared to the untreated control from one independent experiment. Treatment of HUVECs with CM from PTCI and VEGF treated SUM149 cells increased mRNA expression of MMP2. Treatment of HUVECs with CM from PTCI treated SUM149 cells increased the mRNA expression of MMP9.

3.6 Characterization of thrombin-dependent substrate activation of rTM EGF3-6 mutants

Different versions of recombinant thrombomodulin (rTM) consisting of the EGF-like domains 3-6 (rTM EGF3-6) were characterized for cofactor ability of thrombin-dependent activation of TAFI or protein C. Specifically, wild-type rTM EGF3-6, rTM EGF3-6 V340A/D341A, and rTM EGF3-6 F376A were characterized. Wang *et al.* characterized the V340A, D341A, and F376A mutations in rTM containing EGF-like repeats 1-6 [82]. The both V340A and D341A were shown to drastically decrease TAFI activation, while only marginally decreasing protein C activation [82]. The F376A mutation was found to severely reduce protein C activation, while maintaining TAFI activation [82]. The cofactor ability of rTM containing EGF-like repeats 3-6 has been determined to have full protein C activation capability (107%) and 82% TAFI activation capability compared to rTM containing the lectin-like domain, EGF-like repeats 1-6, and the serine/threonine rich domain [82, 149]. These mutations in rTM containing only EGF3-6 have yet to be characterized, but are hypothesized to maintain the substrate activation capabilities as determined by Wang and colleagues [82].

Using the colorimetric substrate, AAFR, initial rate of TAFI activation was quantified using the rTM EGF3-6 mutants and thrombin (Fig. 3.12A). rTM EGF3-6 V340A/D401A supported a significantly decreased initial rate of TAFI activation in the presence of thrombin. rTM EGF3-6 F376A had a similar initial rate of TAFI activation compared to wild-type rTM EGF3-6 in the presence of thrombin (Fig. 3.12A).

Using the colorimetricc substrate, S-2366, initial rate of protein C activation was quantified using the rTM EGF3-6 mutants and thrombin (Fig. 3.12B). rTM EGF3-6 V340A/D401A had a similar initial rate of protein C activation in the presence of thrombin. rTM EGF3-6 F376A had a significantly decreased rate of protein C activation compared to wild-type rTM EGF3-6 in the presence of thrombin (Fig. 3.12B).

The results indicate that the rTM EGF3-6 mutants have expected cofactor abilities. rTM EGF3-6 D340A/V341A has significantly decreased TAFI activation but retains protein C activation capability in comparison to wild-type rTM EGF3-6. rTM EGF3-6 F376A has significantly decreased protein C activation but retains TAFI activation in comparison to wild-type rTM EGF3-6.

A

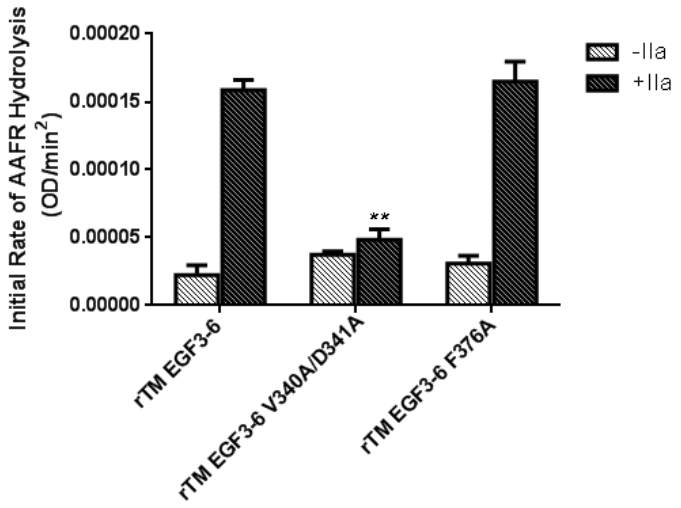
Initial Rate of AAFR Hydrolysis (OD/min^2)
0.00020
0.00015
0.00010
0.00005
0.00000
**
-IIa
+IIa
rTM EGF3-6
rTM EGF3-6 V340A/D341A
rTM EGF3-6 F376A

B

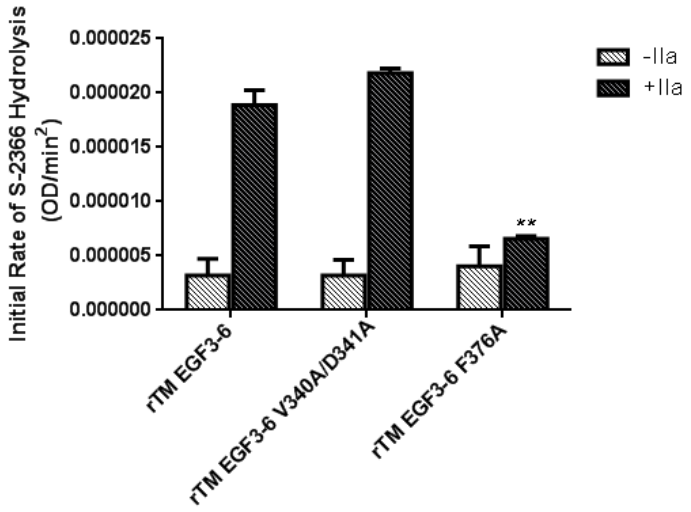
Initial Rate of S-2366 Hydrolysis (OD/min^2)
0.000025
0.000020
0.000015
0.000010
0.000005
0.000000
**
-IIa
+IIa
rTM EGF3-6
rTM EGF3-6 V340A/D341A
rTM EGF3-6 F376A

Figure 3.12 Characterization of cofactor ability of rTM EGF3-6 mutants

The cofactor ability of rTM EGF3-6 (wild-type), rTM EGF3-6 V340A/D3401A, and rTM EGF3-6 F376A for thrombin-dependent activation of TAFI or protein C was determined. **(A)** Thrombin-dependent activation of TAFI by measuring initial rate of AAFR hydrolysis of rTM EGF3-6 mutants using 10 nM of the rTM EGF3-6 mutants and 25 nM of thrombin (IIa). TAFI was allowed to be activated by the rTM EGF3-6 mutants and IIa for 10 minutes at room temperature before IIa was inhibited by PPACK. rTM EGF3-6 V340A/D341A has significantly decreased TAFI activation compared to wild-type rTM EGF3-6 in the presence of IIa. Values are expressed as mean ± SEM from 3-5 independent experiments. ** $p < 0.01$ verses rTM EGF3-6. **(B)** Thrombin-dependent activation of protein C by measuring initial rate of S-2366 hydrolysis of rTM EGF3-6 mutants using 10 nM of the rTM EGF3-6 mutants and 25 nM of IIa. Protein C was allowed to be activated by the rTM EGF3-6 mutants and IIa for 30 minutes at 37°C before IIa was inhibited by PPACK. rTM EGF3-6 F376A has significantly decreased protein C activation compared to wild-type rTM EGF3-6 in the presence of IIa. Values are expressed as mean ± SEM from three independent experiments. ** $p < 0.01$ verses rTM EGF3-6.

3.7 Effect of treatment with rTM EGF3-6 mutants on tube formation in endothelial cells and in co-culture systems containing endothelial and breast cancer cells

The role that TM plays in angiogenesis is not yet firmly established. Some studies have suggested that rTM containing the EGF-like repeats and the serine/threonine-rich domain is angiogenic [93]. Other studies have found through the lectin-like domain TM is anti-angiogenic [95]. TM has been shown to be antimetastatic and this was found to be dependent on the ability of thrombin to bind to TM [91]. Since inhibition of TAFIa resulted in increased tube formation (Fig. 3.3-3.5), we decided to test the effect on endothelial tube formation that the rTM EGF3-6 mutations would have. The V340A/D341A mutant of rTM EGF3-6 was shown to allow thrombin dependent activation of protein C but not TAFI, and the F376A mutant of rTM EGF3-6 was shown to allow thrombin-dependent activation of TAFI but not protein C (Fig. 3.12). We therefore hypothesized addition of wild-type rTM EGF3-6 would decrease endothelial cell tube formation (i.e., have the opposite effect of inhibiting TAFIa), and that this effect would be retained by the F376A mutant but not the V340A/D341A mutant.

Tube formation assays using HUVECs on Cultrex were used, and were treated with either rTM EGF3-6 (wild-type), rTM EGF3-6 V340A/D41A, or rTM EGF3-6 F376A (Fig. 3.13A). Treatment with wild-type rTM EGF3-6 did not significantly affect relative tube length (Fig. 3.13B). Treatment with rTM EGF3-6 V340A/D341A significantly increased relative endothelial tube length compared to the control and compared to wild-type, 1.4-fold and 1.5-fold respectively (Fig. 3.13B). Treatment with

rTM EGF3-6 F376A significantly decreased relative endothelial tube length by 1.2-fold compared to the control and compared to wild-type (Fig. 3.13B).

The effect on endothelial tube formation in co-culture systems consisting of breast cancer cells using the rTM EGF3-6 mutants was also assessed. The cultures consisting of either HUVECs and SUM149 cells (Fig. 3.14A) or HUVECs and MDA-MB-231 cells (Fig. 3.15A) were treated with either rTM EGF3-6 (wild-type), rTM EGF3-6 V340A/D41A, or rTM EGF3-6 F376A. Both co-culture systems produced nearly identical results compared to each other. Treatment with wild-type rTM EGF3-6 did not affect relative endothelial tube length in either co-culture system (Fig. 3.14B & Fig. 3.15B). Treatment with rTM EGF3-6 V340A/D341A significantly increased relative endothelial tube length compared to control and compared to wild-type by 1.3-fold in both co-culture systems (Fig. 3.14B & Fig. 3.15B). Treatment with rTM EGF3-6 F376A significantly decreased relative endothelial tube length compared to control by 1.2-fold in both co-culture systems (Fig. 3.14B & Fig. 3.15B). Treatment with rTM EGF3-6 F376A significantly decreased relative endothelial tube length compared to wild-type rTM EGF3-6 by 1.2-fold in co-cultured HUVECs and SUM149 cells (Fig. 3.14B).

Overall, treatment with rTM EGF3-6 had no effect on endothelial tube formation, treatment with rTM EGF3-6 rTM EGF3-6 V340A/D341A increased endothelial tube formation, and treatment rTM EGF3-6 F376A decreased endothelial tube formation. The results on endothelial tube formation with wild-type rTM EGF3-6 are not consistent with our hypothesized outcome, but do suggest an anti-angiogenic role for TAFI and a pro-angiogenic role for protein C.

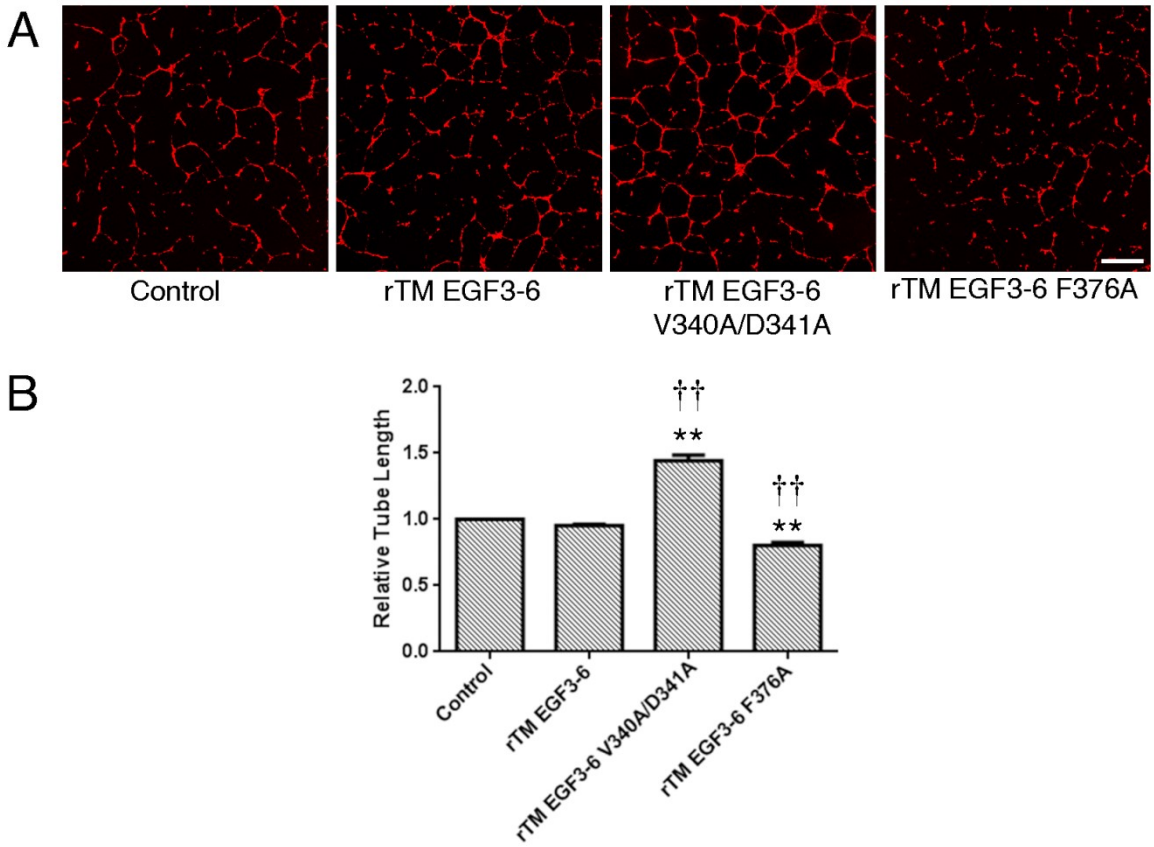

Figure 3.13 Effect of differing cofactor ability of rTM EGF3-6 on endothelial tube formation

(A) HUVECs labelled with Cell Tracker Orange (red) were seeded on top of Cultrex and treated with 10 nM of either rTM EGF3-6, rTM EGF3-6 V340A/D341A, or rTM EGF3-6 F376A. Cells were imaged 18 hours after HUVECs were seeded using confocal microscopy. Images above were obtained at 40× magnification. Scale bar, 500 μm. **(B)** Quantification of endothelial tube formation. To quantify tube formation 8-10 images were obtained at 100× magnification. Tube length was determined by measuring total tube length divided by total tube number, and is expressed relative to that in the control untreated cells. Values are expressed as mean ± SEM from 6-10 independent experiments. Asterisks: **p< 0.01 verses control, daggers: †† p< 0.01 verses rTM EGF3-6. Treatment with rTM EGF3-6 V340A/D341A significantly increased relative tube length of HUVECs compared to control and to rTM EGF3-6. Treatment with rTM EGF3-6 F376A significantly decreased relative tube length of HUVECs compared to control and to rTM EGF3-6.

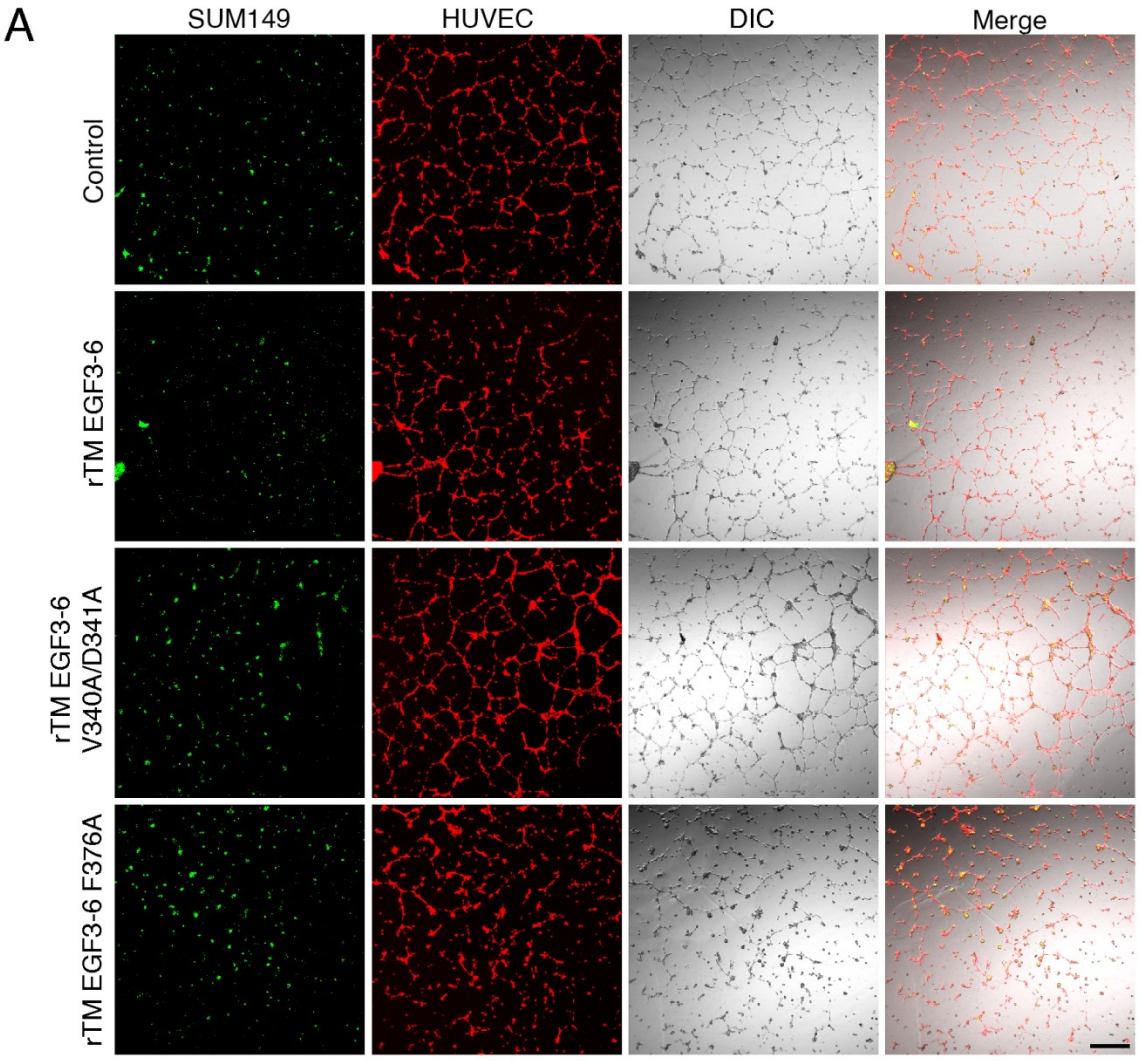
A
SUM149
HUVEC
DIC
Merge
Control
rTM EGF3-6
rTM EGF3-6 V340A/D341A
rTM EGF3-6 F376A

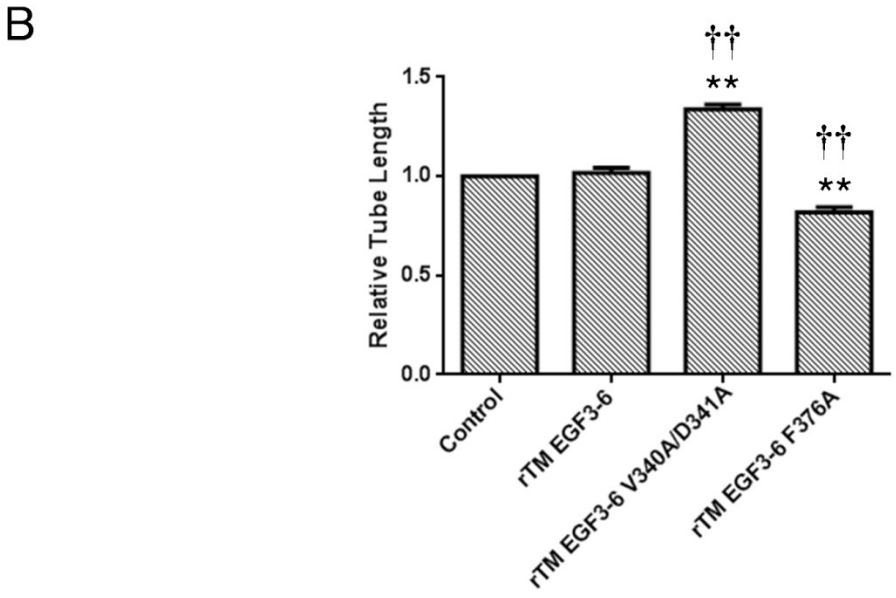
B
Relative Tube Length
1.5
1.0
0.5
0.0
††
**
††
**
Control
rTM EGF3-6
rTM EGF3-6 V340A/D341A
rTM EGF3-6 F376A

Figure 3.14 Effect of differing cofactor ability of rTM EGF3-6 on endothelial tube formation in a co-culture system with HUVECs and SUM149 cells

(A) SUM149 cells labelled with Cell Trace Far Red (green) were seeded on top of Cultrex, after 24 hours HUVECs labelled with Cell Tracker Orange (red) were seeded on top of the SUM149 cells and Cultrex. The co-cultures were treated with 10 nM of either rTM EGF3-6, rTM EGF3-6 V340A/D341A, or rTM EGF3-6 F376A. Cells were imaged 18 hours after HUVECs were seeded using confocal microscopy. Images above were obtained at 40× magnification. Scale bar, 500 μm. **(B)** Quantification of endothelial tube formation. To quantify tube formation 8-10 images were obtained at 100× magnification. Tube length was determined by measuring total tube length divided by total tube number, and is expressed relative to that in the control untreated cells. Values are expressed as mean ± SEM from 5-8 independent experiments. Asterisks: **p< 0.01 verses control, daggers: †† p< 0.01 verses rTM EGF3-6. Treatment with rTM EGF3-6 V340A/D341A significantly increased relative tube length of HUVECs compared to control and to rTM EGF3-6. Treatment with rTM EGF3-6 F376A significantly decreased relative tube length of HUVECs compared to control and to rTM EGF3-6.

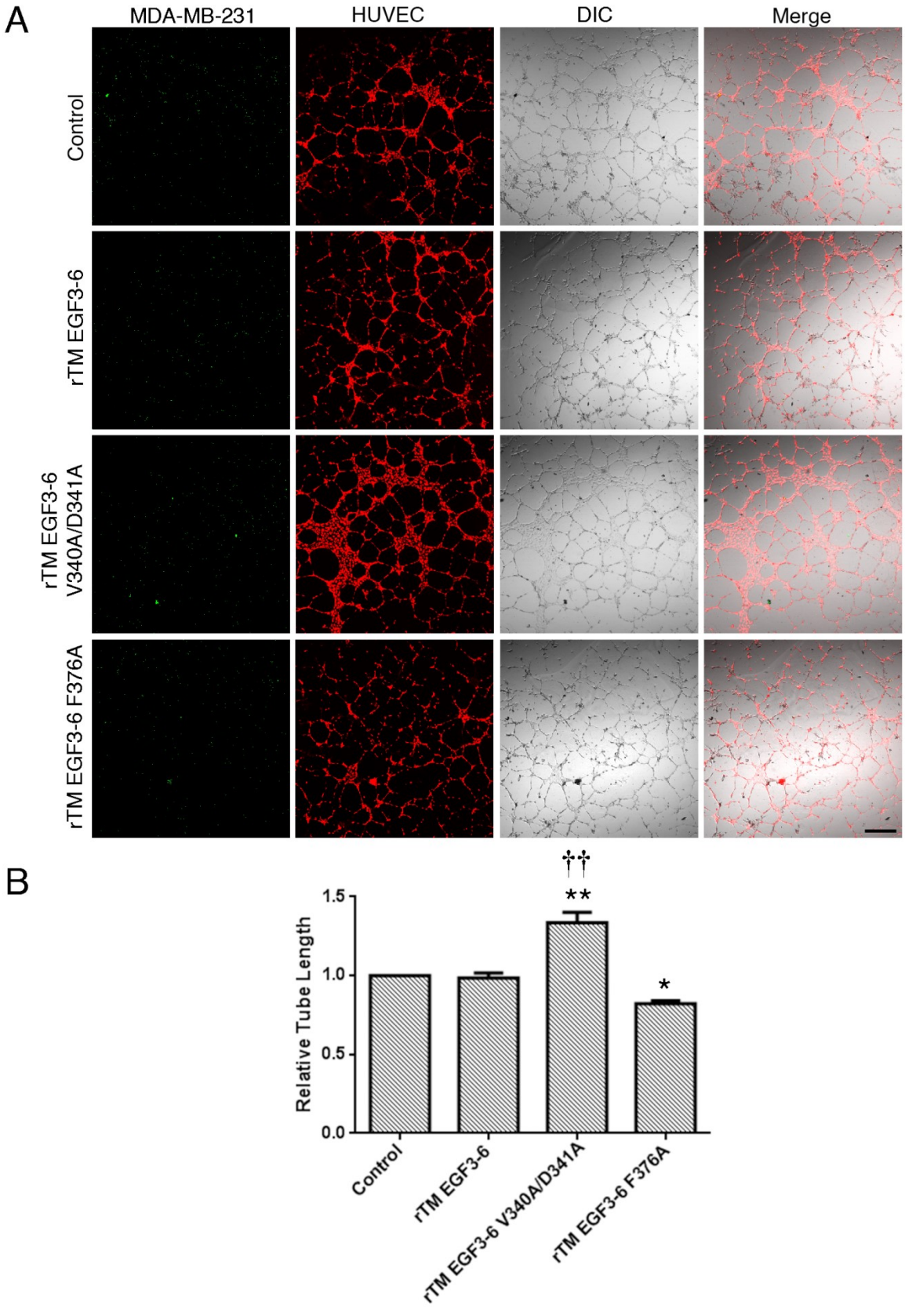
A
MDA-MB-231
HUVEC
DIC
Merge
Control
rTM EGF3-6
rTM EGF3-6 V340A/D341A
rTM EGF3-6 F376A
B
Relative Tube Length
1.5
1.0
0.5
0.0
**
††
*
Control
rTM EGF3-6
rTM EGF3-6 V340A/D341A
rTM EGF3-6 F376A

Figure 3.15 Effect of differing cofactor ability of rTM EGF3-6 on endothelial tube formation in a co-culture system with HUVECs and MDA-MB-231 cells

(A) MDA-MB-231 cells labelled with Cell Trace Far Red (green) were seeded on top of Cultrex, after 24 hours HUVECs labelled with Cell Tracker Orange (red) were seeded on top of the MDA-MB-231 cells and Cultrex. The co-cultures were treated with 10 nM of either rTM EGF3-6, rTM EGF3-6 V340A/D341A, or rTM EGF3-6 F376A. Cells were imaged 18 hours after HUVECs were seeded using confocal microscopy. Images above were obtained at 40× magnification. Scale bar, 500 μm. **(B)** Quantification of endothelial tube formation. To quantify tube formation 8-10 images were obtained at 100× magnification. Tube length was determined by measuring total tube length divided by total tube number, and is expressed relative to that in the control untreated cells. Values are expressed as mean ± SEM from 5-6 independent experiments. Asterisks: * $p<0.05$, ** $p< 0.01$ verses control, daggers: †† $p< 0.01$ verses rTM EGF3-6. Treatment with rTM EGF3-6 V340A/D341A significantly increased relative tube length of HUVECs compared to control and to rTM EGF3-6. Treatment with rTM EGF3-6 F376A significantly decreased relative tube length of HUVECs compared to control.

3.8 Effect of treatment with rTM EGF3-6 mutants on proteolysis of DQ-collagen IV by endothelial cells and by co-culture systems containing endothelial and breast cancer cells

We next tested the effect that the rTM EGF3-6 mutants had on proteolysis of DQ-collagen IV by endothelial cells and by endothelial cells in co-culture with breast cancer cells. We hypothesized that treatment with rTM EGF3-6 V340A/D341A would increase proteolysis of DQ-collagen IV, while treatment with rTM EGF3-6 F376A would decrease proteolysis of DQ-collagen IV. We hypothesized this due to the results obtained in endothelial tube formation assays using treatment with the rTM EGF3-6 mutants which suggested an anti-angiogenic role for TAFI and a pro-angiogenic role for protein C.

HUVECs were seeded on top of Cultrex mixed with DQ-collagen IV and were treated with either rTM EGF3-6 (wild-type), rTM EGF3-6 V340A/D41A, or rTM EGF3-6 F376A (Fig. 3.16A). Degradation products of DQ-collagen IV were localized predominantly intracellularly when HUVECs were treated with the rTM EGF3-6 mutants (Fig. 3.16A). Treatment of HUVECs with wild-type rTM EGF3-6 or rTM EGF3-6 F376A significantly decreased proteolysis of DQ-collagen IV, 1.2-fold and 1.4-fold relative to the control, respectively (Fig. 3.16B). Treatment of HUVECs with rTM EGF3-6 V340A/D341A significantly increased proteolysis of DQ-collagen IV, 1.9-fold relative to the control (Fig. 3.16B). Treatment of HUVECs with rTM EGF3-6 V340A/D341A also significantly increased proteolysis of DQ-collagen IV compared to wild-type by 2.3-fold (Fig. 3.16B).

Co-culture systems containing endothelial cells and breast cancer cells were used to look the effect of the rTM EGF3-6 mutants on proteolysis of DQ-collagen by both endothelial and breast cancer cells in the same environment. HUVECs co-cultured with SUM149 cells (Fig. 3.17A) or MDA-MB-231 cells (Fig. 3.18A) were treated with either rTM EGF3-6, rTM EGF3-6 V340A/D41A, or rTM EGF3-6 F376A. In both co-culture systems there was a mix of intracellular and pericellular proteolysis (Fig. 3.17A & Fig. 3.18A). The co-culture system containing HUVECs and SUM149 cells exhibited predominately pericellular proteolysis (Fig. 3.17A). Treatment with rTM EGF3-6 V340A/D341A increased intracellular proteolysis of DQ-collagen IV in the co-culture system containing HUVECs and MDA-MB-231 cells (Fig. 3.18A). Treatment with wild-type rTM EGF3-6 did not significantly affect proteolysis of DQ-collagen IV in either co-culture system (Fig. 3.17B & Fig. 3.18B). Treatment with rTM EGF3-6 F376A decreased proteolysis of DQ-collagen IV by 1.2-fold in the both co-culture systems compared to the control, although this was not considered significant (Fig. 3.17B & Fig. 3.18B). Treatment with rTM EGF3-6 F376A decreased proteolysis of DQ-collagen IV significantly compared to wild-type by 1.4-fold in the co-culture system containing HUVECs and SUM149 cells (Fig. 3.17B). Treatment with rTM EGF3-6 V340A/D341A significantly increased proteolysis of DQ-collagen IV in the both co-culture systems (1.4-fold in the HUVEC and SUM149 co-culture, and 1.6-fold in the HUVEC and MDA-MB-231 co-culture) compared to control and compared to wild-type (1.3-fold in the HUVEC and SUM149 co-culture, and 1.6-fold in the HUVEC and MDA-MB-231 co-culture) (Fig. 3.17B & Fig. 3.18B).

Overall, treatment with wild-type rTM EGF3-6 decreased proteolysis of DQ-collagen IV by HUVECs alone, but did not have an effect on proteolysis of DQ-collagen IV in either co-culture system. Treatment with rTM EGF3-6 V340A/D341A increased proteolysis of DQ-collagen IV by HUVECs alone and by both co-culture systems. Treatment with rTM EGF3-6 F376A decreased proteolysis of DQ-collagen IV by HUVECs alone and by both co-culture systems. The results we obtained for the proteolysis of DQ-collagen IV in all systems (HUVEC monoculture and both co-culture systems) treated with the rTM EGF3-6 mutants are consistent with what we'd expect given the effect on endothelial tube formation we saw using the rTM EGF3-6 mutants. The effect of the rTM EGF3-6 mutants in both the endothelial tube formation assays and the DQ-collagen IV proteolysis assays are similar. These results suggest that TAFI activation plays an anti-angiogenic role in ECM proteolysis

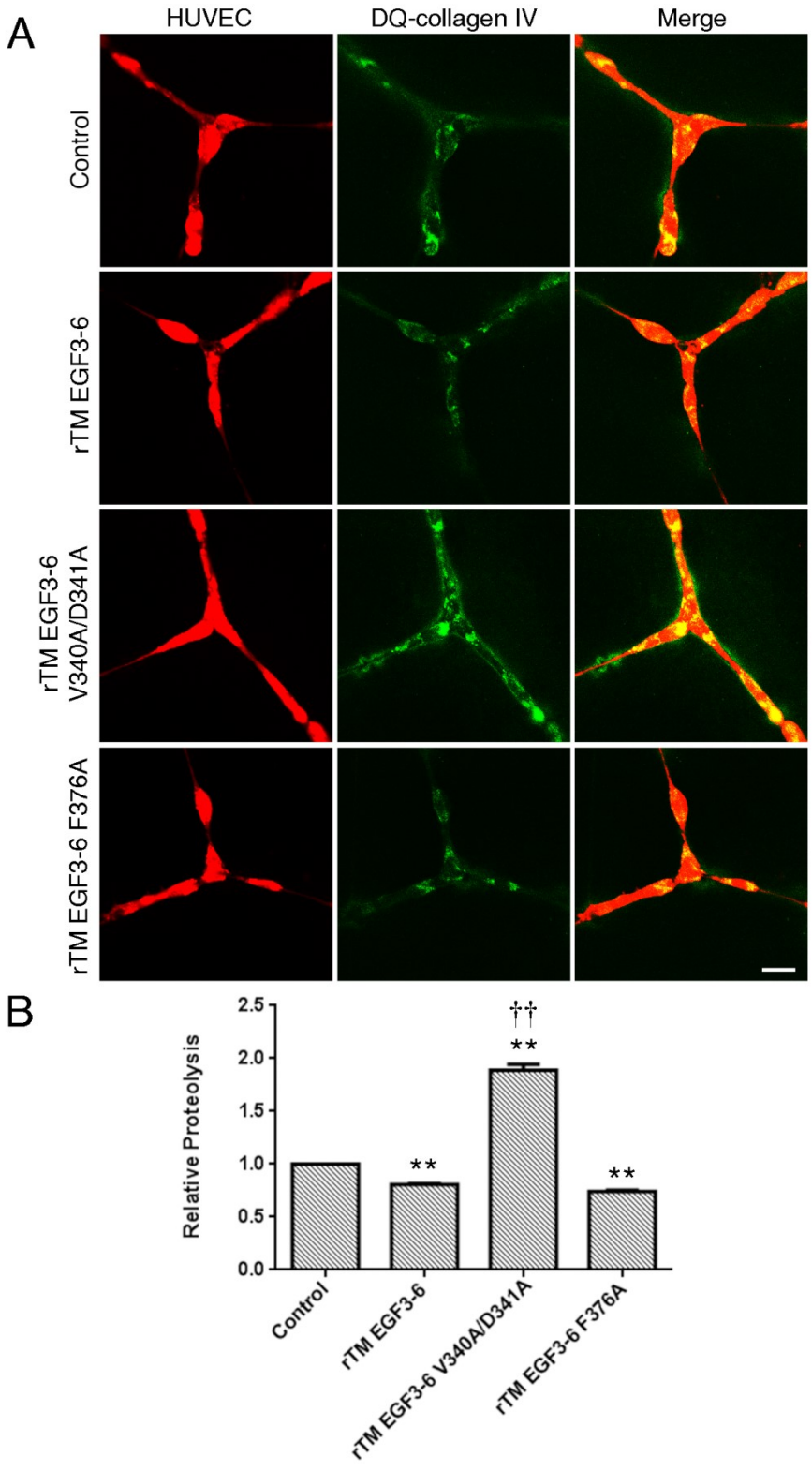
A
HUVEC
DQ-collagen IV
Merge
Control
rTM EGF3-6
rTM EGF3-6 V340A/D341A
rTM EGF3-6 F376A
B
Relative Proteolysis
2.5
2.0
1.5
1.0
0.5
0.0
**
**
††
**
Control
rTM EGF3-6
rTM EGF3-6 V340A/D341A
rTM EGF3-6 F376A

Figure 3.16 Effect of differing cofactor ability of rTM EGF3-6 on proteolysis of DQ-collagen IV by endothelial cells

(A) HUVECs labelled with Cell Tracker Orange (red) were seeded on top of Cultrex mixed with DQ-collagen IV in a 35 mm glass bottom culture dish and treated with 10 nM of either rTM EGF3-6, rTM EGF3-6 V340A/D341A, or rTM EGF3-6 F376A. Cells were imaged 18 hours after seeding HUVECs using confocal microscopy. DQ-collagen IV cleavage products (green) were present predominantly intracellularly. Merge images show intracellular (yellow) and pericellular proteolysis (green). Images were obtained at 600× magnification. Representative images from the equatorial plane of a Z-stack are shown. Scale bar, 30 μm. **(B)** Quantification of proteolysis of DQ-collagen IV. To quantify proteolysis three equatorial planes from 3-4 different images from one experiment were quantified. Total integrated intensity of DQ-collagen IV florescence divided by total HUVEC area was calculated and expressed relative to the control. Values are expressed as mean ± SEM from five independent experiments. Asterisks: **$p < 0.01$ verses control, daggers: †† $p < 0.01$ verses rTM EGF3-6. Treatment with both rTM EGF3-6 and rTM EGF3-6 F376A significantly decreased relative proteolysis of DQ-collagen IV by HUVECs compared to control. Treatment with rTM EGF3-6 V340A/D341A significantly increased relative proteolysis of DQ-collagen IV by HUVECs compared to control and to rTM EGF3-6.

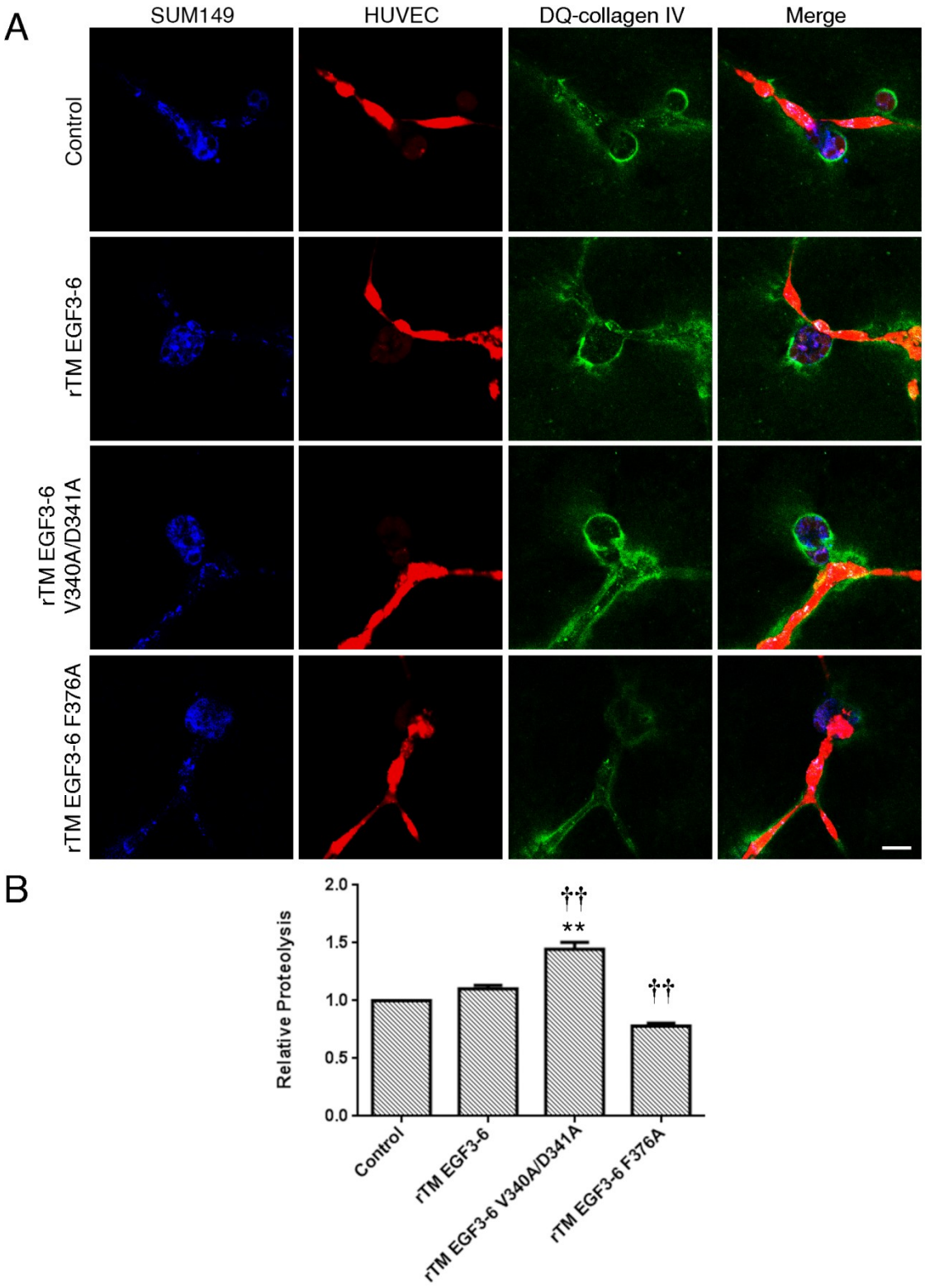
A
SUM149
HUVEC
DQ-collagen IV
Merge
Control
rTM EGF3-6
rTM EGF3-6 V340A/D341A
rTM EGF3-6 F376A
B
Relative Proteolysis
2.0
1.5
1.0
0.5
0.0
**
††
††
Control
rTM EGF3-6
rTM EGF3-6 V340A/D341A
rTM EGF3-6 F376A

Figure 3.17 Effect of differing cofactor ability of rTM EGF3-6 on proteolysis of DQ-collagen IV by co-cultured HUVECs and SUM149 cells

(A) SUM149 cells labelled with Cell Trace Far Red (blue) were seeded on top of Cultrex mixed with DQ-collagen IV in a 35 mm glass bottom culture dish. After 24 hours HUVECs labelled with Cell Tracker Orange (red) were seeded on top of the SUM149 cells and Cultrex mixed with DQ-collagen IV. The co-cultures were treated with 10 nM of either rTM EGF3-6, rTM EGF3-6 V340A/D341A, or rTM EGF3-6 F376A. Cells were imaged 18 hours after HUVECs were seeded using confocal microscopy. DQ-collagen IV cleavage products (green) were present predominately pericellularly. Merge images show pericellular proteolysis (green) surrounding the co-cultured cells. Images were obtained at 600× magnification. Representative images from the equatorial plane of a Z-stack are shown. Scale bar, 30 μm. **(B)** Quantification of proteolysis of DQ-collagen IV. To quantify proteolysis three equatorial planes from 3-4 different images from one experiment were quantified. Total integrated intensity of DQ-collagen IV florescence divided by total combined cell area of HUVECs and SUM149 cells was calculated and expressed relative to the control. Values are expressed as mean ± SEM from 3-7 independent experiments. Asterisks: **$p < 0.01$ verses control, daggers: †† $p < 0.01$ verses rTM EGF3-6. Treatment with rTM EGF3-6 V340A/D341A significantly increased relative proteolysis of DQ-collagen IV by co-cultured HUVECs and SUM149 cells compared to control and to rTM EGF3-6.Treatment with rTM EGF3-6 F376A significantly decreased relative proteolysis of DQ-collagen IV by co-cultured HUVECs and SUM149 cells compared to rTM EGF3-6.

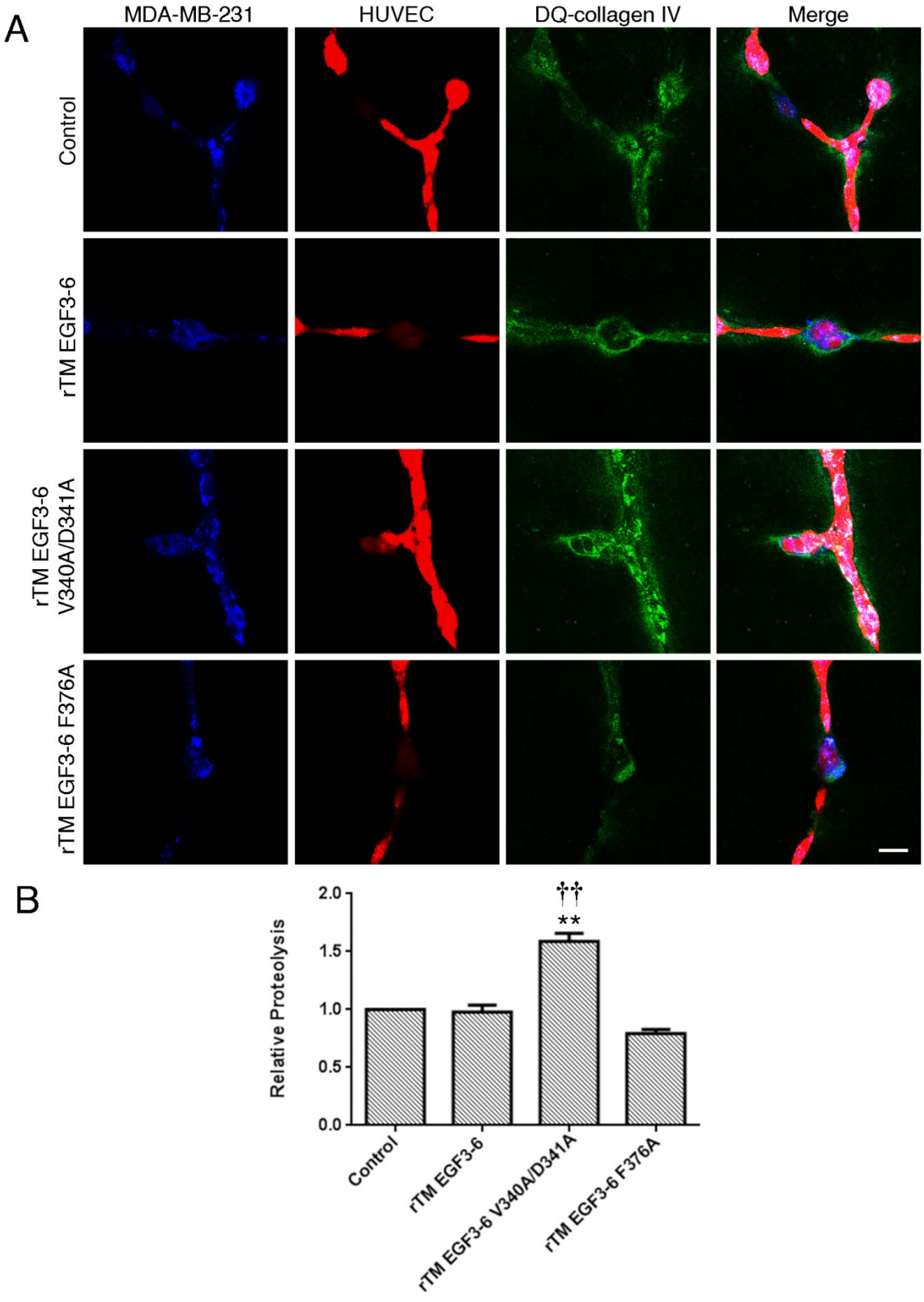
A
MDA-MB-231
HUVEC
DQ-collagen IV
Merge
Control
rTM EGF3-6
rTM EGF3-6 V340A/D341A
rTM EGF3-6 F376A
B
Relative Proteolysis
2.0
1.5
1.0
0.5
0.0
**
††
Control
rTM EGF3-6
rTM EGF3-6 V340A/D341A
rTM EGF3-6 F376A

Figure 3.18 Effect of differing cofactor ability of rTM EGF3-6 on proteolysis of DQ-collagen IV by co-cultured HUVECs and MDA-MB-231 cells

(A) MDA-MB-231 cells labelled with Cell Trace Far Red (blue) were seeded on top of Cultrex mixed with DQ-collagen IV in a 35 mm glass bottom culture dish. After 24 hours HUVECs labelled with Cell Tracker Orange (red) were seeded on top of the MDA-MB-231 cells and Cultrex mixed with DQ-collagen IV. The co-cultures were treated with 10 nM of either rTM EGF3-6, rTM EGF3-6 V340A/D341A, or rTM EGF3-6 F376A. Cells were imaged 18 hours after HUVECs were seeded using confocal microscopy. DQ-collagen IV cleavage products (green) were present both intracellularly and pericellularly. Merge images show pericellular proteolysis (green) surrounding the co-cultured cells. Images were obtained at 600× magnification. Representative images from the equatorial plane of a Z-stack are shown. Scale bar, 30 μm. **(B)** Quantification of proteolysis of DQ-collagen IV. To quantify proteolysis three equatorial planes from 3-4 different images from one experiment were quantified. Total integrated intensity of DQ-collagen IV florescence divided by total combined cell area of HUVECs and MDA-MB-231 cells was calculated and expressed relative to the control. Values are expressed as mean ± SEM from 3-4 independent experiments. Asterisks: **$p < 0.01$ verses control, daggers: †† $p < 0.01$ verses rTM EGF3-6. Treatment with rTM EGF3-6 V340A/D341A significantly increased relative proteolysis of DQ-collagen IV by co-cultured HUVECs and MDA-MB-231 cells compared to control and to rTM EGF3-6.

Chapter 4 Discussion and Conclusions

Thrombomodulin (TM) known mostly for its role in the regulation of vascular hemostasis, has also been shown to play an antimetastatic role in cancer. TM expression has been shown to be inversely correlated to tumour prognosis and malignancy [86, 87]. TM has been shown to decrease invasion, proliferation, and metastasis [79, 87, 90]. A study conducted by Horowitz *et al.* determined the antimetastatic effects of TM were dependent on its ability to bind thrombin [91]. However, this study did not determine which substrate of thrombin-TM, TAFI or protein C, was responsible for these effects. Moreover, TAFI has been shown to inhibit pericellular plasminogen activation through cleavage of carboxyl-terminal lysine residues *in vitro* and *in vivo* [76, 125, 126]. Pericellular plasminogen activation has been implicated in metastasis and tumour angiogenesis through degradation of ECM, regulation of MMP activity, and release of growth factors from ECM [36]. Higuchi *et al.* found TAFIa inhibited plasminogen activation in HT1080 cells resulting in decreased invasion [128]. We therefore hypothesized that due to the role that TAFI plays in the regulation of pericellular plasminogen activation it was the substrate of thrombin-TM responsible for the antimetastatic effects of TM.

Tumour angiogenesis is a hallmark of cancer: without it tumours could not grow beyond 1-2mm^3 [2, 6, 14]. Moreover, highly angiogenic tumours have greater metastatic potential, and metastasis is responsible for 90% of cancer deaths [2]. A previous study showed TAFIa inhibits wound healing angiogenesis on a plasma clot [130]. Another study suggested absence of TAFI inhibited healing of colonic anastomoses through

overactivation of angiogenesis and plasmin [121]. These results suggest that TAFIa plays a role in inhibition of wound healing angiogenesis and potentially tumour angiogenesis. Plasminogen activation plays a role in tumour angiogenesis through degradation of vascular ECM and basement membrane allowing endothelial cells to invade and proliferate into surrounding stroma [36]. There are conflicting reports on the role of TM in angiogenesis. Some studies suggest that it is anti-angiogenic through the lectin-like domain, while others suggest that it is angiogenic through the EGF-like domain [93–95].

We decided to determine the role TAFIa plays in tumour angiogenesis through inhibition of TAFIa, and through manipulation of cofactor ability of TM. In breast cancer patients low TM is strongly correlated with poor prognosis and high relapse rate [89]. Unpublished data from our laboratory have shown that breast cancer cells, including SUM149 and MDA-MB-231 cells, express both TM and TAFI. Unpublished data from our laboratory also shows that TAFIa inhibits pericellular plasminogen activation in these breast cancer cell lines. We therefore used SUM149 and MDA-MB-231 breast cancer cells in these experiments because they provided an appropriate cellular model to evaluate tumour angiogenesis. We found that TAFIa plays a role in inhibition of tumour angiogenesis, and further clarified a role for TM in angiogenesis.

4.1 Inhibition of TAFIa increases tumour angiogenesis

Through inhibition of TAFIa with PTCI there was an increase in crucial components of angiogenesis; namely endothelial cell proliferation, invasion, tube formation, and ECM proteolysis. Endothelial tube formation and ECM proteolysis were also increased when TAFIa was inhibited in co-culture systems consisting of endothelial cells and breast cancer cells. These results suggest that TAFIa plays a role in inhibition of tumour angiogenesis.

4.1.1 Inhibition of TAFIa increases endothelial tube formation as a function of decreased inhibition of pericellular plasminogen activation

TAFIa has been implicated as an anti-angiogenic factor in the context of wound healing angiogenesis [130]. Guimarães *et al.* showed TAFIa decreased tube formation on a 3D-plasma clot matrix [130]. This study determined that TAFIa decreased tube formation through inhibition of plasminogen activation on a fibrin matrix [130]. To date, no study has examined the role that TAFIa plays in endothelial tube formation in the context of tumour angiogenesis, where plasminogen activation is pericellular, supported by cell-surface plasminogen receptors, rather than occurring on a fibrin matrix.

Endothelial cells grown on reconstituted basement membrane form tube-like structures *in vitro* that mimic angiogenesis, in which tube formation can be quantified [134, 135]. Using this system we looked at the effect that inhibition of TAFIa had on tube formation. Inhibition of TAFIa significantly increased tube formation expressed as the

relative length of the endothelial cell tubes (Fig 3.3). In order to make this system relevant in the context of tumour angiogenesis, we also examined the effect of inhibition of TAFIa on endothelial tube formation using two different co-culture systems using endothelial and breast cancer cells. The endothelial tube networks formed around the cancer spheroids on the reconstituted basement membrane. Inhibition of TAFIa significantly increased endothelial tube formation in both co-culture systems (Fig. 3.4 & Fig. 3.5). There was no difference in the relative tube length increase due to PTCI treatment between the HUVEC monocultures and either co-culture system. There was, however, an apparent increase in proliferation of the endothelial cells in the MDA-MB-231 and HUVEC co-culture system (Fig. 3.5) compared to the HUVEC monoculture (Fig. 3.3), and the SUM149 and HUVEC co-culture system (Fig. 3.4). This could be due to the fact that MDA-MB-231 cells are a more malignant cell line than HUVECs (a noncancerous cell line) and SUM149 cells, which could lead to an increased production of factors that increase proliferation [150].

Previous studies have shown that uPA bound to uPAR can enhance endothelial cell organization into tubes [151]. Since uPA/uPAR can activate plasminogen [41], and TAFIa can inhibit pericellular plasminogen activation [76, 125, 126], this could be the mechanism of tube formation seen in our study. These results suggest that TAFIa decreases formation of tumour angiogenesis, potentially through inhibition of pericellular plasminogen activation.

There are some limitations to the tube formation assay used. The formation of tube-like structures could in part be a function of increased cell proliferation or increased cell adhesion, although this limitation could be argued to be a part of the differentiation

process that leads to the formation of tube-like structures on Cultrex [145]. Cultrex also contains many growth stimulating factors which leads to a gross stimulation of endothelial cells [145]. This results in large amounts of tube-like structures in the control, which causes increases in tube formation from pro-angiogenic factors to be less apparent [145]. Although Cultrex has been shown to direct endothelial cell differentiation, it is questionable whether the tube-like structures formed contain a lumen [145]. Therefore, the tube-like structures formed may not closely resemble blood vessels [145]. There is a lack of homogeneity in the tube-like structures formed which is another limitation of this assay [145]. Therefore, other morphological studies will have to be completed to further support these results, such as aortic ring assays. Angiogenic vessels grow from an aortic ring; the microvascular outgrowth can be quantified [145]. These assays have their own sets of limitations, such as variability of the aortic rings which can influence the outgrowth of microvessels [145].

4.1.2 Inhibition of TAFIa increases ECM proteolysis as a function of decreased inhibition of pericellular plasminogen activation

In order for endothelial tube formation to occur the vascular basement membrane must be locally degraded by proteolytic enzymes [152]. Proteolysis of the ECM also plays an important role in invasion and metastasis of tumour cells [153]. Using a 3D live-cell proteolysis assay, we examined the effect of TAFIa inhibition on degradation of DQ-collagen IV, a quenched fluorescent derivative of type IV collagen [136]. This assay allows for the imaging and quantification of pericellular and intracellular proteolysis [153]. We examined proteolysis of DQ-collagen IV by endothelial cells, and by two co-

culture systems containing endothelial cells (HUVECs) and breast cancer cells (SUM149 or MDA-MB-231 cells). The co-culture systems act to recapitulate a tumour microenvironment [154].

Inhibition of TAFIa increased total proteolysis of DQ-collagen IV in all three systems tested (Fig. 3.6-3.8). The HUVECs alone exhibited predominantly intracellular proteolysis. The co-culture consisting of HUVECs and SUM149 cells exhibited both pericellular and intracellular proteolysis (Fig. 3.7). The co-culture system consisting of HUVECs and MDA-MB-231 cells predominantly exhibited pericellular proteolysis (Fig. 3.8). Different proteases and pathways are involved in pericellular proteolysis as compared to intracellular proteolysis [136, 153]. The proteases involved in pericellular proteolysis are MMPs, serine proteases (including components of the plasminogen activation system), and cysteine proteases [136, 153]. Intracellular proteolysis involves endocytosis of DQ-collagen IV by the live cells, and degradation of the substrate in the lysosome [153, 155, 156]. Intracellular proteolysis can also occur after partial degradation of DQ-collagen IV with pericellular proteases, after which endocytosis and further degradation in the lysosome can occur [157]. In this manner the same proteolytic enzymes can be involved in pericellular and intracellular proteolysis [157]. Within the lysosome cysteine proteases degrade the DQ-collagen IV [136, 153]. Treatment of the HUVEC monoculture with PTCI increased intracellular proteolysis as compared to the control (Fig. 3.6), whereas treatment with PTCI increased pericellular proteolysis as compared to the control in both the co-culture systems (Fig. 3.7 & Fig. 3.8). This result suggests that inhibition of TAFIa in the breast cancer cells plays a larger role in pericellular proteolysis than inhibition of TAFIa in the endothelial cells. Alternatively,

these results could suggest that there is more pericellular proteolysis in a real tumour microenvironment since the co-cultures mimic a tumour microenvironment.

Inhibition of TAFIa could lead to increased pericellular proteolysis, and potentially intracellular proteolysis, through decreased inhibition of pericellular plasminogen activation. This is the potential mechanism because pericellular proteolysis can be caused by degradation of the ECM by components of the plasminogen activation system [136, 153], and plasmin can liberate and activate MMPs from the ECM [38].

Treatment of HUVECs alone with PTCI (Fig. 3.6) increased proteolysis of DQ-collagen IV more than treatment of either co-culture system with PTCI (Fig. 3.7 & Fig. 3.8). This could be due to the fact that the cancer cell lines are more malignant and invasive then the non-cancerous HUVECs, which causes them to have inherently more proteolytic activity. Therefore, the effect of PTCI on proteolysis of DQ-collagen IV by the co-culture systems appears less than in the HUVEC monoculture. Unpublished data from our laboratory have shown that there is more TAFI and TM expression in HUVECs than either breast cancer cell line. This could suggest that there is more TAFI activation in HUVECs compared to either breast cancer cell line. Therefore, the effect of inhibiting TAFIa is greater in HUVECs alone than in either co-culture system. There was no difference in relative tube length between the HUVEC monoculture and either co-culture system (Fig. 3.3-3.5) in contrast to what is seen with the proteolysis of DQ-collagen IV in the HUVEC monoculture compared to the co-culture systems (Fig. 3.6-3.8). This could suggest that TAFIa plays a larger role in proteolysis than in tube formation.

4.1.3 Differing effects of TAFIa inhibition on secretion and mRNA expression of MMP2 and MMP9

MMP2 and MMP9 have been implicated in angiogenesis through degradation of the ECM [53]. MMPs are also upregulated in many cancers, and have been shown to increase invasion and metastasis by degrading the ECM [49, 50]. MMPs have been implicated in pericellular proteolysis, and potentially in intracellular proteolysis through partial degradation of ECM components before endocytosis and lysosomal degradation [136, 153, 157]. Due to the significant increase in proteolysis of DQ-collagen IV by endothelial cells and endothelial cells co-cultured with breast cancer cells when treated with PTCI, we wanted to see the effect of TAFIa inhibition on secretion of pro-MMP2 and pro-MMP9, and mRNA expression of MMP2 and MMP9. We also wanted to determine the effect on mRNA expression and secretion of these MMPs on breast cancer cells alone, endothelial cells alone, and endothelial cells treated with CM from treated breast cancer cells. These systems were used to determine if the effects on MMP secretion and expression were cell specific, and to determine if soluble factors from PTCI-treated breast cancer cells can influence secretion and expression of MMPs in endothelial cells. Previous studies have shown that tumour-stromal cell interactions can lead to expression of MMPs [139, 158]. Once pro-MMP2 or pro-MMP9 have been made they are stored in the cytosol and are secreted by vesicles [159, 160]. Using gelatin zymography, bands from SUM149 or HUVEC media were assumed to be pro-MMP2 and pro-MMP9 because they migrated identically to recombinant pro-MMP2 and pro-MMP9 that were loaded as controls (Fig. 3.9-3.11). Results were also assumed to reflect a change in secretion of pro-MMP2 and pro-MMP9 from the cells in response to PTCI or

VEGF. Transcriptional regulation of MMP2 and MMP9 is complex and is not completely understood, but many cytokines, oncogenes, and growth factors have been shown to increase mRNA expression of these MMPs [161].

When SUM149 cells were treated with PTCI there was a significant increase in the secretion of pro-MMP2 and pro-MMP9, but there was no effect on mRNA expression of MMP2 or MMP9 (Fig. 3.9). When HUVECs were treated with PTCI there was no effect on pro-MMP2 secretion (no pro-MMP9 secretion was detected in these cells), but there was increased mRNA expression of both MMP2 and MMP9 (Fig. 3.10). These results suggest that inhibition of TAFIa increases secretion and mRNA expression of MMPs in a cell specific manner.

In order to see the effect that the tumour microenvironment has on MMP2 and MMP9 secretion and mRNA expression in endothelial cells, CM from treated SUM149 cells was used to treat HUVECs. Treatment of HUVECs with CM from untreated SUM149 cells resulted in a slight increase in secretion of pro-MMP2 (Fig. 3.11A). HUVECs treated with CM from PTCI treated SUM149 cells had significantly increased secretion of pro-MMP2 and increased mRNA expression of MMP2 and MMP9 (Fig. 3.11). These results show dynamic interplay between components of the tumour cell microenvironment. The secreted soluble factors produced from SUM149 cells treated with PTCI resulted in significantly increased secretion of pro-MMP2 by HUVECs, which was not seen in HUVECs treated with PTCI. These results suggest inhibition of TAFIa in SUM149 cells can alter soluble factors that can exert a paracrine effect on HUVECs.

Both PTCI treated SUM149 cells, and HUVECs treated with CM from PTCI treated SUM149 cells resulted in increased secretion of pro-MMPs, likely due to some mechanism of stored vesicle release [159, 160]. Both PTCI treated SUM149 cells, and HUVECs treated with CM from PTCI treated SUM149 cells resulted in increased mRNA expression of MMP2 and MMP9. The specific mechanism of how these treatments influenced MMP2 and MMP9 mRNA expression remain to be investigated. Many inflammatory mediators increase the mRNA expression of MMP2 and MMP9, such as IL-6, IL-1β, TNFα, and TNFβ [161, 162]. Interestingly, the anaphylatoxins, C3a and C5a, induce IL-6 and IL-1β expression [163–165]. TAFIa has been shown to inactivate C3a and C5a [117].Therefore inhibition of TAFIa could increase C3a and C5a leading to increased IL-6 and IL-1β, and therefore increased mRNA expression of MMP2 and MMP9. In this manner a function of TAFIa separate from pericellular plasminogen activation could play a role in the antimetastatic effect of TAFI.

These results taken together suggest inhibition of TAFIa results in differing secretion and mRNA expression of MMP2 and MMP9 dependent on cell type, and TAFIa inhibited SUM149 cells secrete soluble factors that can exert a paracrine effect on HUVECs.

4.2 Manipulation of TM cofactor activity suggests TAFIa plays a role in inhibition of tumour angiogenesis

TM has been shown to be antimetastatic and these effects are attributable to thrombin binding [91]. We hypothesized that TAFI was the substrate of thrombin-TM responsible for these effects due to its role in the inhibition of pericellular plasminogen activation [76, 125, 126, 128]. Using different mutations of recombinant TM (rTM) containing EGF-like repeats 3-6, responsible for substrate binding and activation, we looked at the effect of TAFI activation on tube formation and ECM proteolysis. We hypothesized that wild-type rTM EGF3-6 would decrease tube formation and ECM proteolysis, since this would result in an increase in TAFIa generation. While the role of TM in angiogenesis has not been firmly established, previous reports have shown that the EGF-like domain of TM may be pro-angiogenic [93]. The rTM EGF3-6 V340A/D341A mutant, on the other hand, would have no effect on these parameters because it is unable to support TAFIa activation (Fig. 3.12). We also used rTM EGF3-6 F376A, which with thrombin can activate TAFI but not protein C (Fig. 3.12). We hypothesized that this mutant would show the same effects as wild-type rTM EGF3-6, as this variant retains the ability to support TAFIa activation. The results, however, confounded our expectations.

Treatment with wild-type rTM EGF3-6 consistently had no effect on endothelial tube formation in any system (Fig. 3.13-3.15). In regards to tube formation, rTM containing all six EGF-like repeats (D2) and the serine/threonine domain (D3) (rTMD23) has been previously shown to significantly increase endothelial tube formation of HUVECs [93, 94]. Previous reports have also shown rTMD2 was less angiogenic than

rTMD23, suggesting the serine/threonine domain has angiogenic activity [93]. The variant of rTM we used in our experiments did not contain the serine/threonine domain, and only contained some of the EGF-like repeats. One possible conclusion from our work is therefore that EGF1-2 harbour pro-angiogenic activity. Treatment with wild-type rTM EGF3-6 significantly decreased proteolysis of DQ-collagen IV by endothelial cells alone compared to control (Fig. 3.16), but did not have a significant effect on proteolysis of DQ-collagen IV by either of the co-culture systems used compared to control (Fig. 3.17 & Fig. 3.18). This result could suggest that HUVECs, a normal human endothelial cell line, are more affected by the antimetastatic effects of TM than the cancer cell lines, which are inherently more proteolytic. Our results, at first glance, appear to suggest that EGF-like repeats 3-6 are neither pro-angiogenic nor anti-angiogenic in regards to endothelial tube formation and ECM proteolysis (in co-culture systems).

Treatment with rTM EGF3-6 V340A/D341A significantly increased tube formation in the endothelial monoculture and the co-culture systems containing endothelial and breast cancer cells compared to control and compared to wild-type rTM EGF3-6 (Fig. 3.13-3.15). Treatment with rTM EGF3-6 V340A/D341A significantly increased proteolysis of DQ-collagen IV by endothelial cells alone and in both co-culture systems significantly compared to control and compared to wild-type rTM EGF3-6 (Fig. 3.16-3.18). This result suggests that absence of TAFI activation increases degradation of type IV collagen. These results are consistent with the results we obtained through inhibition of TAFIa with PTCI.

On the other hand, treatment with rTM EGF3-6 F376A significantly decreased tube formation in all three systems used compared to control (Fig 3.13-3.15). Treatment

with rTM EGF3-6 F376A also significantly decreased tube formation in endothelial cells alone and the co-culture system consisting of HUVECs and SUM149 cells compared to wild-type rTM EGF3-6 (Fig. 3.14). Treatment with rTM EGF3-6 F376A decreased proteolysis in all three systems in which it was tested, although the decrease was only significant compared to control in the HUVEC monoculture (Fig. 3.16), and significant compared to wild-type rTM EGF3-6 in the HUVEC and SUM149 co-culture (Fig. 3.17). This mutant resulted in very little pericellular proteolysis in each of the three systems tested (Fig. 3.16-3.18). This result suggests that this mutant results in inhibition of proteases involved in pericellular proteolysis, such as plasmin and MMPs [157], consistent with its ability to support TAFI activation. Inhibition of pericellular plasminogen activation can lead to decreased plasmin and MMPs [41]. Hence, increased activation of TAFI by rTM EGF3-6 F376A could result in decreased pericellular proteolysis by inhibition of plasminogen activation.

These findings suggest that, in fact, the wild-type rTM EGF3-6 harbours both pro- and anti-angiogenic effects that essentially cancel each other out. The pro-angiogenic effects are mediated through activation of protein C. The anti-angiogenic effects are mediated through activation of TAFI. When activation of TAFI is prevented (the V340A/D341A mutant), the pro-angiogenic effects of TM are observable. When activation of PC is prevented (the F376A mutant), the anti-angiogenic effects of TM are observable. The role of TM in angiogenesis is not fully established, but our results using wild-type rTM EGF3-6 have added insight into its role. The lectin-like domain (D1) of TM was found to elicit anti-angiogenic effects through use of rTM containing only the lectin-like domain (rTMD1) [95]. rTMD1 was found to inhibit angiogenesis through

interaction with Lewis Y antigen thereby preventing it from its pro-angiogenic activities [95]. Previous reports have shown that rTM containing EGF-like repeats 1-6 exhibited mitogenic effects in Swiss 3T3 fibroblast cells [166]. In addition, rTMD2 (containing EGF1-6) and rTMD23 (containg EGF1-6 and serine/threonine-like domain) were found to stimulate HUVEC proliferation [93]. Furthermore, rTMD23 was found to be more mitogenic than rTMD2 [93]. Treatment with rTMD23 was shown to increase angiogenesis *in vitro* and *in vivo* [93].We found that the EGF-like repeats 3-6 were not mitogenic. Our results taken together with previous reports potentially pin-point the specific domains within TM responsible for the reported angiogenic effects. The serine/threonine-like domain may have pro-angiogenic properties because rTMD23 was more pro-angiogenic than rTMD2 [93], and we found EGF-like repeats 3-6 are not pro-angiogenic. The serine/threonine-like domain facilitates the attachment of a chondroitin sulfate (CS) moiety [78]. In fact, there are reports that CS is pro-angiogenic. CS from sea cucumber has been shown to be pro-angiogenic in the presence of fibroblast growth factor-2 (FGF-2) [167]. CS has also been shown to increase sprouting angiogenesis by binding TGF-β, VEGF, and PDGF [168]. Previous reports showing EGF-like domains 1-6 have pro-angiogenic properties [93, 166], considered with our result that EGF-like repeats 3-6 do not stimulate angiogenesis, suggest that EGF-like repeats 1 and 2 are responsible for the observed pro-angiogenic effects. Our results highlight the complex role TM plays in angiogenesis. In the full-length TM protein, the lectin-like domain is anti-angiogenic, the serine/threonine-like domain is pro-angiogenic, and EGF-like repeats 1-2 appear to be pro-angiogenic, EGF-like repeats 3-6 appear to have both anti-

angiogenic (through TAFI activation) and pro-angiogenic (through protein C activation) effects.

Our results are also consistent with the idea that TAFIa is an anti-angiogenic factor. On the other hand, the mutations of rTM EGF3-6 could be eliciting effects on tube formation and proteolysis of DQ-collagen IV due to protein C being a pro-angiogenic factor. The decrease in angiogenesis observed with rTM EGF3-6 F376A treatment could have been due to a loss of protein C activation. The increase in angiogenesis observed with rTM EGF3-6 V340A/D341A treatment could have been due to protein C activation. The role of protein C in cancer is not fully understood. There are reports that APC promotes proliferation, invasion, migration, angiogenesis, and DNA synthesis, as well as inhibition of apoptosis mediated by binding of APC to EPCR [97–99, 169]. Other studies have suggested APC limits extravasation of cancer cells, and overexpression of EPCR reduces metastasis *in vivo* [101, 102]. A recent study used mutants of rTMD23 that lack protein C activation (E357A, R385S, and D400A), and determined their effect on angiogenesis [94]. This study found that treatment with the mutants increased angiogenesis comparable to wild-type rTMD23, and therefore concluded that rTMD23 induced angiogenesis independent of protein C activation [94]. However, one of the mutations used in this study (E375A) had been previously shown to abolish thrombin binding to TM, consequently neither TAFI or protein C can be activated by this mutant [82]. Therefore, this study cannot clearly rule out the involvement of protein C.

A key experiment yet to be completed in our studies is the use of a mutant form of rTM EGF3-6 without the ability to bind thrombin, such as Q387P or E357A [81, 82]. The antimetastatic effects of TM have been shown to be dependent on thrombin binding [91],

and we found effects on angiogenesis were substrate activation dependent. We observed a cancelation of anti-angiogenic effects of TAFI activation and pro-angiogenic effects of protein C activation when using wild-type rTM EGF3-6, resulting in no effect on angiogenesis. We therefore hypothesize that a mutant without the ability to bind thrombin would also lead to no change in angiogenesis because neither TAFI nor protein C can be activated. Our studies using PTCI to inhibit TAFIa suggested that TAFIa decreases angiogenesis through pericellular plasminogen activation. These results support that the results we saw using rTM EGF3-6 mutants are an effect of TAFIa, since similar effects were seen with PTCI as were obtained with rTM EGF3-6 V340A/D341A. Further studies will have to be completed to determine the role of protein C activation on angiogenesis using the rTM EGF3-6 mutants. Treatment with an inhibitor of APC and rTM EGF3-6 V340A/D341A should be completed to determine the role of APC on angiogenesis. If both the anti-angiogenic effects TAFI activation and the pro-angiogenic effects of protein C activation are equal, inhibition of APC when treating with the V340A/D341A mutant should result in no effect on angiogenesis since there will be neither TAFIa nor APC generation. Similarly, an experiment using treatment of both PTCI and the F376A mutant should be completed to determine the role of TAFIa on angiogenesis. Assuming that both the anti-angiogenic effects TAFI activation and the pro-angiogenic effects of protein C activation are equal, inhibition of TAFIa when treating with the F376A mutant should result in no effect on angiogenesis since there will be neither TAFIa nor APC generation. These experiments should help determine the anti-angiogenic and pro-angiogenic activities of EGF3-6 of TM.

The same trends were observed when the rTM EGF3-6 mutants were used as seen with PTCI treatment on increased proliferation of HUVECs in the MDA-MB-231 and HUVEC co-culture, suggesting that both the rTM EGF3-6 and PTCI treatments share a common underlying mechanism. Similarly, treatment of HUVECs alone with the rTM EGF3-6 mutants (Fig. 3.16) resulted in proportionally larger effects than with either co-culture system (Fig. 3.17 & Fig. 3.18) on the proteolysis of DQ-collagen IV as seen with treatment with PTCI. This again suggests treatments with rTM EGF3-6 and PTCI share a common underlying mechanism. There was a slight increase in the effect of treatment with rTM EGF3-6 V340A/D341A on proteolysis of DQ-collagen IV in the co-culture system containing MDA-MB-231 cells and HUVECs (Fig. 3.18) as compared to the co-culture system containing SUM149 cells and HUVECs (Fig. 3.17). Our laboratory has found that there is less TM and TAFI expression in the more metastatic MDA-MB-231 cells than in SUM149 cells. There would likely be more TAFI available to be activated in the SUM149 cells than the MDA-MB-231 cells. Treatment with rTM EGF3-6 V340A/D341A should have resulted in a larger increase in proteolysis in the co-culture system containing SUM149 cells since there would be a larger overall change in the amount of TAFI activation compared to that in the MDA-MB-231 cells. Therefore, this result may not have been due to a difference in TAFI activation and potentially could be attributed to protein C activation. The amount of protein C expressed in these cell lines has not been determined. On the other hand, the amount of TAFI that can be activated by these breast cancer cell lines could differ from the amount of TAFI expressed. Treatment with rTM EGF3-6 F376A did not result in a significant decrease in proteolysis of DQ-collagen IV compared to control in either of the co-culture systems (Fig. 3.17 & Fig.

3.18), but there was a significant decrease in the HUVEC monoculture (Fig. 3.16). This could suggest that using this mutant may not be effective on treatment of tumour angiogenesis of highly metastatic cancers since these breast cancer cell lines are highly invasive metastatic cell lines. However, by the time cancer cells become highly metastatic treating tumour angiogenesis is usually ineffective. Therefore, these results might suggest that treatment with rTM EGF3-6 F376A would be more effective at an earlier stage of cancer.

Taken together these results suggest that TAFI activation, using TM as a cofactor, plays a significant role in endothelial tube formation and on proteolysis of type IV collagen. Our findings also represent proof-of-principle that stimulation of TAFI activation in the tumour microenvironment using a variant of TM that cannot support protein C activation might be a viable strategy to inhibit tumour angiogenesis.

4.3 Alternate mechanisms of TAFIa antimetastatic effects

We hypothesized that TAFIa is responsible for the antimetastatic effects of TM through inhibition of pericellular proteolysis by cleaving carboxyl-terminal lysine residues from plasminogen receptors. However, TAFIa can also inactivate some inflammatory mediators that may play roles in cancer. TAFIa can inactivate these inflammatory mediators through removal of carboxyl-terminal lysine and arginine residues from C3a, C5a, bradykinin (BK), and thrombin-cleaved OPN (OPN-R) [77, 117].

The anaphylatoxins, C3a and C5a, are potent leukocyte chemoattractants [77], and have been implicated in cancer. C3a and C5a have been shown to increase proliferation, angiogenesis, invasion, migration, and growth factor/cytokine production [164]. As mentioned previously (4.1.3), they can increase mRNA expression of IL-6 and IL-1β which can potentially increase MMP2 and MMP9 mRNA expression [161–165]. C3a and C5a also stimulate secretion of VEGF, the key mediator of angiogenesis [164, 170].

BK plays a role in inflammation by increasing vasodilation and vascular permeability [77], it has also been shown to have metastatic properties. BK has been shown to increase migration, MMP9 mRNA expression and secretion in prostate cancer cells [171]. BK has also been shown to increase proliferation in epithelial breast cancer cells [172]. BK has been implicated in tumour angiogenesis by promoting VEGF expression [173].

OPN is involved in inflammation, but also has many metastatic properties [77]. OPN expression has been shown to be elevated in many cancers, especially in breast cancer where increased expression correlates with poor prognosis [174]. OPN is involved in cell adhesion, migration, invasion, and proliferation [174]. OPN has been implicated in the plasminogen activation system through integrin signaling and stimulation of uPA [174]. OPN can also up regulate pro-MMP2 [174]. OPN can induce VEGF expression, thereby increasing angiogenesis [175]. OPN can be cleaved by thrombin resulting in a carboxyl-terminal arginine residue (OPN-R). OPN-R has been shown to be more metastatic that OPN through increased adhesion, migration, and spreading of various cell types [119, 175]. OPN-R has also been shown to upregulate the proinflammatory effects

of OPN [77]. TAFIa has been shown cleave OPN-R forming OPN-L [77]. OPN-L has been shown to reduce the pro-inflammatory effects of OPN-R [77]. OPN-L has also been shown to decrease cell adhesion compared to OPN-R in Jurkat cells and sinovocytes [77, 176].

Inactivation of these inflammatory mediators by TAFIa suggests that there are alternate mechanisms of antimetastatic effects of TAFIa.

4.4 Future Directions

The results from this study suggest that TAFIa plays a role in decreasing tumour angiogenesis. However, further experiments have to be completed to strengthen these findings.

Specifically, we need to look at the effect on endothelial cell invasion and proliferation, and MMP mRNA expression and secretion with the rTM EGF3-6 mutants as completed with inhibition of TAFIa with PTCI. These experiments should be completed to further show an effect of these mutants on angiogenesis *in vitro*. As mentioned previously, to confirm the role of APC in the effects on angiogenesis of the rTM mutants, we need to complete experiments inhibiting TAFIa and APC in these mutants.

A stable variant of TAFI, CIIQY [177], in our laboratory has recently been shown to inhibit breast cancer cell invasion, migration, and degradation of DQ-collagen IV (unpublished). It is also the first direct evidence that TAFIa plays an antimetastatic role.

This variant of TAFI should be used to determine a direct effect of TAFIa on tumour angiogenesis in the future.

We also want to look at the effect of TAFIa on angiogenesis *in vivo* using zebrafish. Zebrafish can be used as an *in vivo* model that allows inexpensive, higher-throughput screening than other available *in vivo* models [145]. Transgenic zebrafish lines with fluorescent (GFP-labelled) blood vessels can be used to image angiogenesis [178]. Sprouting intersegmental vessels (ISVs), and subintestinal vein (SIVs) vessels do so by angiogenesis, and can be easily quantified [145, 179]. We could test the rTM EGF3-6 mutants, or stable TAFI, and determine the effect of TAFIa on angiogenesis. Mammalian tumour cells can be xenotransplanted into zebrafish embryos and used to study tumour angiogenesis, invasion, and metastasis [179]. This system allows for the delivery of a limited number of cells which mimics the initial stages of tumour angiogenesis [179]. Moreover, fluorescently labelled tumour cells and vasculature can be easily visualized allowing analysis of temporal and spatial relationship between the cells [179]. We could fluorescently labelled MDA-MB-231 or SUM149 breast cancer cells and inject them, along with rTM EGF3-6 mutants, or stable TAFI, and look at the effect of TAFIa on tumour angiogenesis *in vivo*.

4.5 Conclusions

In conclusion, this study determined inhibition of TAFIa with PTCI increased angiogenesis and tumour angiogenesis *in vitro* by increasing cell proliferation, invasion, endothelial tube formation, proteolysis of DQ-collagen IV, and secretion and mRNA expression of MMP2 and MMP9. These results most likely occurred due to a decrease in inhibition of pericellular plasminogen activation by TAFIa. Also, using rTM containing EGF-like repeats 3-6 with differing cofactor ability, TAFIa was determined to decrease angiogenesis and tumour angiogenesis *in vitro* through endothelial tube formation and DQ-collagen IV proteolysis experiments. These effects indirectly suggest TAFIa decreases angiogenesis. Further experiments are required to confirm the effects seen with certain rTM EGF3-6 mutants reflected effects on protein C activation. Furthermore, a direct effect of TAFIa on angiogenesis needs to be tested using a stable variant of TAFI. Additionally, *in vivo* experiments using zebrafish need to be completed to look at both angiogenesis and tumour angiogenesis in a more biologically relevant system. These results are promising in suggesting an anti-angiogenic role for TAFIa, and could eventually lead to the production of a therapeutic to prevent tumour angiogenesis using rTM EGF3-6 F376A or a stable variant of TAFI.

References

1. Weinberg, R. A. How Cancer Arises. *Sci. Am.* **275,** 62–70 (1996).

2. Hanahan, D. & Weinberg, R. A. The hallmarks of cancer. *Cell* **100,** 57–70 (2000).

3. Cancer statistics at a glance - Canadian Cancer Society. at <https://www.cancer.ca/en/cancer-information/cancer-101/cancer-statistics-at-a-glance/?region=on>

4. Croce, C. M. Oncogenes and cancer. *N. Engl. J. Med.* **358,** 502–511 (2008).

5. Vineis, P., Schatzkin, A. & Potter, J. D. Models of carcinogenesis: An overview. *Carcinogenesis* **31,** 1703–1709 (2010).

6. Hanahan, D. & Weinberg, R. A. Hallmarks of cancer: The next generation. *Cell* **144,** 646–674 (2011).

7. Risau, W. Mechanisms of angiogenesis. *Nature* **386,** 671–674 (1997).

8. Hanahan, D. & Folkman, J. Patterns and emerging mechanisms of the angiogenic switch during tumorigenesis. *Cell* **86,** 353–364 (1996).

9. Bergers, G. & Benjamin, L. E. Tumorigenesis and the angiogenic switch. *Nat. Rev. Cancer* **3,** 401–410 (2003).

10. Pepper, M. S. Role of the Matrix Metalloproteinase and Plasminogen Activator – Plasmin Systems in Angiogenesis. *Arterioscler. Thromb.* 1104–1117 (2001). doi:10.1161/hq0701.093685

11. Folkman, J. Angiogenesis in cancer, vascular, rheumatoid and other disease. *Nat. Med.* **1,** 27–31 (1995).

12. Folkman, J. Angiogenesis. *Annu. Rev. Med.* **57,** 1–18 (2006).

13. Folkman, J. Tumor Angiogenesis: Therapeutic Implications. *N. Engl. J. Med.* **285,** 1182–1186 (1971).

14. Gimbrone, M., Leapman, S., Cotran, R. & Folkman, J. Tumor Dormancy In Vivo By Prevention of Neovascularization. *J. Exp. Med.* **136,** 261–276 (1972).

15. Stephenson, J. A., Goddard, J. C., Dennison, A. R. & Morgan, B. Tumour Angiogenesis : A Growth Area — From John Hunter to Judah Folkman and Beyond Hunter to Folkman — A Slow Beginning. *J. Cancer Res.* **2013,** 1–6 (2013).

16. Zetter, B. R. Angiogenesis and tumor metastasis. *Annu. Rev. Med.* **49,** 407–424 (1998).

17. Baluk, P., Hashizume, H. & McDonald, D. M. Cellular abnormalities of blood vessels as targets in cancer. *Curr. Opin. Genet. Dev.* **15,** 102–111 (2005).

18. Carmeliet, P. & Jain, R. K. Angiogenesis in cancer and other diseases. *Nature* **407,** 249–257 (2000).

19. Talmadge, J. E. & Fidler, I. J. AACR centennial series: The biology of cancer metastasis: Historical perspective. *Cancer Res.* **70,** 5649–5669 (2010).

20. Chambers, A. F. & Matrisian, L. M. Changing Views of the Role of Matrix. *J. Natl. cancer insitute* **89,** 1260–1270 (1997).

21. Ferrara, N. Vascular endothelial growth factor: Basic science and clinical progress. *Endocr. Rev.* **25,** 581–611 (2004).

22. Senger, D. R. *et al.* Tumor cells secrete a vascular permeability factor that promotes accumulation of ascites fluid. *Science.* **219,** 983–985 (1983).

23. Ferrara, N. & Henzel, W. J. Pituitary follicular cells secrete a novel heparin-binding growth factor specific for vascular endothelial cells. *Biochem. Biophys. Res. Commun.* **161,** 851–858 (1989).

24. Ferrara, N. VEGF as a therapeutic target in cancer. *Oncology* **69,** 11–16 (2005).

25. Carmeliet, P. VEGF as a key mediator of angiogenesis in cancer. *Oncology* **69,** 4–10 (2005).

26. Park, J. E., Keller, G. A. & Ferrara, N. The vascular endothelial growth factor (VEGF) isoforms: differential deposition into the subepithelial extracellular matrix and bioactivity of extracellular matrix-bound VEGF. *Mol. Biol. Cell* **4,** 1317–1326 (1993).

27. Pepper, M., Ferrara, N., Orci, L. & Montesano, R. Vascular Endothelial Growth Factor (VEGF) Induces Plasminogen Activators and Plasminogen Activator Inhibitor-1 in Microvascular Endothelial Cells. *Biochem. Biophys. Res. Commun.* **181,** 902–906 (1991).

28. Mandriota, S. *et al.* Vascular Endothelial Growth Factor increases Urokinase Receptor Expression in Vascular Endohelial Cells. *J Biol Chem.* **270,** 9709–9716 (1995).

29. Hollborn, M. *et al.* Positive feedback regulation between MMP-9 and VEGF in human RPE cells. *Investig. Ophthalmol. Vis. Sci.* **48,** 4360–4367 (2007).

30. Dvorak, H. F., Brown, L. F., Detmar, M. & Dvorak, A. M. Vascular permeability factor/vascular endothelial growth factor, microvascular hyperpermeability, and angiogenesis. *Am. J. Pathol.* **146,** 1029–1039 (1995).

31. Masood, R. *et al.* Vascular endothelial growth factor (VEGF) is an autocrine growth factor for VEGF receptor-positive human tumors. *Blood* **98,** 1904–1913 (2001).

32. Sitohy, B., Nagy, J. A. & Dvorak, H. F. Anti-VEGF/VEGFR therapy for cancer: Reassessing the target. *Cancer Res.* **72,** 1909–1914 (2012).

33. Hayes, D. F. Bevacizumab treatment for solid tumors: boon or bust? *JAMA* **305,** 506–508 (2011).

34. Jain, R. K., Duda, D. G., Clark, J. W. & Loeffler, J. S. Lessons from phase III clinical trials on anti-VEGF therapy for cancer. *Nat. Clin. Pract. Oncol.* **3,** 24–40 (2006).

35. Andreasen, P. A., Egelund, R. & Petersen, H. H. The plasminogen activation system in tumor growth, invasion, and metastasis. *Cell. Mol. life Sci.* **57,** 25–40 (2000).

36. Ulisse, S., Baldini, E., Sorrenti, S. & D'Armiento, M. The urokinase plasminogen activator system: a target for anti-cancer therapy. *Curr. Cancer Drug Targets* **9,** 32–71 (2009).

37. Godier, A. & Hunt, B. J. Plasminogen receptors and their role in the pathogenesis of inflammatory, autoimmune and malignant disease. *J. Thromb. Haemost.* **11,** 26–34 (2013).

38. Deryugina, E. I. & Quigley, J. P. Cell surface remodeling by plasmin: A new function for an old enzyme. *J. Biomed. Biotechnol.* **2012,** 1–21 (2012).

39. Plow, E. F., Doeuvre, L. & Das, R. So many plasminogen receptors: Why? *J. Biomed. Biotechnol.* **2012,** 1–7 (2012).

40. Blasi, F. & Carmeliet, P. uPAR: a versatile signalling orchestrator. *Nat. Rev. Mol. Cell Biol.* **3,** 932–943 (2002).

41. Smith, H. W. & Marshall, C. J. Regulation of cell signalling by uPAR. *Nat. Rev. Mol. Cell Biol.* **11,** 23–36 (2010).

42. Christensen, B., Schack, L., Kläning, E. & Sørensen, E. S. Osteopontin is cleaved at multiple sites close to its integrin-binding motifs in milk and is a novel substrate for plasmin and cathepsin D. *J. Biol. Chem.* **285,** 7929–7937 (2010).

43. Sidenius, N. & Blasi, F. The urokinase plasminogen activator system in cancer: Recent advances and implication for prognosis and therapy. *Cancer Metastasis Rev.* **22,** 205–222 (2003).

44. Look, M. P. *et al.* Pooled analysis of prognostic impact of urokinase-type plasminogen activator and its inhibitor PAI-1 in 8377 breast cancer patients. *J. Natl. Cancer Inst.* **94,** 116–128 (2002).

45. Pepper, M. S., Vassalli, J. D., Montesano, R. & Orci, L. Urokinase-type plasminogen activator is induced in migrating capillary endothelial cells. *J Cell Biol* **105,** 2535–2541 (1987).

46. Bajou, K. *et al.* Absence of host plasminogen activator inhibitor 1 prevents cancer invasion and vascularization. *Nat. Med.* **4,** 923–938 (1998).

47. Deng, G., Curriden, S. A., Wang, S., Rosenberg, S. & Loskutoff, D. J. Is plasminogen activator inhibitor-1 the molecular switch that governs urokinase receptor-mediated cell adhesion and release? *J. Cell Biol.* **134,** 1563–1571 (1996).

48. Stefansson, S. & Lawrence, D. A. The serpin PAI-1 inhibits cell migration by blocking integrin αvβ3 binding to vitronectin. *Nature* **383,** 441–443 (1996).

49. Kessenbrock, K., Plaks, V. & Werb, Z. Matrix Metalloproteinases: Regulators of the Tumor Microenvironment. *Cell* **141,** 52–67 (2010).

50. Page-McCaw, A., Ewald, A. J. & Werb, Z. Matrix metalloproteinases and the regulation of tissue remodelling. *Nat. Rev. Mol. Cell Biol.* **8,** 221–233 (2007).

51. Van Wart, H. E. & Birkedal-Hansen, H. The cysteine switch: a principle of regulation of metalloproteinase activity with potential applicability to the entire matrix metalloproteinase gene family. *Proc. Natl. Acad. Sci. U. S. A.* **87,** 5578–5582 (1990).

52. Sternlicht, M. & Werb, Z. How Matrix metalloproteinases regulate cell behavior. *Annu Rev Cell Biol* **17,** 463–516 (2001).

53. Egeblad, M. & Werb, Z. New functions for the matrix metalloproteinases in cancer progression. *Nat. Rev. Cancer* **2,** 161–174 (2002).

54. Itoh, T. *et al.* Reduced angiogenesis and tumor progression in gelatinase A-deficient mice. *Cancer Res.* **58,** 1048–1051 (1998).

55. Vu, T. H. *et al.* MMP-9/gelatinase B is a key regulator of growth plate angiogenesis and apoptosis of hypetrophic chondrocytes. *Cell* **93,** 411–422 (1998).

56. Zhou, Z. *et al.* Impaired endochondral ossification and angiogenesis in mice deficient in membrane-type matrix metalloproteinase I. *Proc. Natl. Acad. Sci. U. S. A.* **97,** 4052–4057 (2000).

57. Lee, S., Jilan, S. M., Nikolova, G. V., Carpizo, D. & Luisa Iruela-Arispe, M. Processing of VEGF-A by matrix metalloproteinases regulates bioavailability and vascular patterning in tumors. *J. Cell Biol.* **169,** 681–691 (2005).

58. Bodary, P. F., Wickenheiser, K. J. & Eitzman, D. T. Recent advances in understanding endogenous fibrinolysis: implications for molecular-based treatment of vascular disorders. *Expert Rev. Mol. Med.* **4,** 1–10 (2002).

59. Rasche, H. Haemostasis and thrombosis: an overview. *Eur. Hear. J. Suppl.* **3,** Q3–Q7 (2001).

60. Boffa, M. B. & Koschinsky, M. L. Curiouser and curiouser: Recent advances in measurement of thrombin-activatable fibrinolysis inhibitor (TAFI) and in understanding its molecular genetics, gene regulation, and biological roles. *Clin. Biochem.* **40,** 431–442 (2007).

61. Wu, K. K. & Thiagarajan, P. Role of endothelium in thrombosis and hemostasis. *Annu. Rev. Med.* **47,** 315–331 (1996).

62. Ruggeri, Z. M. Platelets in atherothrombosis. *Nat. Med.* **4,** 1227–1234 (2002).

63. Bouma, B. N. & Mosnier, L. O. Thrombin activatable fibrinolysis inhibitor (TAFI)--how does thrombin regulate fibrinolysis? *Ann. Med.* **38,** 378–388 (2006).

64. Nesheim, M. Thrombin and fibrinolysis. *Chest* **124,** 33–39 (2003).

65. Opal, S. M. & Esmon, C. T. Bench-to-bedside review: functional relationships between coagulation and the innate immune response and their respective roles in the pathogenesis of sepsis. *Crit. Care* **7,** 23–38 (2003).

66. Dahlbäck, B. & Villoutreix, B. O. Regulation of blood coagulation by the protein C anticoagulant pathway: Novel insights into structure-function relationships and molecular recognition. *Arterioscler. Thromb. Vasc. Biol.* **25,** 1311–1320 (2005).

67. Broze, G. J. & Higuchi, D. A. Coagulation-dependent inhibition of fibrinolysis: role of carboxypeptidase-U and the premature lysis of clots from hemophilic plasma. *Blood* **88,** 3815–3823 (1996).

68. Foley, J. H., Kim, P. Y., Mutch, N. J. & Gils, A. Insights into thrombin activatable fibrinolysis inhibitor function and regulation. *J. Thromb. Haemost.* **11,** 306–315 (2013).

69. Plow, E. F., Freaney, D. E., Plescia, J. & Miles, L. A. The plasminogen system and cell surfaces: Evidence for plasminogen and urokinase receptors on the same cell type. *J. Cell Biol.* **103,** 2411–2420 (1986).

70. Mosnier, L. O., Meijers, J. C. M. & Bouma, B. N. Regulation of fibrinolysis in plasma by TAFI and protein C is dependent on the concentration of thrombomodulin. *Thromb. Haemost.* **85,** 5–11 (2001).

71. Esmon, C. T. The Protein C Pathway. *Chest* **124,** 26S–32S (2003).

72. Esmon, N. L., Owen, W. G. & Esmon, C. T. Isolation of a membrane bound cofactor for thrombin catalyzed activation of protein C. *J. Biol. Chem.* **257,** 859–864 (1982).

73. Rezaie, A. R. Regulation of the protein C anticoagulant and antiinflammatory pathways. *Curr. Med. Chem.* **17,** 2059–2069 (2010).

74. Nesheim, M. *et al.* Thrombin, thrombomodulin and TAFI in the molecular link between coagulation and fibrinolysis. *Thromb. Haemost.* **78,** 386–91 (1997).

75. Bajzar, L., Morser, J. & Nesheim, M. TAFI, or plasma procarboxypeptidase B, couples the coagulation and fibrinolytic cascades through the thrombin-thrombomodulin complex. *J. Biol. Chem.* **271,** 16603–16608 (1996).

76. Redlitz, A., Tan, A. K., Eaton, D. L. & Plow, E. F. Plasma Cabrboxypeptidases as Regulators of the Plasminogen System. *J. Clin. Invest.* **96,** 2534–2538 (1995).

77. Myles, T. *et al.* Thrombin Activatable Fibrinolysis Inhibitor, a Potential Regulator of Vascular Inflammation. *J. Biol. Chem.* **278,** 51059–51067 (2003).

78. Conway, E. M. Thrombomodulin and its role in inflammation. *Semin. Immunopathol.* **34,** 107–125 (2012).

79. Zhang, Y. *et al.* Thrombomodulin Modulates Growth of Tumor Cells Independent of its. *J. Clin. Invest.* **101,** 1301–1309 (1998).

80. Wen, D. *et al.* Human thrombomodulin: Complete cDNA sequence and chromosome localization of the gene. *Biochemistry* **26,** 4350–4357 (1987).

81. Nagashima, M., Lundh, E., Leonard, J. C., Morser, J. & Parkinson, J. F. Alanine-scanning mutagenesis of the epidermal growth factor-like domains of human thrombomodulin identifies critical residues for its cofactor activity. *J. Biol. Chem.* **268,** 2888–2892 (1993).

82. Wang, W., Nagashima, M., Schneider, M., Morser, J. & Nesheim, M. Elements of the primary structure of thrombomodulin required for efficient thrombin-activable fibrinolysis inhibitor activation. *J. Biol. Chem.* **275,** 22942–22947 (2000).

83. Boffa, M. C. & Karmochkine, M. Thrombomodulin: an overview and potential implications in vascular disorders. *Lupus* **7,** S120–S125 (1998).

84. Glaser, C. B. *et al.* Oxidation of a specific methionine in thrombomodulin by activated neutrophil products blocks cofactor activity: A potential rapid mechanism for modulation of coagulation. *J. Clin. Invest.* **90,** 2565–2573 (1992).

85. Li, Y., Kuo, C., Shi, G. & Wu, H. The role of thrombomodulin lectin-like domain in inflammation. *J. Biomed. Sci.* **19,** 34 (2012).

86. Horowitz, N. A. & Palumbo, J. S. Mechanisms coupling thrombomodulin to tumor dissemination. *Thromb. Res.* **129,** S119–S121 (2012).

87. Menschikowski, M. *et al.* Regulation of thrombomodulin expression in prostate cancer cells. *Cancer Lett.* **322,** 177–184 (2012).

88. Ogawa, H. *et al.* Expression of thrombomodulin in squamous cell carcinoma of the lung: its relationship to lymph node metastasis and prognosis of the patients. *Cancer Lett.* **149,** 95–103 (2000).

89. Kim, S. J. *et al.* Thrombomodulin is a new biological and prognostic marker for breast cancer: an immunohistochemical study. *Anticancer Res.* **17,** 2319–2323 (1997).

90. Hosaka, Y., Higuchi, T., Tsumagari, M. & Ishii, H. Inhibition of invasion and experimental metastasis of murine melanoma cells by human soluble thrombomodulin. *Cancer Lett.* **161,** 231–240 (2000).

91. Horowitz, N. A. *et al.* Thrombomodulin is a determinant of metastasis through a mechanism linked to the thrombin binding domain but not the lectin-like domain. *Blood* **118,** 2889–2895 (2011).

92. Weiler-Guettler, H. *et al.* A targeted point mutation in thrombomodulin generates viable mice with a prethrombotic state. *J. Clin. Invest.* **101,** 1983–1991 (1998).

93. Shi, C. S. *et al.* Evidence of human thrombomodulin domain as a novel angiogenic factor. *Circulation* **111,** 1627–1636 (2005).

94. Kuo, C. H. *et al.* FGFR1 mediates recombinant thrombomodulin domain-induced angiogenesis. *Cardiovasc. Res.* **105,** 107–117 (2015).

95. Kuo, C. H. *et al.* The recombinant lectin-like domain of thrombomodulin inhibits angiogenesis through interaction with Lewis Y antigen. *Blood* **119,** 1302–1313 (2012).

96. Bouwens, E. A. M., Stavenuiter, F. & Mosnier, L. O. Mechanisms of anticoagulant and cytoprotective actions of the protein C pathway. *J. Thromb. Haemost.* **11,** 242–253 (2013).

97. Van Sluis, G. L., Büller, H. R. & Spek, C. A. The role of activated protein C in cancer progression. *Thromb. Res.* **125 Suppl ,** S138–S142 (2010).

98. Spek, C. A. & Arruda, V. R. The protein C pathway in cancer metastasis. *Thromb. Res.* **129,** S80–S84 (2012).

99. Uchiba, M. *et al.* Activated protein C induces endothelial cell proliferation by mitogen-activated protein kinase activation in vitro and angiogenesis in vivo. *Circ. Res.* **95,** 34–41 (2004).

100. Beaulieu, L. M. & Church, F. C. Activated protein C promotes breast cancer cell migration through interactions with EPCR and PAR-1. *Exp. Cell Res.* **313,** 677–687 (2007).

101. Van Sluis, G. L. *et al.* Endogenous activated protein C limits cancer cell extravasation through sphingosine-1-phosphate receptor 1-mediated vascular endothelial barrier enhancement. *Blood* **114,** 1968–1973 (2009).

102. Bezuhly, M. *et al.* Role of activated protein C and its receptor in inhibition of tumor metastasis. *Blood* **113,** 3371–3374 (2009).

103. Antoń, I. *et al.* Receptor of activated protein C promotes metastasis and correlates with clinical outcome in lung adenocarcinoma. *Am. J. Respir. Crit. Care Med.* **186,** 96–105 (2012).

104. Hendriks, D., Scharpé, S., van Sande, M. & Lommaert, M. P. Characterisation of a carboxypeptidase in human serum distinct from carboxypeptidase N. *J. Clin. Chem. Clin. Biochem.* **27,** 277–285 (1989).

105. Campbell, W. & Okada, H. An arginine specific carboxypeptidase generated in blood during coagulation or inflammation which is unrelated to carboxypeptidase N or its subunits. *Biochem. Biophys. Res. Commun.* **162,** 933–939 (1989).

106. Eaton, D. L., Malloy, B. E., Tsai, S. P., Henzel, W. & Drayna, D. Isolation, molecular cloning, and partial characterization of a novel carboxypeptidase B from human plasma. *J. Biol. Chem.* **266,** 21833–21838 (1991).

107. Wang, W., Hendriks, D. F. & Scharpé, S. S. Carboxypeptidase U, a plasma carboxypeptidase with high affinity for plasminogen. *J. Biol. Chem.* **269,** 15937–15944 (1994).

108. Bajzar, L., Manuel, R. & Nesheim, M. E. Purification and characterization of TAFI, a thrombin-activable fibrinolysis inhibitor. *J. Biol. Chem.* **270,** 14477–14484 (1995).

109. Bajzar, L. & Nesheim, M. The effect of activated protein C on fibrinolysis in cell-free plasma can be attributed specifically to attenuation of prothrombin activation. *J. Biol. Chem.* **268,** 8608–8616 (1993).

110. Lin, J. H. H. *et al.* Identification of human thrombin-activatable fibrinolysis inhibitor in vascular and inflammatory cells. *Thromb. Haemost.* **105,** 999–1009 (2011).

111. Hori, Y. *et al.* Insulin enhanced thrombin-activable fibrinolysis inhibitor expression through PI3 kinase/Akt pathway. *Int. J. Mol. Med.* **15,** 265–268 (2005).

112. Marx, P. F. *et al.* Crystal structures of TAFI elucidate the inactivation mechanism of activated TAFI: A novel mechanism for enzyme autoregulation. *Blood* **112,** 2803–2809 (2008).

113. Boffa, M. B., Wang, W., Bajzar, L. & Nesheim, M. E. Plasma and recombinant thrombin-activable fibrinolysis inhibitor (TAFI) and activated TAFI compared with respect to glycosylation, thrombin/thrombomodulin-dependent activation, thermal stability, and enzymatic properties. *J. Biol. Chem.* **273,** 2127–2135 (1998).

114. Valnickova, Z. *et al.* Post-translational modifications of human thrombin-activatable fibrinolysis inhibitor (TAFI): Evidence for a large shift in the isoelectric point and reduced solubility upon activation. *Biochemistry* **45,** 1525–1535 (2006).

115. Mao, S. S., Cooper, C. M., Wood, T., Shafer, J. A. & Gardell, S. J. Characterization of plasmin-mediated activation of plasma procarboxypeptidase B. Modulation by glycosaminoglycans. *J. Biol. Chem.* **274,** 35046–35052 (1999).

116. Marx, P. F., Dawson, P. E., Bouma, B. N. & Meijers, J. C. M. Plasmin-mediated activation and inactivation of thrombin-activatable fibrinolysis inhibitor. *Biochemistry* **41,** 6688–6696 (2002).

117. Campbell, W. D., Lazoura, E., Okada, N. & Okada, H. Inactivation of C3a and C5a octapeptides by carboxypeptidase R and carboxypeptidase N. *Microbiol. Immunol.* **46,** 131–134 (2002).

118. Smith, L. L. *et al.* Protein Chemistry and Structure : Osteopontin N-terminal Domain Contains a Cryptic Adhesive Sequence Recognized by Osteopontin N-terminal Domain Contains a Cryptic Adhesive Sequence Recognized by α9β1 Integrin. *J. Biol. Chem.* **271,** 28485–28491 (1996).

119. Senger, D. R., Perruzzi, C. A., Papadopoulos-Sergiou, A. & Van de Water, L. Adhesive properties of osteopontin: regulation by a naturally occurring thrombin-cleavage in close proximity to the GRGDS cell-binding domain. *Mol. Biol. Cell* **5,** 565–574 (1994).

120. Renckens, R. *et al.* Absence of Thrombin-Activatable Fibrinolysis Inhibitor Protects against Sepsis-Induced Liver Injury in Mice. *J. Immunol.* **175,** 6764–6771 (2005).

121. Te Velde, E. A. *et al.* Impaired healing of cutaneous wounds and colonic anastomoses in mice lacking thrombin-activatable fibrinolysis inhibitor. *J. Thromb. Haemost.* **1,** 2087–2096 (2003).

122. Romer, J. *et al.* Impaired wound healing in mice with a disrupted plasminogen gene. *Nat. Med.* **2,** 287–292 (1996).

123. Boffa, M. B. TAFI and wound healing: Closing a knowledge gap. *J. Thromb. Haemost.* **1,** 2075–2077 (2003).

124. Drew, A. F., Liu, H., Davidson, J. M., Daugherty, C. C. & Degen, J. L. Wound-healing defects in mice lacking fibrinogen. *Blood* **97,** 3691–3698 (2001).

125. Swaisgood, C. M., Schmitt, D., Eaton, D. & Plow, E. F. In vivo regulation of plasminogen function by plasma carboxypeptidase B. *J. Clin. Invest.* **110,** 1275–1282 (2002).

126. Okumura, N., Koh, T., Hasebe, Y., Seki, T. & Ariga, T. A novel function of thrombin-activatable fibrinolysis inhibitor during rat liver regeneration and in growth-promoted hepatocytes in primary culture. *J. Biol. Chem.* **284,** 16553–16561 (2009).

127. Reijerkerk, A. *et al.* Tumor growth and metastasis are not affected in thrombin-activatable fibrinolysis inhibitor-deficient mice. *J. Thromb. Haemost.* **2,** 769–779 (2004).

128. Higuchi, T., Nakamura, T., Kakutani, H. & Ishii, H. Thrombomodulin suppresses invasiveness of HT1080 tumor cells by reducing plasminogen activation on the cell surface through activation of thrombin-activatable fibrinolysis inhibitor. *Biol. Pharm. Bull.* **32,** 179–185 (2009).

129. Atkinson, J. M., Pullen, N. & Johnson, T. S. An inhibitor of thrombin activated fibrinolysis inhibitor (TAFI) can reduce extracellular matrix accumulation in an in vitro model of glucose induced ECM expansion. *Matrix Biol.* **32,** 277–287 (2013).

130. Guimarães, A. H. C. *et al.* TAFI and pancreatic carboxypeptidase B modulate in vitro capillary tube formation by human microvascular endothelial cells. *Arterioscler. Thromb. Vasc. Biol.* **27,** 2157–2162 (2007).

131. Mock, W. L. & Stanford, D. J. Anisylazoformylarginine: A superior assay substrate for carboxypeptidase B type enzymes. *Bioorganic Med. Chem. Lett.* **12,** 1193–1194 (2002).

132. Sakata, T. *et al.* Study of chromogenic substrate on protein C activity assay--in patients treated with warfarin. *Japanese J. Clin. Pathol.* **38,** 937–941 (1990).

133. Cell Proliferation Reagent WST-1. at <http://lifescience.roche.com/shop/products/cell-proliferation-reagent-wst-1>

134. Grant, D. S., Lelkes, P. I., Fukuda, K., Kleinman, H. K. & Al, G. Intracellular Mechanisms Involved in Basement Membrane. *Vitr. Cell. Dev. Biol.* **27A,** 327–336 (1991).

135. Kubota, Y., Kleinman, H. K., Martin, G. R. & Lawley, T. J. Role of laminin and basement membrane in the morphological differentiation of human endothelial cells into capillary-like structures. *J. Cell Biol.* **107,** 1589–1598 (1988).

136. Sameni, M., Dosescu, J., Moin, K. & Sloane, B. F. Functional Imaging of Proteolysis: Stromal and Inflammatory Cells Increase Tumor Proteolysis. *Mol. Imaging* **2,** 159–175 (2003).

137. Sloane, B. F., Sameni, M., Podgorski, I., Cavallo-Medved, D. & Moin, K. Functional imaging of tumor proteolysis. *Annu. Rev. Pharmacol. Toxicol.* **46,** 301–315 (2006).

138. Sameni, M. *et al.* Imaging and quantifying the dynamics of tumor-associated proteolysis. *Clin. Exp. Metastasis* **26,** 299–309 (2009).

139. Mohamed, M. M. *et al.* Interleukin-6 increases expression and secretion of cathepsin B by breast tumor-associated monocytes. *Cell. Physiol. Biochem.* **25,** 315–324 (2010).

140. Wang, L. *et al.* Matrix metalloproteinase 2 (MMP2) and MMP9 secreted by erythropoietin-activated endothelial cells promote neural progenitor cell migration. *J. Neurosci.* **26,** 5996–6003 (2006).

141. Livak, K. J. & Schmittgen, T. D. Analysis of relative gene expression data using real-time quantitative PCR and the 2-ΔΔCT Method. *Methods* **25,** 402–408 (2001).

142. Clare, G. M., Gronenborn, A. M., Nilges, J. M. & Ryan, C. A. Three-Dimensional Structure of Potato Carboxypeptidase Inhibitor in Solution. A Study Using Nuclear Magnetic Resonance , Distance Geometry , and Restrained Molecular Dynamics. *Biochemistry* **26,** 8012–8023 (1987).

143. Ryan, C. A., Hass, G. M. & Kuhn, R. W. Purification and Properties of a Carboxypeptidase Inhibitor from Potatoes. *J. Biol. Chem.* **249,** 5495–5500 (1974).

144. Foley, J. H., Kim, P. & Nesheim, M. E. Thrombin-activable fibrinolysis inhibitor zymogen does not play a significant role in the attenuation of fibrinolysis. *J. Biol. Chem.* **283,** 8863–8867 (2008).

145. Staton, C. A. *et al.* Current methods for assaying angiogenesis in vitro and in vivo. *Int. J. Exp. Path.* **85,** 233–248 (2004).

146. Cavallo-Medved, D. *et al.* Live-cell imaging demonstrates extracellular matrix degradation in association with active cathepsin B in caveolae of endothelial cells during tube formation. *Exp. Cell Res.* **315,** 1234–1246 (2009).

147. LeBleu, V. S., Macdonald, B. & Kalluri, R. Structure and function of basement membranes. *Exp. Biol. Med.* **232,** 1121–1129 (2007).

148. Toth, M., Sohail, A. & Fridman, R. Assessment of gelatinases (MMP-2 and MMP-9) by gelatin zymography. *Methods Mol. Biol.* **878,** 121–35 (2012).

149. Parkinson, J. F., Nagashima, M., Kuhn, I., Leonard, J. & Morser, J. Structure-function studies of the epidermal growth factor domains of human thrombomodulin. *Biochem. Biophys. Res. Commun.* **185,** 567–576 (1992).

150. Holliday, D. L. & Speirs, V. Choosing the right cell line for breast cancer research. *Breast cancer Res.* **13,** 215 (2011).

151. Schnaper, H. W. *et al.* Plasminogen activators augment endothelial cell organization in vitro by two distinct pathways. *J. Cell. Physiol.* **165,** 107–118 (1995).

152. Van Hinsbergh, V. W. M., Engelse, M. A. & Quax, P. H. A. Pericellular proteases in angiogenesis and vasculogenesis. *Arterioscler. Thromb. Vasc. Biol.* **26,** 716–728 (2006).

153. Sameni, M., Moin, K. & Sloane, B. F. Imaging Proteolysis by Living Human Breast Cancer Cells. *Neoplasia* **2,** 496–504 (2000).

154. Sameni, M. *et al.* Imaging and quantifying the dynamics of tumor-associated proteolysis. *Clin. Exp. Metastasis* **26,** 299–309 (2009).

155. Ahram, M. *et al.* Rac1-induced endocytosis is associated with intracellular proteolysis during migration through a three-dimensional matrix. *Exp. Cell Res.* **260,** 292–303 (2000).

156. Sameni, M., Dosescu, J. & Sloane, B. F. Imaging proteolysis by living human glioma cells. *Biol. Chem.* **382,** 785–788 (2001).

157. Everts, V., Van Der Zee, E., Creemers, L. & Beertsen, W. Phagocytosis and intracellular digestion of collagen, its role in turnover and remodelling. *Histochem. J.* **28,** 229–245 (1996).

158. Tang, Y., Kesavan, P., Nakada, M. T. & Yan, L. Tumor-stroma interaction: positive feedback regulation of extracellular matrix metalloproteinase inducer (EMMPRIN) expression and matrix metalloproteinase-dependent generation of soluble EMMPRIN. *Mol. Cancer Res.* **2,** 73–80 (2004).

159. Taraboletti, G. *et al.* Shedding of the matrix metalloproteinases MMP-2, MMP-9, and MT1-MMP as membrane vesicle-associated components by endothelial cells. *Am. J. Pathol.* **160,** 673–680 (2002).

160. Ginestra, A. *et al.* Urokinase Plasminogen-Activator and Gelatinases Are Associated with Membrane-Vesicles Shed by Human HT1080 Fibrosarcoma Cells. *J. Biol. Chem.* **272,** 17216–17222 (1997).

161. Mauviel, A. Cytokine regulation of metalloproteinase gene expression. *J. Cell. Biochem.* **53,** 288–295 (1993).

162. Kossakowska, A. E. *et al.* Interleukin-6 regulation of matrix metalloproteinase (MMP-2 and MMP-9) and tissue inhibitor of metalloproteinase (TIMP-1) expression in malignant non-Hodgkin's lymphomas. *Blood* **94,** 2080–2089 (1999).

163. Sayah, S., Ischenko, A. M., Zhakhov, A., Bonnard, A. S. & Fontaine, M. Expression of cytokines by human astrocytomas following stimulation by C3a and C5a anaphylatoxins: Specific increase in interleukin-6 mRNA expression. *J. Neurochem.* **72,** 2426–2436 (1999).

164. Rutkowski, M. J., Sughrue, M. E., Kane, A. J., Mills, S. A. & Parsa, A. T. Cancer and the complement cascade. *Mol. Cancer Res.* **8,** 1453–1465 (2010).

165. Monsinjon, T. *et al.* Regulation by complement C3a and C5a anaphylatoxins of cytokine production in human umbilical vein endothelial cells. *FASEB J.* **17,** 1003–1014 (2003).

166. Hamada, H. *et al.* The epidermal growth factor-like domain of recombinant human thrombomodulin exhibits mitogenic activity for Swiss 3T3 cells. *Blood* **86,** 225–233 (1995).

167. Tapon-Bretaudière, J. *et al.* A fucosylated chondroitin sulfate from echinoderm modulates in vitro fibroblast growth factor 2-dependent angiogenesis. *Mol. cancer Res.* **1,** 96–102 (2002).

168. Jan, S. Le *et al.* Functional overlap between chondroitin and heparan sulfate proteoglycans during VEGF-induced sprouting angiogenesis. *Arterioscler. Thromb. Vasc. Biol.* **32,** 1255–1263 (2012).

169. Beaulieu, L. M. & Church, F. C. Activated protein C promotes breast cancer cell migration through interactions with EPCR and PAR-1. *Exp. Cell Res.* **313,** 677–687 (2007).

170. Nozaki, M. *et al.* Drusen complement components C3a and C5a promote choroidal neovascularization. *Proc. Natl. Acad. Sci. U. S. A.* **103,** 2328–2333 (2006).

171. Yu, H., Lin, T. & Tang, C. Bradykinin enhances cell migration in human prostate cancer cells through B2 receptor/PKCδ/c-Src dependent signaling pathway. *Prostate* **73,** 89–100 (2013).

172. Greco, S. *et al.* Bradykinin stimulates cell proliferation through an extracellular-regulated kinase 1 and 2-dependent mechanism in breast cancer cells in primary culture. *J. Endocrinol.* **186,** 291–301 (2005).

173. Yu, H. *et al.* Bradykinin promotes vascular endothelial growth factor expression and increases angiogenesis in human prostate cancer cells. *Biochem. Pharmacol.* **87,** 243–253 (2014).

174. El-Tanani, M. K. *et al.* The regulation and role of osteopontin in malignant transformation and cancer. *Cytokine Growth Factor Rev.* **17,** 463–474 (2006).

175. Senger, D. R. *et al.* Stimulation of endothelial cell migration by vascular permeability factor/vascular endothelial growth factor through cooperative mechanisms involving the αvβ3 integrin, osteopontin, and thrombin. *Am. J. Pathol.* **149,** 293–305 (1996).

176. Sharif, S. A. *et al.* Thrombin-activatable carboxypeptidase B cleavage of osteopontin regulates neutrophil survival and synoviocyte binding in rheumatoid arthritis. *Arthritis Rheum.* **60,** 2902–2912 (2009).

177. Ceresa, E. *et al.* Comparative evaluation of stable TAFIa variants: Importance of α-helix 9 and β-sheet 11 for TAFIa (in)stability. *J. Thromb. Haemost.* **5,** 2105–2112 (2007).

178. Lawson, N. D. & Weinstein, B. M. In vivo imaging of embryonic vascular development using transgenic zebrafish. *Dev. Biol.* **248,** 307–318 (2002).

179. Tobia, C., Gariano, G., De Sena, G. & Presta, M. Zebrafish embryo as a tool to study tumor/endothelial cell cross-talk. *Biochim. Biophys. Acta - Mol. Basis Dis.* **1832,** 1371–1377 (2013).

Vita Auctoris

NAME:	Jennifer Balun
PLACE IF BIRTH:	Windsor, ON
YEAR OF BIRTH:	1991
EDUCTATION:	University of Windsor B.Sc. Honours Biochemistry with Thesis with distinction Windsor, ON, 2013
	University of Windsor M.Sc. in Chemistry and Biochemistry Windsor, ON, 2015